ABSTRACT

GRAHAM, WILLIAM DARNELL. Bacterial Cellulose: Investigating the Structural and Mechanical Properties of Bacterial Cellulose Under Biologically Relevant Conditions. (Under the direction of Joel J. Pawlak & Amy M. Grunden).

Advancements in colloidal and polymer chemistry have expanded the commercial applications of cellulose to include the development of high strength composite films for the production of energy efficient liquid displays, high-fidelity biosensors and acoustic diaphragms for high quality audio speakers. Additionally, cellulose is the most abundant polymer on earth making it the most logical candidate precursor for the replacement of fossil fuels. Although the commercial promise of cellulose is high, the establishment of cellulose as a global commodity is significantly hindered by the inefficiencies in cellulose liberation and processing. The current model associated with cellulose liberation from lignin and hemicellulose relies on the use of highly basic reagents resulting in significant alterations to cellulose native structure. The research detailed here examines the inherent properties of cellulose in its most native state using bacterial cellulose (BC) synthesized by *Gluconacetobacter hansenii* (*G. hansenii*) strain ATCC 23769 as a model; with the intent of improving cellulose liberation and saccharification techniques through the understanding of the biochemical complexities of *in vivo* cellulose. Previously characterized for the protection BC provides *G. hansenii* against mechanical, chemical and physiological stress, the degree of resistance BC affords *G. hansenii* against antibiotics is investigated here. The addition of kanamycin (kan) at a concentration of 50 μg ml^{-1} to wild type cultures of *G. hansenii* results in the selection of high cellulose producing phenotypes. Furthermore, it is demonstrated that when cultured in the presence of 5% (v/v) cellulase, a complete loss in kan resistance is observed in wild type cultures of *G. hansenii*. The stability of BC structure when exposed to

mechanical, chemical and thermal influence is also examined. An 88% drop in the intensity of the $1\bar{1}0$ peak (16.4º) of BC x-ray diffractograms is observed when BC samples are prepared by cryo-homogenization and pressed into film using 670 MPa of pressure, resulting in a 21% reduction in calculated crystallinity. A 100% improvement in the saccharification efficiency of cyro-homogenized BC despite a negligible change in observed degree of polymerisation (DP_n) from 606 ± 41 to 541 ± 42 after homogenization is seen. The influence of salinity on the crystalline structure of never dried BC was investigated by XRD, and it was demonstrated that the addition of salt at a concentration of 19 mmol l^{-1} restores intensity to otherwise unobservable crystalline peaks 110 (14.6°) and $1\bar{1}0$ (16.4°) of wet cellulose. Additionally, an observed shift of 1° in peak $1\bar{1}0$ as a consequence of aqueous water leaving BC during desiccation is reported. When purified BC samples are dried using a freeze dryer, the native structure of the BC is preserved and the 1º shift from 16.4° to 17.4° in the $1\bar{1}0$ peak is not observed. The influence of low concentrations of NaOH and heat on native cellulose structure was investigated using a protease purification technique that preserves the intrinsic hydrogen bonding of unpurified BC. The treatment of BC with proteinase K (PK) resulted in BC purity comparable to BC treated using the industry standard 1% (v/w) NaOH thermal bath treatment. PK treated BC however exhibited a 10% reduction in thermal stability as determined by TGA and DSC suggesting the preservation of BC native structure. Furthermore, the treatment of BC with PK resulted in the enhanced saccharification efficiency of BC as well as a reduction of 44% in observed BC DP_n. Finally this novel purification technique is used to demonstrate that cellulose synthesized by *G. hansenii* under agitated conditions is structurally the same as BC synthesized under static conditions.

Bacterial Cellulose: A Model for Deconstructing Cellulose Native Structure

by
William Darnell Graham

A dissertation submitted to the Graduate Faculty of
North Carolina State University
in partial fulfillment of the
requirements for the degree of
Doctor of Philosophy

Forest Biomaterials and Microbiology

Raleigh, North Carolina

2013

APPROVED BY:

_____	_____
Dr. Joel J. Pawlak Committee Co-Chair	Dr. Amy M. Grunden Committee Co-Chair
_____	_____
Dr. Candace H. Haigler	Dr. Sunkyu Park

DEDICATION

I dedicate this work to my mother, Dr. Priscilla Anne Graham, who worked her way up from being a teacher's aid to becoming an educational administrator, while raising three children. You are and always will be an inspiration to me. Through your example I learned that with a little creativity, hard work and dedication anything can be achieved. I also dedicate this work to my father, Master Sergeant William G. Graham for instilling in me discipline and a strong sense of work ethic. I thank you for teaching me the difference between success and victory and that victory can only be obtained through strong resolve.

BIOGRAPHY

William Darnell Graham was born on a small Marine Corp base in Havelock North Carolina. Who William Darnell Graham is and his ambitions in life are best defined by the following statement: History has taught us that the sum of any individual's life is not measured in wealth but in his or her contributions to the advancement of humanity. Innovations in technology and medicine are made every day by research teams around the world who are able to combine ideas and develop unique and creative ways to solve complex problems. The foundation for this type of research begins in the classroom and ends with an idea. It is my career aspiration to obtain a position of influence that will allow me to facilitate a collaborative environment where ideas are turned into reality. A deconstruction of my life as the son of a teacher and a Marine Drill Sergeant would reveal a man driven by a blue collar work ethic, where work input equals work output, but is also experienced in the complex nature of society and the importance of education. It is my ultimate desire to become an individual of influence whose legacy will involve the bettering of humanity through the nurturing of the next generation of researchers whose values are rooted in creative thinking and collaboration.

ACKNOWLEDGMENTS

I would like to thank Dr. Pawlak and Dr. Grunden for believing in me and providing me with a safe and secure environment to develop professionally. Words can not express my gratitude to the both of you for providing me with timeless advice and stern words of encouragement. I hold you both in the highest regard, and I hope that your personal mandate of exemplary mentoring never changes. Dr. Haigler, I thank you for your candor regarding my work and ideas. Your brutal honesty and your attention to detail has helped me to become a more thoughtful and thorough scientist. I want to thank Dr. Park for providing me with an open door anytime I needed assistance. Finally, I would like to thank my mentor and friend, Dr. Franck Vendeix. Your advice and support over the years has been invaluable. As a token of my gratitude, I dedicate the following poem to each of you. Each verse personifies your individual contributions to my professional evolution.

If

By Rudyard Kipling

If you can keep your head when all about you
Are losing theirs and blaming it on you;
If you can trust yourself when all men doubt you,
But make allowance for their doubting too:
If you can wait and not be tired by waiting,
Or, being lied about, don't deal in lies,
Or being hated don't give way to hating,
And yet don't look too good, nor talk too wise;

If you can dream---and not make dreams your master;
If you can think---and not make thoughts your aim,
If you can meet with Triumph and Disaster
And treat those two impostors just the same:.
If you can bear to hear the truth you've spoken
Twisted by knaves to make a trap for fools,
Or watch the things you gave your life to, broken,
And stoop and build'em up with worn-out tools;

If you can make one heap of all your winnings
And risk it on one turn of pitch-and-toss,
And lose, and start again at your beginnings,
And never breathe a word about your loss:

If you can force your heart and nerve and sinew

To serve your turn long after they are gone,

And so hold on when there is nothing in you

Except the Will which says to them: "Hold on!"

If you can talk with crowds and keep your virtue,

Or walk with Kings---nor lose the common touch,

If neither foes nor loving friends can hurt you,

If all men count with you, but none too much:

If you can fill the unforgiving minute

With sixty seconds' worth of distance run,

Yours is the Earth and everything that's in it,

And---which is more---you'll be a Man, my son

This work was supported by the USDA under the National Needs Fellowship program Award No. 2010-38420-20399. The writers also like to thank Susan Gardner and Dr. Olsen's lab for the use of their lab space and equipment during this study.

TABLE OF CONTENTS

LIST OF TABLES

LIST OF FIGURES

CHAPTER 1:

Literature Review

Bacterial cellulose: A model fiber for understanding cellulose structure

William D. Graham,[1,2]

Amy Grunden[2] and Joel Pawlak[1,*]

[1]Department of Forest Biomaterials, North Carolina State University, Raleigh NC 27695

[2]Department of Microbiology, North Carolina State University Raleigh NC 27695

Summary

A biosynthetic marvel, bacterial cellulose fibers are unique for their structural purity and nano-assembly. Bacterial cellulose exhibits increased water retention, crystallinity, tensile strength and biodegradability compared to plant based cellulose and has proven industrial and biomedical uses. This review discusses the current understanding of bacterial cellulose *in vivo* assembly, synthesis, regulation and physiochemical properties with emphasis on native cellulose structure. The current and potential applications for bacterial cellulose as an industrial biopolymer are also addressed.

Keywords: *Acetobacter xylinum*, *Gluconacetobacter hansenii* 23769, Bacterial Cellulose, Cyclic di-GMP, nano-fiber

1.1 Introduction

The pursuit of an international economy rooted in clean, sustainable energy has generated a renewed interest in cellulosic research. Globally abundant, cellulose provides a more environmentally friendly alternative to fossil fuels (Singh *et al*. 2010). Advancements in fermentation technology and carbon recycling has led to the development of innovative techniques for converting lignocellulosic biomass into fermentable sugars for biofuel production (Lin and Tanaka 2006; Tengerdy and Szakacs 2003). Despite these advancements, a major hurdle for the global acceptance of lignocellulosic based fuels is the cost associated with cellulose processing and saccharification (Ajanovic *et al*. 2012; Margeot *et al*. 2009). A potential solution to this economic barrier is the exploitation of bacteria that can synthesize cellulose from low value sugars generated from the liberation of cellulose from lignin and hemicellulose (Ishihara *et al*. 2002; Kurosumi *et al*. 2009; Tokoh *et al*. 2002). Historically rooted in the food industry, BC has gained interest from textiles, biomedical and industrial related fields for its nano-scale and unique properties (Iguchi *et al*. 2000; Siro and Plackett 2010). Exhibiting increased crystallinity, water retention and tensile strength compared to plant based cellulose, the potential commercial applications for BC are vast (Shoda and Sugano 2005).

Cellulose is a linear homopolysaccharide consisting of repeating units of D-glucose linked together with a β-1,4 linkage (Fig. 1-1) (Klemm *et al*. 2005). In higher plants, cellulose fibrils are interwoven with glycoproteins, heteropolysaccharides and aromatic compounds *in vivo*. Functioning as inherent architectural elements, cellulose provides a unique blend of chemical resilience, mechanical support and flexibility to plant cell walls (McNeil *et al*. 1984).

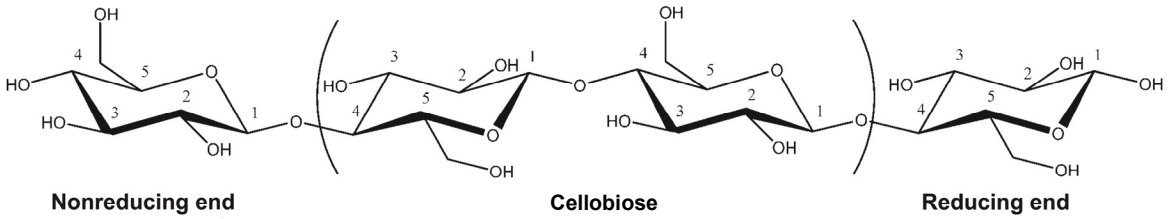

Figure 1-1 Chemical structure of cellulose (Habibi *et al*. 2010).

These characteristics are essential for other cellulose synthesizing organisms such as algae and oomycetes. Structurally reinforced with cellulose fibrils, the cell walls of algae differ in their polysaccharide composition. Generally consisting of more acidic polysaccharides, the polydispersity of these polymers is a reflection on the environmental requirements for mechanical strength, osmotic regulation and nutrient diffusion (Kloareg and Quatrano 1988). Different from plant and algae, oomycetes, formerly known as cellulosic fungi, contain only a small amount of cellulose. The primary role of cellulose in these organisms is to provide support during cell wall production and expansion (Blum *et al*. 2012; Bulone *et al*. 1992).

In a divergent class of microorganisms, cellulose is synthesized *in vivo* but secreted *ex vivo* in the form of an extra cellular polymeric substance (EPS) (Flemming *et al*. 2007). The secretion of EPS has been observed in algae, fungi and bacteria (Douwes *et al*. 1999; Jugdaohsingh *et al*. 1998). Bacterial EPS secretion has been widely studied and characterized because of the critical role it plays in the formation of biofilms. A biofilm is defined as a structured community of micro-organisms growing in a self-synthesized matrix of heteropolysacharides adherent to a living or non-living surface (Hall-Stoodley *et al*. 2004). Biofilm formation has gained notoriety among a diverse set of research fields, for the antimicrobial resistant properties it provides pathogenic bacteria (Costerton *et al*. 1999). Within the family of identified biofilming bacteria, only a small set of species belonging to

genera *Sarcina, Agrobacterium, Rhizobium, Achromobacter, Pseudomonas* and *Salmonella* synthesize cellulose. *Acetobacter, Azotobacter,* and recently identified gram positive *Rhodococcus* also synthesize cellulose but do not produce adhering polysaccharides and are not classified as biofilm associated organisms (Shoda and Sugano 2005; Tanskul *et al*. 2013). Considered an archetype for BC synthesis, *Acetobacter* are the most efficient producers of cellulose from a variety of carbon substrates (Mikkelsen *et al*. 2009; Ramana *et al*. 2000).

Several species of *Acetobacter* have been investigated for their ability to synthesize cellulose, with *Acetobacter xylinum* being the most widely characterized (Bielecki *et al*. 2005). *Acetobacter xylinum* was renamed *Gluconacetobacter hansenii* (*G. hansenii*) in 2006 after the microorgansims 16S rRNA sequence was determined (Lisdiyanti *et al*. 2006). *G. hansenii* is an aerobic, gram negative, rod shaped bacterium that was first isolated in 1886 for the purpose of vinegar production (Brown 1886). *G. hansenii* was not identified as a model organism for cellulose synthesis research until the late 1950s when Hestrin *et al* identified optimal growth conditions for cellulose production (Schramm and Hestrin 1954). The continued cultivation of *G. hansenii* under laboratory conditions resulted in the identification and cataloging of sub species, referred to as strains, of *G. hansenii* and their primary carbon source(s) (Table 1-1) (Chawla *et al*. 2009). The complete genome of *G. hansenii* ATCC (American Type Culture Collection) 23769 was completed in 2010 (Iyer *et al*. 2010). Although *G. hansenii* 23769 does not produce the highest yield of cellulose under general static conditions (Ishihara *et al*. 2002), strain 23769 is a vital tool for the continued investigation of cellulose biosynthesis and regulation as a result of the organism's sequenced genome.

Table 1-1. Cellulose producing *Gluconacetobacter* and their growth conditions

Strain	Culture conditions	Carbon source	Supplement	Culture time (h)	Yield (g/L)	Reference
Acetobacter xylinum (*G. Hansenii*)						
BRC 5	Agitated	Glucose	Oxygen, Ethanol,	50	15.3	Yang *et al.* 1998
ATCC 35959 (NCIMB 8746)	Agitated	Glucose	Oxygen, Agar	120	3.98	Toyosaki *et al.* 1995
PJK	Agitated	Glucose	Ethanol	48	1.72	Park *et al*. 2003
NUST4.1	Stir tank reactor	Glucose	Soduim alginate	120	6	Zhou *et al.* 2007
V6	Agitated	Glucose	Ethanol	192	4.16	Son *et al.* 2003
Sp. A9	Agitated	Glucose	Ethanol	192	15.2	Son *et al.* 2001
E_{25}	Agitated	Glucose	None	168	3.5	Krystynowicz *et al.* 2002
RKY5	Agitated	Glycerol	None	144	5.63	Kim et al. 2006
sp. st-60-12 & Co-Culture *Lactobacallis mali* JCM1116	Agitated	Sucrose	Co-Culture	72	4.2	Seto *et al*. 2006
K3	Static	Mannitol	Green tea	168	3.34	Nguyen *et al*. 2008
IFO 13,773	Static	Glucose	Lignosulfonate	168	10.1	Keshk andSameshima 2006a
IFO 13,773	Static	Molasses	None	168	5.76	Keshk and Sameshima 2006b
ATCC 23769 (NCIB 8246)	Static	Glucose	None	672	3.21	Ishihara *et al.* 2002
ATCC 53524	Static	Sucrose	None	96	3.83	Mikkelsen *et al*. 2009
ATCC 7000178 BPR2001 (JCM 9730)	Static	Molasses	None	72	7.82	Bae and Shoda 2004
ATCC 7000178 BPR2001 (JCM 9730)	Bioreactor	Fructose	Agar oxygen	72	14.1	Bae *et al.* 2004
Acetobacter pasteurianus						
ATCC 10245	Static	Glucose	None	672	0.4	Ishihara *et al.* 2002
IFO 14814	Static	Glucose	None	672	0.78	Ishihara *et al.* 2002
Gluconacetobacter medellensis						
G. medellensis	Static	Sucrose	None	336	4.5	Castro *et al.* 2012

1.2 Bacterial cellulose biosynthesis and regulation

The development of an *in vitro* assay for investigating the biochemical pathways involved in cellulose biogenesis was achieved in 1958 using cell free extracts isolated from *G. hansenii* (Colvin 1957; Glaser 1958; Greathouse 1957). Further refinement of this technique resulted in the isolation of a stable bacterial cellulose (BC) synthase using digitonin (Lin *et al*. 1985). A trans-membrane protein, BC synthase has a molecular mass of 400 – 500 kDa (Chawla *et al*. 2009). The polymerization of glucose into cellulose is catalyzed by conserved β-glycosyltransferase residues contained in the globular region of the cellulose synthase (Saxena and Brown 2005). Advancements in molecular cloning resulted in the identification of the *acs* operon for BC synthase (Saxena and Brown 1995; Saxena *et al*. 1994). The operon is composed of three genes, *acsAB*, *acsC* and *acsD*, with *acsAB* enconding BC synthase (AcsAB) (Lin *et al*. 1990; Saxena *et al*. 1994). Predicted to be localized to the cytoplasm, BC synthase is composed of a catalytic domain and a regulatory domain (Chawla *et al*. 2009; Mayer *et al*. 1991). A recent study using *G. hansenii* 23769 suggest the BC synthase is processed into three polypeptide subunits, with the regulatory domain located in the cytoplasm and the catalytic domain oriented in the cytosol (Iyer *et al*. 2013).

The regulatory domain binds cyclic diguanylate (c-di-GMP), which has been demonstrated to allosterically activate the enzyme (Mayer *et al*. 1991; Ross *et al*. 1987). The mechanism for recognition and binding of c-di-GMP is still being investigated with the most recent study, using BC synthase isolated from *G. hansenii*, suggesting the conserved PilZ region of the regulatory domain functions as a receptor for c-di-GMP binding (Fujiwara

et al. 2013).

c-di-GMP is a universal regulator of biofilm formation, motility, EPS production and multicellular behavior in a diverse set of bacteria (Amikam and Galperin 2006). This universal regulation is achieved through the binding of ci-di-GMP to effector molecules that undergo conformational changes, transcriptional activation, DNA binding, protein-protein interactions, depression of genes, localization, and enhanced enzymatic activity (Boyd and O'Toole 2012; Tuckerman *et al*. 2009). The biochemical pathways associated with c-di-GMP signaling are complex in nature consisting of a network of enzymes and effector molecules that sense and respond to environmental signals to adjust *in vivo* levels of c-di-GMP for the regulation of phenotypic outputs (Boyd and O'Toole 2012). The synthesis and regulation of c-di-GMP *in vivo* is mediated by a set of proteins containing conserved amino acid motifs (Fig. 1-2). c-di-GMP is synthesized from GTP by diguanylate cyclases (DGCs) that contain the conserved domain GGDEF. The linearization and deactivation of c-di-GMP into 5'-phosphoguanylyl-guanosine (pGpG) is mediated by phosphodiesterase (PDEs) which contains the conserved region EAL. In some bacteria, the activity of the EAL is heavily dependent on the presence of Mg^{2+} ions, and is strongly inhibited by Ca^{2+} ions (Christen *et al*. 2005). These conserved regions are found in several different effector molecules containing sensing domains that allow the bacteria to respond to a diverse set of external stimuli (Mills *et al*. 2011). In *G. hansenii*, the phosphodiesterase A1 protein (AxPDEA1) was found to be most active in the deoxyheme conformation, resulting in linearizing of c-di-GMP and the down regulation of cellulose synthesis in response to low oxygen concentrations (Chang *et al*. 2001). At present, the regulation of BC synthesis in *G. hansenii* 23769 by c-di-GMP in response to additional external stimuli has yet to be investigated.

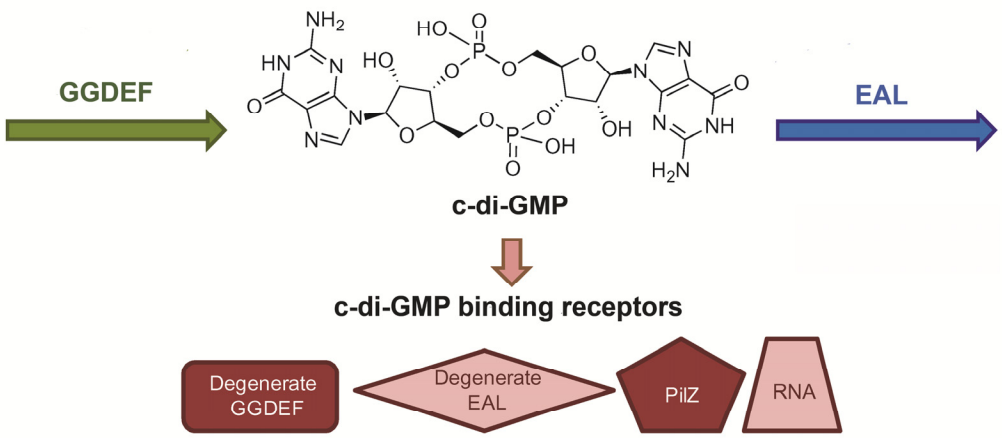

Figure 1-2 cyclic diguanylate metabolism. c-di-GMP is synthesized from GTP by diguanylate cyclases containing GGDEF domains (green) and is degraded into pGpG by phosphodiesterase domains containing either EAL or HD-GYP domains (blue). Depending on c-di-GMP binding receptor expression patterns and binding affinities to c-di-GMP, different receptors (red) will be activated. Binding receptors can be highly diverse and include proteins with a variety of domains as well as RNA motifs (Mills *et al*. 2011).

The β-glycosyltransferase region of BC synthase binds to uridine diphosphate glucose (UDPGlc) and processively polymerizes glucose molecules with a β-1,4 linkage into a cellulose chain (Kudlicka and Brown Jr 1997; Saxena *et al*. 1995; Saxena and Brown Jr 2000). Cellulose synthesis by *G. hansenii* can be broken down into four enzymatic steps (Fig. 1-3). The initial step involves the phosphorylation of glucose to glucose-6-phosphate (Glc-6-P) by glucokinase (Benziman and Rivetz 1972). Glc-6-P is then isomerized by phosphoglucomutase into glucose-1-phosphate (Glc-1-P). UDPGlc is then synthesized from Glc-1-P by UDPG-phosphorylase. The formation of UDPGlc initiates cellulose synthesis by the BC synthase enzyme complex (Chawla *et al*. 2009). Efforts are being made to determine the complete structure of a biologically relevant BC synthase through protein isolation, crystallization and molecular dynamics simulations (Hu *et al*. 2010; Morgan *et al*. 2012). The challenge associated with structural studies involving a membrane associated

biosynthetic complex is the ability to simulate *in vivo* conditions that favor proper protein folding and interaction. In a study performed by Morgan *et al*, the crystal structure of *Rhodobacter sphaeroides* cellulose synthase complex BcsA-Bcs-B containing a translocating polysaccharide, was solved providing researchers with a model for understanding the architecture of cellulose synthase during glucan chain elongation. Their results suggest that BcsA forms a channel where the polymerization of glucose occurs one monomer at a time and not two monomers at a time as previously theorized (Morgan *et al* 2012).

The refinement of carbon atom labeling techniques led to the illumination of the biochemical pathways in bacteria that govern the flux of hexoses into the cellulose synthesis pathway (Benziman and Burger-Rachamimov 1962; Weinhouse and Benziman 1976; Weinhouse and Benziman 1972). *G. hansenii* can metabolize carbon by two amphibolic pathways; pentose phosphate pathway for the oxidation of carbohydrates and the citrate cycle for the oxidation of organic acids and related compounds (Fig. 1-3) (Benziman and Mazover 1973; Gromet *et al*. 1957; Swissa and Benziman 1976). The oxidative dissimilation of carbohydrates by these pathways results in the formation of hexose phosphate (Glc-6-P), which is the intermediate for UDPGlc (Gromet *et al*. 1957; Schramm *et al*. 1957). More specifically, the generation of hexoses *in vivo* is the indirect result of the pentose phosphate pathway and gluconeogenic pathway (Weinhouse and Benziman 1974). The shuttling of hexoses into the cellulose synthesis pathway is regulated by the enzymatic activity of NAD-linked glucose 6 phosphate dehydrogenase (Benziman and Mazover 1973). Specific to *G. hansenii*, NADP-glucose 6 phosphate dehydrogenase converts Glc-6-P into 6-phosphogluconate for pentose phosphate metabolism. In the presence of high levels of ATP, $NADP^+$ levels are low relative to NADPH, resulting in the shuttling of Glc-6-P into the

cellulose synthesis pathway. In contrast, functioning as an energy-linked control mechanism, low levels of ATP result in increased $NADP^+$ levels and the conversion of G-6-P into 6-phosphogluconate initiating pentose phosphate metabolism (Benziman and Mazover 1973). The metabolism of glucose by *G. hansenii* is slightly different, in that exogenous glucose (hexose) can be directly phosphorylated without entering the pentose phosphate pathway (Benziman and Rivetz 1972). Despite the high conversion rate of glucose to UDPGlc, the problem associated with glucose as the primary carbon source for cellulose

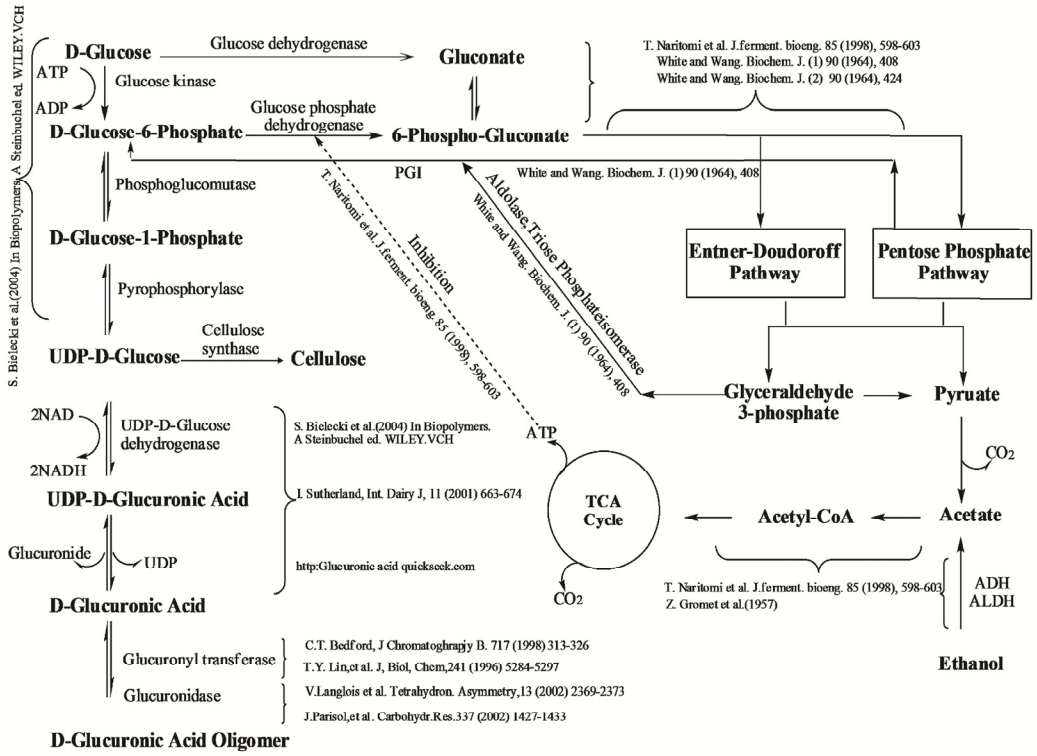

Figure 1-3 Proposed biochemical pathways for metabolism and cellulose production by *G. hansenii* (Ha et al. 2011).

production is the formation of gluconate as a by-product in the medium resulting in a decreased pH profile and a reduction in cellulose synthesis (De Wulf *et al*. 1999; Hwang *et al*. 1999; Keshk and Sameshima 2006a). In more recent studies, alternative carbon sources like α-linked glucuronic acid-based oligosaccharide (SSGO) have been used to cultivate *G. hansenii* in an effort to reduce gluconate accumulation, thereby stabilizing the culture pH for better cellulose production. SSGO is a byproduct produced during cellulose synthesis by *G. hansenii*. When used as an additive to glucose based media, cellulose production was enhanced resulting in a cellulose yield of 10.5 g l^{-1} compared to the 7.4 g l^{-1} observed with glucose-only based media (Ha *et al*. 2011; Ul-Islam *et al*. 2013).

1.3 Carbon sources

The influence of various carbon sources on cellulose production by *G. hansenii* has also been investigated (Ramana *et al*. 2000). Ultimately strain specific (Table 1-1), sucrose is the most efficient carbon source for cellulose production by *G. hansenii* when glucose is not available (Embuscado *et al*. 1994). The successful cloning and expression of sucrose synthase in *G. hansenii* was achieved by Nakai *et al* 1999, where cellulose production in the presence of sucrose was increased by 1.6 fold compared to wild type *G. hansenii* (Nakai *et al*. 1999) through the sequestering of free UDP *in vivo*. The utilization of D-xylose for cellulose synthesis by *G. hansenii* was investigated by Ishihara *et al* 2002. The results from this study demonstrated that when cultured in the presence of xylose isomerase, the efficiency of cellulose production by *G. hansenii* from a mixture of D-xylose/D-xylulose is significantly enhanced (Ishihara *et al*. 2002). The use of ethanol as the primary carbon

source resulted in low yield cellulose production. However, when ethanol is used in combination with glucose the efficiency of cellulose production was enhanced in some strains of *G. hansenii* (Jung *et al*. 2005; Li *et al*. 2012; Masaoka *et al*. 1993; Park *et al*. 2003a). Maltose, glycerol and starch have also been investigated; however, cellulose yields were considerably lower compared to glucose based cultures (Masaoka *et al*. 1993). The efficiency of cellulose production by *G. hansenii* is most improved when substrates are used in combination. Culture medium containing a mixture of carbohydrates such as sucrose, fructose and glucose, resulted in an increase in cellulose yield relative to culture media containing only one carbohydrate (Keshk and Sameshima 2006b; Kongruang 2008; Nakai *et al*. 1999). This observation resulted in the development of statistical optimization techniques that maximize cellulose synthesis (Mohite *et al*. 2012).

1.4 Cellulose fibril assembly and extrusion

Time course experiments aimed at characterizing the biogenesis of cellulose by *G. hansenii* suggest the ability of a single cell to polymerize up to 200,000 glucose molecules per second into cellulose (Hestrin and Schramm 1954). The polymerization of glucose by BC synthase signifies the initiation of cellulose biogenesis, which includes polymerization, crystallization and extrusion (Brown and Saxena 2000). The mechanism associated with the formation of a possible precellulosic polymer in the cytoplasm is not well understood. The two prominent models for this mode of action differ concerning the involvement of a lipid intermediate (De Iannino *et al*. 1988). The nascent cellulose strand, referred to as a protofibril, is approximately 1.5 nm in diameter (Benziman *et al*. 1980; Haigler 1985). The

profibrils are spun out of the cell in the form of ribbon-shaped microfibrils through small pores (50 to 80) that run along the long axis of the cell surface (Fig. 1-4) (Brown *et al*. 1976; Zaar 1979). It is postulated that the β-1,4 glucan chains, upon extrusion, aggregate into units of 10 to 15 chains known as tactoidal aggregates that are 3.5 nm in diameter. Microfibril crystallization occurs as the tactoidal glucan bundles assemble at the cell surface (Benziman *et al*. 1980). In a theorized cell directed assembly, the highly crystalline microfibrils form loosely wound helical bundles of 1000 individual glucan chains, in a precise hierarchical fashion (Ross *et al*. 1991). The mutual orientation of associated glucan chains and the mutual orientation of subsequent chain bundles is the result of the coupling of polymerization and crystallization *in vivo*, explaining the initial predominance of the less structurally stable cellulose I polymorph (Benziman *et al*. 1980).

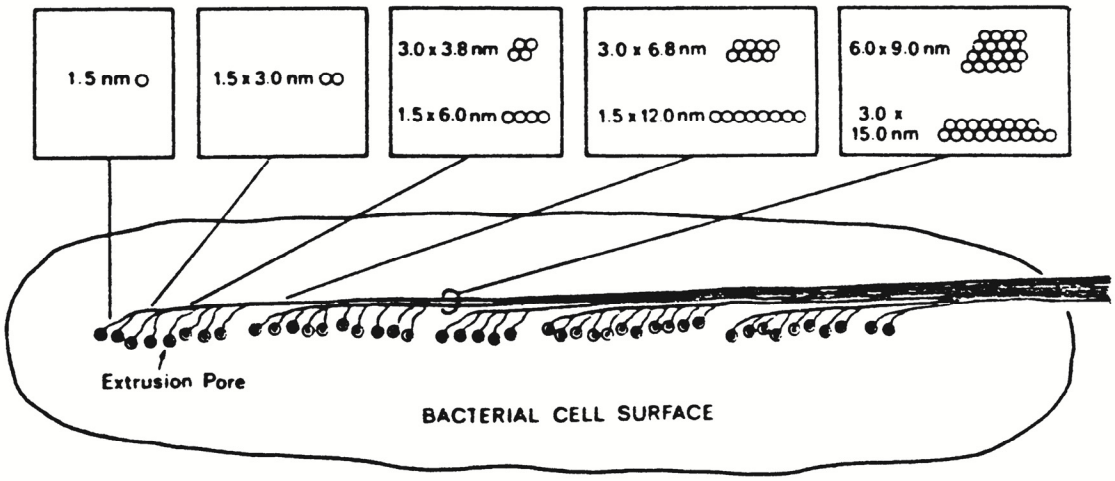

Figure 1-4. Generalized model of ribbon assembly in *G. hansenii*, showing a possible mechanism of origin or microfibrils and separate fibrillar subunits within the ribbon. Shown in the boxes are possible packing arrangements of 1.5 nm tactoidal aggregates (Haigler 1985).

1.5 Bacterial cellulose structure

Cellulose I is theorized to represent the most native form of cellulose. However, attempts to synthesize BC under *in vitro* conditions results in the formation of the more thermodynamically stable cellulose II, which supports the concept that crystallization accompanies or follows very closely, to polymerization *in vivo* (O'sullivan 1997). Under *in vivo* conditions factors such pH and the presence of counter ions can significantly influence native hydrogen bonding. The existence of two subpolymorphs of cellulose I, referred to as Iα and Iβ, was discovered in 1984 by cross-polarization magic angle spinning (CP-MAS) (Atalla and Vanderhart 1984; Vanderhart and Atalla 1984). Both Iα and Iβ polymorphs adopt a parallel chain configuration, but differ in their hydrogen bonding patterns, suggesting a difference in crystalline structure (Habibi *et al*. 2010). Cellulose Iα exhibits a triclinic motif consisting of only one chain per unit cell (Nishiyama *et al*. 2003). In comparison, cellulose Iβ exists in a monoclinic unit cell having two cellulose chains (Nishiyama *et al*. 2002). Bacterial cellulose generally consists of 70% Iα polymorph, which is the highest percentage in nature, whereas the Iβ allomorph is dominant in plant based cellulose (Yamamoto *et al*. 1996). The *in situ* ratio of Iα to Iβ varies among cellulose producing organisms, suggesting the two polymorphs natively co-exist with Iα representing nascent microfibrils (O'sullivan 1997). However, several groups have demonstrated the conversion of Iα polymorph to Iβ polymorph through environmental factors such as temperature and pH (Yamamoto *et al*. 1989). Iα polymorph undergoes a re-annealing event to the more thermal stable Iβ conformation at a temperature of 260°C (Nakagaito *et al*. 2005). This observation suggests, the heterogeneous nature of cellulose I may be a result of the ability of cellulose Iα to interconvert to Iβ as a result of environmental factors (Maunu *et al*. 2000; O'sullivan 1997).

Cellulose II is the industrial preferred cellulose conformation, exhibiting enhanced thermal stability compared to the cellulose I polymorph. The irreversible conversion of cellulose I to cellulose II is achieved through mercerization, which involves swelling of native fibers in concentrated NaOH or regeneration, which involves the solubilization and precipitation of cellulose I resulting in the re-annealing of glucose chains into the cellulose II conformation (O'sullivan 1997). Cellulose III can be reversibly formed from I and II, by treatment with liquid ammonia. The application of heat to cellulose III results in the formation of cellulose IV (Park *et al*. 2010).

1.6 Culture conditions

The efficiency of cellulose production by *G. hansenii* is dictated by carbon source availability and the accumulation of metabolic by-products that cause unfavorable growth conditions (Chawla *et al*. 2009). As discussed previously in this article, the optimization of media components based on *G. hansenii* strain is essential for high yield cellulose production (Chawla *et al*. 2009; Embuscado *et al*. 1994). Other environmental factors such as temperature, culture type (agitated or static) oxygen diffusion and pH also influence cellulose synthesis.

The most efficient production of cellulose by *G. hansenii* occurs under static conditions between 28°C and 30°C (Gromet *et al*. 1957). Culturing *G. hansenii* under agitated conditions results in the formation of cellulose negative (Cel^-) phenotypes, which become more enriched over time in comparison to wild type phenotypes, resulting in low cellulose production (Kim *et al*. 2007). The appearance of cellulose negative mutants of *G.*

hansenii has been explicitly investigated and well characterized (Valla and Kjosbakken 1982). Cel^- mutants form colonies on agar plates that are smooth in appearance and easily identified without visual aid. Unlike wild type cells, Cel^- mutants excrete a water soluble EPS in large quantities (Valla and Kjosbakken 1981). Whereas, wild type phenotypes produce colonies that excrete cellulose in large quantities, giving rise to their distinctive wrinkled appearance. This observed difference in colony morphology as a result of cellulose synthesis was confirmed by a luminescent assay using the chemical Calcofluor White, which in the presence of cellulose is visible when exposed to UV light (Cannon and Anderson 1991).

Although the rate of mutation varies from strain to strain, the accumulation of Cel^- mutants was found to be more the result of biological selection than spontaneous mutation (Valla and Kjosbakken 1982). More specifically, under agitated conditions wild type cells become entrapped in cellulose aggregates that resemble spheres (Fig. 1-5), whereas Cel^- mutants grow as individual cells. A random sampling of an agitated culture will contain a large population of Cel- mutants as a result of the number of wild type cells entangled in cellulose spheres that cannot be selected by pipettor. Thus, when transferred to a new culture, the Cel- population is further enriched (Valla and Kjosbakken 1982). Chemical mutagenesis can also induce a high population of Cel- mutants in various strains. Molecular analysis of Cel- mutants from specific strains of *G. hansenii*, suggest the majority of the observed mutations do not reside in the structural genes of cellulose synthesis, since the cellulose production from a population of Cel- phenotypes could be induced by antibiotics that inhibit protein synthesis. These observations may indicate that cellulose synthesis in *G. hansenii* is subject to a fast responding molecular switch that deserves further characterization (Valla and Kjosbakken 1982). Wild type *G. hansenii* have the selective

advantage when cultivated under static conditions. Cellulose synthesis by wild type *G. hansenii* is high at the air liquid interface resulting in the formation of a cellulose pad referred to as a pellicle (Fig. 1-6). It is currently theorized that the pellicle remains at the surface of

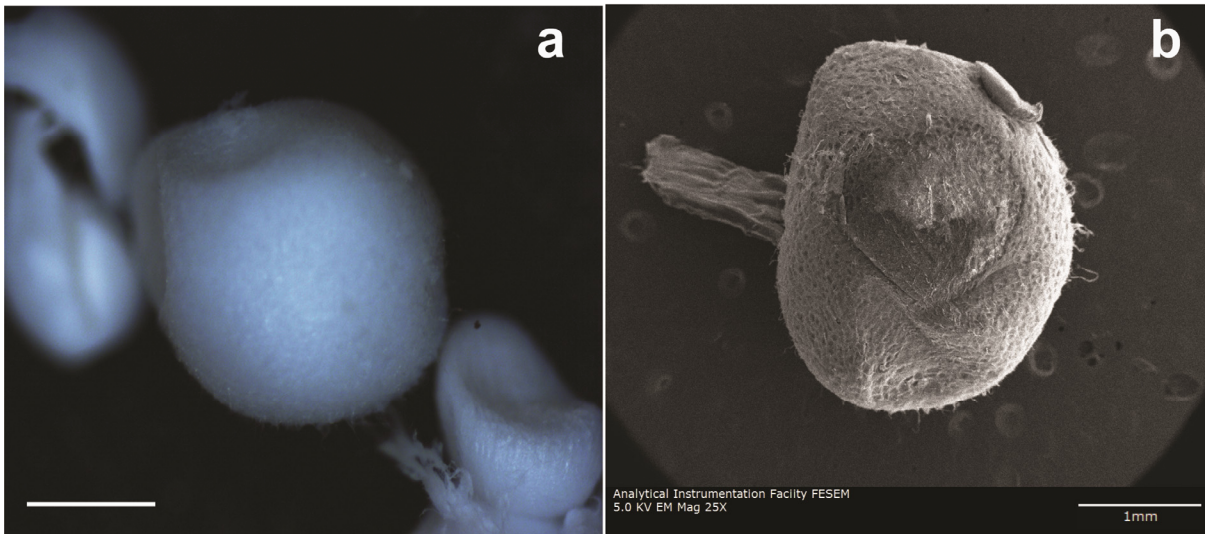

Figure 1-5 Bacterial spheres (a) Light microscope image of BC spheres: Scale bar = 1mm (b) SEM of BC Sphere.

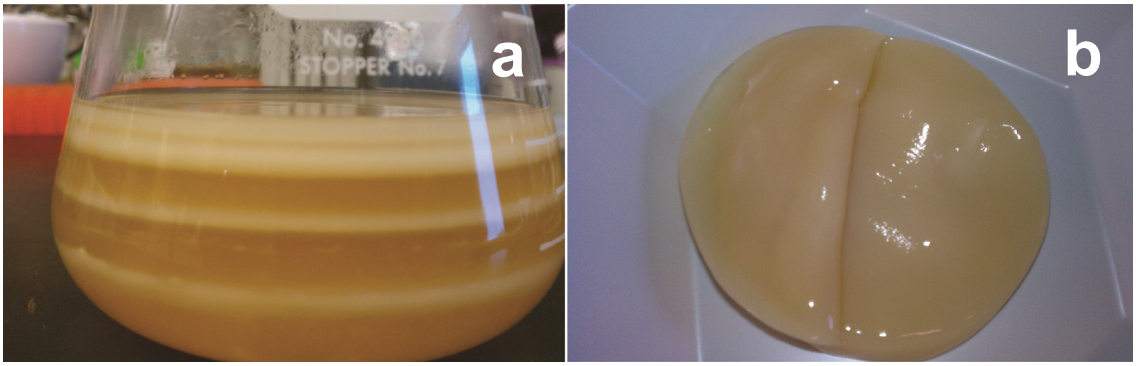

Figure 1-6 Bacterial cellulose pellicle (a) in culture (b) isolated from media.

media as a result of CO_2 trapping (Ross *et al*. 1991). The Cel^- mutants are relegated to the bottom of the culture where oxygen supply is limited. After a few generations the Cel^- population is significantly reduced whereas wild type cells are able to continue to grow and thrive on atmospheric oxygen (Valla and Kjosbakken 1982). A more recent study demonstrated the reduction of Cel^- mutants in agitated cultures through the addition of 1% *v*/*v* ethanol (Jung *et al*. 2005; Li *et al*. 2012). Active investigations into reducing/preventing the generation of Cel^- mutants in *G. hansenii* cultures using novel approaches, such as bioreactors, are ongoing (Chawla *et al*. 2009; Huang and Chen 2013). In addition to the formation of Cel^- phenotypes, it has been suggested that under agitated conditions wild type *G. hansenii* produces cellulose with a higher ratio of the Iβ polymorph (Czaja *et al*. 2004). It is theorized that shear stress from agitation interferes with nascent strand association and crystallization resulting in the formation of the more stable Iβ polymorph (Watanabe *et al*. 1998; Yamamoto *et al*. 1996).

An obligate aerobe, oxygen is essential for the production of cellulose by *G. hansenii* (Hestrin and Schramm 1954). The dissolved oxygen concentration in the culture medium can significantly influence the rate of cellulose production. Under agitated conditions, if the concentration of dissolved oxygen becomes too high and in the presence of excess glucose, the rate of gluconate conversion is significantly raised resulting in the down regulation of cellulose synthesis as a consequence of low pH. Cultures that contain low concentrations of dissolved oxygen are unable to grow efficiently and synthesize cellulose (Tantratian *et al*. 2005). Investigation into alternative culture techniques using a fed batch culture scheme identified a value of 10% saturation as the ideal dissolved concentration of oxygen for optimal cellulose synthesis by *G. hansenii* (Hwang *et al*. 1999). At present, the use of viscosity inducing factors to reduce culture shear stress, while providing optimal oxygen

diffusion, is being actively investigated (Kim *et al*. 2012).

Cellulose synthesis by *G. hansenii* occurs optimally at a culture pH range of 4 to 6 depending on strain. The rate of cellulose synthesis decreases exponentially once the pH of the culture falls below 4 (Masaoka *et al*. 1993). Depending on the culture technique, the stabilization of culture pH using buffers like corn steep liquor (CSL) (Noro *et al*. 2004; Sharma *et al*. 2012), has been met with great success; however, in a study performed by Hwang *et al*, it was demonstrated that the decrease in culture pH under static conditions enhanced the efficiency of cellulose production by *G. hansenii* over extended culture periods (Hwang *et al*. 1999). At present, the use of complex rotary and submerged bioreactors designed to optimize cellulose production through the mediation of dissolved oxygen content, pH and viscosity is actively being investigated (Chawla *et al*. 2009; Huang and Chen 2013).

1.7 Harvesting and purification

Crude BC harvested from bacterial cultures contain a number of impurities that include protein, cell mass and media components. These secondary organics must be removed before the polymer can be used for industrial refinement or analytical evaluation. The most common method of purification, referred to as 1% base treatment, involves the treatment with an alkali, generally sodium hydroxide, heat and organic acid (Nakai *et al*. 1998; Sutherland 1998). The period of time for each treatment step can vary depending on the study, with a typical treatment scheme represented in figure 1-7. For medical applications the BC is washed in 3% (*v*/*v*) NaOH for a minimum of 12 h then exposed to 3%

(*v*/*v*) HCl until a pH of 7 is reached. After a thorough washing in deionized water, the cellulose is autoclaved to ensure complete sterilization (Seto *et al*. 2006; Yang *et al*. 2012). The technique used for water removal from purified cellulose is dependent on the end application. The most common method of drying BC for the purpose of making film involves oven drying the polymer at 90°C (Norouzian *et al*. 2011). Freeze drying is the preferred method for removing water from BC purified for analytical studies because of the preservation of the native structure of the cellulose (Maneerung *et al*. 2008; Ul-Islam *et al*. 2013).

1.8 Bacterial cellulose properties

Chemically identical, BC differs from plant based cellulose in the degree of polymerization (DP) with BC exhibiting a DP of 2,000 – 6,000 and plant based cellulose exhibiting a DP of 13,000 to 14,000 (Jonas and Farah 1998). Consisting of 1000 glucan chains, the helical ribbons intersect to form nano-fibrils and nano-fibril bundles. When cultured under static conditions, the helical bundles form a complex network of cellulose nano-fibers (3-8 nm) (Fig. 1-4) (Morgan *et al*. 2012; Ross *et al*. 1991). The nano-fibers of this ultrafine and pure matrix are highly uniaxially oriented resulting in the unique properties of high crystallinity, high tensile strength and high moldability (George *et al*. 2005; White and Brown 1981). One hundred times thinner than most plant based fibers, the water holding properties of BC (by mass) is 100 times higher than their plant based counterparts (Schrecker and Gostomski 2005; Watanabe *et al*. 1998). The exploitation of the self-assembly properties of BC are currently being investigated using magnetic nanoparticles

covalently attached to the surface of *G. hansenii* cells, resulting in the ability to direct BC synthesis in predetermined macrostructures (Park *et al*. 2012; Sano *et al*. 2010; Sureshkumar *et al*. 2010).

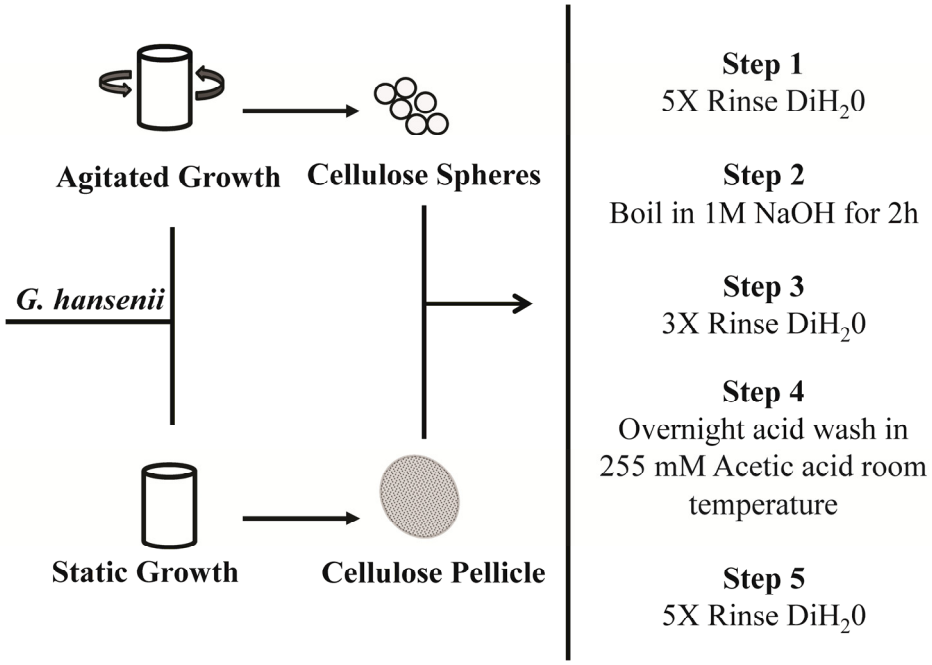

Figure 1-7 1% Base treatment scheme for purifying bacterial cellulose.

The dissolution of cellulose can be achieved using concentrated acid, such as sulfuric acids, hydrochloric acid or nitric acid. Equally effective, cellulose can also be dissolved in NaOH solutions that are 8.5% (*v*/*v*) or higher in concentration. The efficiency of NaOH solutions can be enhanced by the addition of 1% (*v*/*v*) urea (Lüaskiewicz 1998). A

relic from the industrial processing and conversion of plant based cellulose, the saccharification of cellulose for the purpose of biofuel generation was initially accomplished by the immersion of the cellulose in strong acid and strong base solutions (Sanchez and Cardona 2008). However, this process was found to be extremely cost prohibitive as a result of the refinement and disposal of the highly corrosive chemical waste generated. This realization resulted in the search for alternative processing techniques that are more efficient and economically viable (Sarkar *et al*. 2012; Teramoto *et al*. 2008). Additionally the treatment of cellulose with strong base has significant influence on the structural characteristics of native cellulose. The submersion of purified cellulose into low concentrations of NaOH results in the swelling of cellulose fibers and mass gain. Although, the transition to a more thermal stable polymorph is desired for industrial purposes, the change in native structure is not ideal for the analytical analysis and chemical modification of native cellulose. Further investigations into cellulose fiber swelling resulted in the generation of the following list that reflects the percent mass gain as a consequence of cellulose submersion into low concentration base solutions: $NaOH>KOH>Na_2CO_3>K_2CO_3$ (George *et al*. 2005). Alkali treated (kraft pulp method) BC was analyzed for enhanced properties in mechanical strength in microfibrillated composites (MFC) (Orts *et al*. 2005). It was found that the bending strength of BC associated film increased from 370 MPa to 425 MPa, while the young's modulus increased from 19 GPa to 28 GPa (Nakagaito and Yano 2008; Orts *et al*. 2005). The mass gain observed from these treatments, have also been found to influence the saccharification rate of cellulose fibers as a result of increased DP (Kuo and Lee 2009).

The addition of heat can also significantly influence the structural aspects of native cellulose. The transition of cellulose Iα to Iβ is achieved at 260°C (Nakagaito *et al*. 2005).

The thermal stability of the cellulose structure is further enhanced by the addition of alkali which results in a shift in degradation temperature from 300°C - 330°C to 343°C – 370°C (Nakagaito *et al*. 2005; Yamamoto *et al*. 1989).

1.9 Current and future applications

Nature's masterpiece cellulose, has evolved to be the world's finest example of light weight, rigid architecture designed for efficient biological and non-biological applications. Quickly advancing to the forefront of technology, the ultrafine and ultrapure nanostructured network of BC makes it ideal for industrial and commercial applications that range from advanced fiber-optics to dietary food supplements. Only recently recognized by the medical industry, the porous nature of BC and its biocompatibility make it ideal for health related applications. A summary of these applications and their future prospects are listed below.

Fiber optics

The integration of BC into nano-composites has led to the development of more energy efficient liquid crystal displays. Transparent nano-woven composites of BC are flexible, making them ideal for the construction of organic light emitting diode (OLED) displays. Exhibiting high thermal stability, the incorporation of BC into nano-composite films, results in reduction of the film's coefficient of thermal expansion (CTE). A major hurdle for OLED development, a reduced CTE minimizes heat fluctuations in OLED circuit assemblies, making the organic based displays more sustainable. Additionally, the enhanced tensile strength and high crystallinity make BC perfect for reinforcing nano-composites. When

meshed in a polymeric matrix for transparent displays, the nano-scale of BC also ensures the prevention of light scattering. Highly biodegradable and renewable in nature, BC is ideal for the future advancement and development of OLED technology that is both efficient in energy consumption and environmentally friendly to manufacture (Ummartyotin *et al*. 2012).

Acoustics

BC has been used to produce high fidelity acoustic speaker diaphragms for a number of years. The low density of BC and its high Young's modulus allow BC derived speaker diaphragms to achieve high sonic velocity for better acoustics without the loss of sound clarity (Nishi *et al*. 1990).

Food supplements

Commercially realized in the late 90s, BC based food products have been a global success. Originating in South-East Asia and now popular all over the world, BC is used as a dessert referred to as nata de coco. Derived from the culturing of *G. hansenii* in coconut based media, the gelatinous mixture of cellulose pellicle, is currently being investigated for its physicochemical potential for the development of liquid membranes designed to trap nitrogen (Matsumoto *et al*. 2012). Typically used as a food thickening agent, BC is high in fiber, making it an ideal dietary supplement. Incompatible with the human digestive tract, Japanese based companies have begun to supplement dietary drinks with BC (Chawla *et al*. 2009).

Medical

In recent years, BC has gained recognition from the medical industry for its unique ability to co-exist with the human body without invoking an immunological response (Helenius *et al*. 2005). BC was first used in a clinical setting as a skin substitute for burn

victims. Serving as a protective barrier against opportunistic pathogens, the highly porous nature of BC allows for the easy transfusion of antibiotics and other antimicrobial compounds into severe wounds (Maneerung *et al*. 2008). In parallel, BC was investigated for the development of a gel based wound dressing, leading to the production of Bioprocess ® and Gengiflex ® dressings for extensive wounds (Helenius *et al*. 2005; Johnson and Neogi 1989). Presently BC is being investigated for the development of scaffolding seeded with epithelial cells for faster and more efficient skin regeneration (Fu *et al*. 2012). On a macromolecular scale, BC fabricated artificial blood vessels and heart valves are currently being evaluated in animal studies (Malm *et al*. 2012). Due to the supportive role of cellulose in plant cell walls, BC is being investigated as cartilage replacement (Costa *et al*. 2012). Composites consisting of BC fibers demonstrated superior porosity compared to plastic and alginate based substitutes. Like the epithelial model discussed previously, BC derived cartilage provides the opportunity for host cell seeding. A BC based mold can function as scaffolding for the eventual regeneration of host cartilage (Azuma *et al*. 2006; Svensson *et al*. 2005). Currently, the chemical modification of BC to function as a drug delivery mechanism is an active area of BC medical research (Dugan *et al*. 2013; Trovatti *et al*. 2012).

1.10 Concluding remarks

The industrial and commercial versatility of BC attest to the polymer's economic potential on a global scale. Given the increasing number of BC applications in medical, food and biotechnology related industries, the development of a novel lignocellulosic saccharifcation

scheme that allows for the efficient production of BC from low value by-products is warranted and could positively contribute to the development of a global economy free of fossil fuels

1.11 References

Ajanovic,A., Jungmeier,G., Beermann,M. and Haas,R. (2012) The Long-Term Prospects of Biofuels in the EU-15 Countries. *Energies* **5**, 3110-3125.

Amikam,D. and Galperin,M.Y. (2006) PilZ domain is part of the bacterial c-di-GMP binding protein. *Bioinformatics* **22**, 3-6.

Atalla,R.H. and Vanderhart,D.L. (1984) Native cellulose: a composite of two distinct crystalline forms. *Science (New York, NY)* **223**, 283.

Azuma,C., Yasuda,K., Tanabe,Y., Taniguro,H., Kanaya,F., Nakayama,A., Chen,Y.M., Gong,J.P. and Osada,Y. (2006) Biodegradation of high-toughness double network hydrogels as potential materials for artificial cartilage. *Journal of Biomedical Materials Research Part A* **81**, 373-380.

Bae,S. and Shoda,M. (2004) Bacterial Cellulose Production by Fed Batch Fermentation in Molasses Medium. *Biotechnology progress* **20**, 1366-1371.

Bae,S., Sugano,Y. and Shoda,M. (2004) Improvement of bacterial cellulose production by addition of agar in a jar fermentor. *Journal of bioscience and bioengineering* **97**, 33-38.

Benziman,M. and Burger-Rachamimov,H. (1962) Synthesis of cellulose from pyruvate by succinate-grown cells of *Acetobacter xylinum*. *Journal of Bacteriology* **84**, 625-630.

Benziman,M., Haigler,C.H., Brown,M.R., White,A.R. and Cooper,K.M. (1980) Cellulose biogenesis: Polymerization and crystallization are coupled processes in *Acetobacter xylinum*. *Proceedings of the National Academy of Sciences* **77**, 6678-6682.

Benziman,M. and Mazover,A. (1973) Nicotinamide adenine dinucleotide-and nicotinamide adenine dinucleotide phosphate-specific glucose 6-phosphate dehydrogenases of *Acetobacter xylinum* and their role in the regulation of the pentose cycle. *Journal of Biological Chemistry* **248**, 1603-1608.

Benziman,M. and Rivetz,B. (1972) Factors Affecting Hexose Phosphorylation in *Acetobacter xylinum*. *Journal of Bacteriology* **111**, 325-333.

Bielecki,S., Krystynowicz,A., Turkiewicz,M. and Kalinowska,H. (2005) Bacterial cellulose. *Biopolymers Online*.

Blum,M., Gamper,H.A., Waldner,M., Sierotzki,H. and Gisi,U. (2012) The cellulose synthase 3 (CesA3) gene of oomycetes: structure, phylogeny and influence on sensitivity to carboxylic acid amide (CAA) fungicides. *Fungal Biology* **116**, 529-542.

Boyd,C.D. and O'Toole,G.A. (2012) Second Messenger Regulation of Biofilm Formation: Breakthroughs in Understanding c-di-GMP Effector Systems. Annual review of cell and developmental biology 28, 439-462.

Brown,A.J. (1886) XLIII.-On an acetic ferment which forms cellulose. *Journal of the Chemical Society, Transactions* **49**, 432-439.

Brown,M.R., Willison,J.H. and Richardson,C.L. (1976) Cellulose biosynthesis in *Acetobacter xylinum*: visualization of the site of synthesis and direct measurement of the in vivo process. *Proceedings of the National Academy of Sciences* **73**, 4565-4569.

Brown,M.R. and Saxena,I.M. (2000) Cellulose biosynthesis: A model for understanding the assembly of biopolymers. *Plant Physiology and Biochemistry* **38**, 57-67.

Bulone,V., Chanzy,H., Gay,L., Girard,V. and vre,M. (1992) Characterization of chitin and chitin synthase from the cellulosic cell wall fungus *Saprolegnia*. *Experimental Mycology* **16**, 8-21.

Cannon,R.E. and Anderson,S.M. (1991) Biogenesis of bacterial cellulose. *Critical Reviews in Microbiology* **17**, 435-447.

Chang,A.L., Tuckerman,J.R., Gonzalez,G., Mayer,R., Weinhouse,H., Volman,G., Amikam,D., Benziman,M. and Gilles-Gonzalez,M.A. (2001) Phosphodiesterase A1, a Regulator of Cellulose Synthesis in *Acetobacter xylinum*, Is a Heme-Based Sensor. *Biochemistry* **40**, 3420-3426.

Chao,Y., Ishida,T., Sugano,Y. and Shoda,M. (2000) Bacterial cellulose production by *Acetobacter xylinum* in a 50 mL internal loop airlift reactor. Biotechnology and bioengineering **68**, 345-352.

Chawla,P.R., Bajaj,I.B., Survase,S.A. and Singhal,R.S. (2009) Microbial cellulose: fermentative production and applications. *Food Technology and Biotechnology* **47**, 107-124.

Cheng,K.C., Catchmark,J.M. and Demirci,A. (2011) Effects of CMC Addition on Bacterial Cellulose Production in a Biofilm Reactor and Its Paper Sheets Analysis. *Biomacromolecules* **12**, 730-736.

Christen,M., Christen,B., Folcher,M., Schauerte,A. and Jenal,U. (2005) Identification and Characterization of a Cyclic di-GMP-specific Phosphodiesterase and Its Allosteric Control by GTP. *Journal of Biological Chemistry* **280**, 30829-30837.

Colvin,J.R. (1957) Formation of cellulose microfibrils in a homogenate of *Acetobacter xylinum*. *Archives of biochemistry and biophysics* **70**, 294.

Costa,L.M.M., Olyveira,G.M.d., Basmaji,P., Valido,D.P., Gois,P.B.P., Junior,R.L.A.C. and Lauro Filho,X. (2012) Novel Otoliths/Bacterial Cellulose Nanocomposites as a Potential Natural Product for Direct Dental Pulp Capping. *Journal of Biomaterials and Tissue Engineering* **2**, 48-53.

Costerton,J.W., Stewart,P.S. and Greenberg,E.P. (1999) Bacterial Biofilms: A Common Cause of Persistent Infections. *Science* **284**, 1318-1322.

Czaja,W., Romanovicz,D. and Brown,M.R. (2004) Structural investigations of microbial cellulose produced in stationary and agitated culture. *Cellulose* **11**, 403-411.

De Iannino,N.I.o., Couso,R.O. and Dankert,M.A. (1988) Lipid-linked intermediates and the synthesis of acetan in *Acetobacter xylinum*. *Journal of General Microbiology* **134**, 1731-1736.

De Wulf,P., Joris,K. and Vandamme,E.J. (1999) Improved cellulose formation by an *Acetobacter xylinum* mutant limited in (keto) gluconate synthesis. *Journal of chemical technology and biotechnology* **67**, 376-380.

Douwes,J., van der Sluis,B., Doekes,G., van Leusden,F., Wijnands,L., van Strien,R., Verhoeff,A. and Brunekreef,B. (1999) Fungal extracellular polysaccharides in house dust as a marker for exposure to fungi: Relations with culturable fungi, reported home dampness, and respiratory symptoms. *Journal of Allergy and Clinical Immunology* **103**, 494-500.

Dugan,J.M., Gough,J.E. and Eichhorn,S.J. (2013) Bacterial cellulose scaffolds and cellulose nanowhiskers for tissue engineering. *Nanomedicine* **8**, 287-298.

Embuscado,M.E., Marks,J.S. and BeMiller,J.N. (1994) Bacterial cellulose. I. Factors affecting the production of cellulose by *Acetobacter xylinum*. *Food Hydrocolloids* **8**, 407-418.

Flemming,H.C., Neu,T.R. and Wozniak,D.J. (2007) The EPS Matrix: The House of Biofilm Cells. *Journal of Bacteriology* **189**, 7945-7947.

Fu,L., Zhang,Y., Li,C., Wu,Z., Zhuo,Q., Huang,X., Qiu,G., Zhou,P. and Yang,G. (2012) Skin tissue repair materials from bacterial cellulose by a multilayer fermentation method. *Journal of Materials Chemistry*.

Fujiwara,T., Komoda,K., Sakurai,N., Tajima,K., Tanaka,I. and Yao,M. (2013) The c-di-GMP recognition mechanism of the PilZ domain of bacterial cellulose synthase subunit A. *Biochemical and Biophysical Research Communications*.

George,J., Ramana,K.V., Sabapathy,S.N. and Bawa,A.S. (2005) Physico-mechanical properties of chemically treated bacterial (*Acetobacter xylinum*) cellulose membrane. *World Journal of Microbiology and Biotechnology* **21**, 1323-1327.

Glaser,L. (1958) The synthesis of cellulose in cell-free extracts of *Acetobacter xylinum*. *Journal of Biological Chemistry* **232**, 627-636.

Greathouse,G.A. (1957) Isolation of a cell-free enzyme system from Acetobacter xylinum capable of cellulose synthesis. *Journal of the American Chemical Society* **79**, 4503-4504.

Gromet,Z., Schramm,M. and Hestrin,S. (1957) Synthesis of cellulose by *Acetobacter xylinum*. 4. Enzyme systems present in a crude extract of glucose-grown cells. *Biochemical Journal* **67**, 679.

Ha,J.H., Shah,N., Ul-Islam,M., Khan,T. and Park,J.K. (2011) Bacterial cellulose production

from a single sugar alpha-linked glucuronic acid-based oligosaccharide. *Process Biochemistry* **46**, 1717-1723.

Habibi,Y., Lucia,L.A. and Rojas,O.J. (2010) Cellulose nanocrystals: chemistry, self-assembly, and applications. *Chemical reviews* **110**, 3479.

Haigler, C. H. (1985) The functions and biogenesis of native cellulose. In *Cellulose chemistry and its applications* pp. 31-83. Ellis Horwood Limited.

Hall-Stoodley,L., Costerton,J.W. and Stoodley,P. (2004) Bacterial Biofilms: from the natural environment to infectious diseases. *Nature Reviews: Microbiology* **2**, 95.

Helenius,G., Backdhal,H., Bodin,A., Nannmark,U., Gatenholm,P. and Risberg,B. (2005) In vivo biocompatibility of bacterial cellulose. *Journal of Biomedical Materials Research Part A* **76**, 431-438.

Hestrin,S. and Schramm,M. (1954) Synthesis of cellulose by *Acetobacter xylinum*. 2. Preparation of freeze-dried cells capable of polymerizing glucose to cellulose. *Biochemical Journal* **58**, 345.

Hu,S.Q., Gao,Y.G., Tajima,K., Sunagawa,N., Zhou,Y., Kawano,S., Fujiwara,T., Yoda,T., Shimura,D. and Satoh,Y. (2010) Structure of bacterial cellulose synthase subunit D octamer with four inner passageways. *Proceedings of the National Academy of Sciences* **107**, 17957-17961.

Huang,Y. and Chen,Y.M. (2013) An Overview of Fermentation Production and Application of Bacterial Cellulose. *Advanced Materials Research* **627**, 878-884.

Hwang,J.W., Yang,Y.K., Hwang,J.K., Pyun,Y.R. and Kim,Y.S. (1999) Effects of pH and dissolved oxygen on cellulose production by Acetobacter xylinum BRC5 in agitated culture. *Journal of bioscience and bioengineering* **88**, 183-188.

Iguchi,M., Yamanaka,S. and Budhiono,A. (2000) Bacterial cellulose: A masterpiece of nature's arts. *Journal of Materials Science* **35**, 261-270.

Ishihara,M., Matsunaga,M., Hayashi,N. and Tiler,V. (2002) Utilization of d-xylose as carbon source for production of bacterial cellulose. *Enzyme and Microbial Technology* **31**, 986-991.

Iyer,P.R., Geib,S.M., Catchmark,J., Kao,T.h. and Tien,M. (2010) Genome sequence of a cellulose-producing bacterium, *Gluconacetobacter hansenii* ATCC 23769. *Journal of Bacteriology* **192**, 4256.

Iyer,P.R., Liu,Y.A., Deng,Y., McManus,J.B., Kao,T.h. and Tien,M. (2013) Processing of cellulose synthase (AcsAB) from *Gluconacetobacter hansenii* 23769. *Archives of biochemistry and biophysics* **529**, 92-98.

Johnson, D. C. and Neogi, A. N. (1989) Sheeted products formed from reticulated microbial cellulose. Google Patents.

Jonas,R. and Farah,L.F. (1998) Production and application of microbial cellulose. *Polymer Degradation and Stability* **59**, 101-106.

Jugdaohsingh,R., Campbell,M.M., Thompson,R.P.H., McCrohan,C.R., White,K.N. and Powell,J.J. (1998) Mucus Secretion by the Freshwater Snail Lymnaea stagnalis Limits Aluminum Concentrations of the Aqueous Environment. *Environmental Science & Technology* **32**, 2591-2595.

Jung,J.Y., Park,J.K. and Chang,H.N. (2005) Bacterial cellulose production by *Gluconacetobacter hansenii* in an agitated culture without living non-cellulose producing cells. *Enzyme and Microbial Technology* **37**, 347-354.

Keshk,S. and Sameshima,K. (2006a) Influence of lignosulfonate on crystal structure and productivity of bacterial cellulose in a static culture. *Enzyme and Microbial Technology* **40**, 4-8.

Keshk,S. and Sameshima,K. (2006b) The utilization of sugar cane molasses with/without the presence of lignosulfonate for the production of bacterial cellulose. *Applied Microbiology and Biotechnology* **72**, 291-296.

Kim,S., Li,H., Oh,I., Kee,C. and Kim,M. (2012) Effect of viscosity-inducing factors on oxygen transfer in production culture of bacterial cellulose. *Korean J. Chem. Eng.* **29**, 792-797.

Kim,Y.J., Kim,J.N., Wee,Y.J., Park,D.H. and Ryu,H.W. (2007) Bacterial cellulose production by *Gluconacetobacter sp.* PKY5 in a rotary biofilm contactor. *Applied biochemistry and biotechnology* **137**, 529-537.

Kim, S. Y., Kim, J. N., Wee, Y. J., Park, D. H. and Ryu, H. W. (2006) Production of bacterial cellulose by *Gluconacetobacter sp. RKY5* isolated from persimmon vinegar. pp. 705-715. *Springer*.

Klemm,D., Heublein,B., Fink,H.P. and Bohn,A. (2005) Cellulose: Fascinating Biopolymer and Sustainable Raw Material. *Angewandte Chemie International Edition* **44**, 3358-3393.

Kloareg,B. and Quatrano,R.S. (1988) Structure of the cell walls of marine algae and ecophysiological functions of the matrix polysaccharides. *Oceanography and Marine Biology: An Annual Review* **26**, 259-315.

Kongruang,S. (2008) Bacterial cellulose production by *Acetobacter xylinum* strains from agricultural waste products. *Applied biochemistry and biotechnology* **148**, 245-256.

Krystynowicz,A., Czaja,W., Wiktorowska-Jezierska,A., Goncalves-Miskiewicz,M., Turkiewicz,M. and Bielecki,S. (2002) Factors affecting the yield and properties of bacterial cellulose. *Journal of Industrial Microbiology and Biotechnology* **29**, 189-195.

Kudlicka,K. and Brown Jr,R.M. (1997) Cellulose and callose biosynthesis in higher plants (I. Solubilization and separation of (1-> 3)-and (1-> 4)-[beta]-glucan synthase activities from mung bean). *Plant Physiology* **115**, 643-656.

Kuo,C.H. and Lee,C.K. (2009) Enhancement of enzymatic saccharification of cellulose by cellulose dissolution pretreatments. *Carbohydrate Polymers* **77**, 41-46.

Kurosumi,A., Sasaki,C., Yamashita,Y. and Nakamura,Y. (2009) Utilization of various fruit juices as carbon source for production of bacterial cellulose by *Acetobacter xylinum* NBRC 13693. *Carbohydrate Polymers* **76**, 333-335.

Li,Y., Tian,C., Tian,H., Zhang,J., He,X., Ping,W. and Lei,H. (2012) Improvement of bacterial cellulose production by manipulating the metabolic pathways in which ethanol and sodium citrate involved. *Applied Microbiology and Biotechnology* 1-9.

Lin,F.C., Brown Jr,R.M., Cooper,J.B. and Delmer,D.P. (1985) Synthesis of fibrils in vitro by a solubilized cellulose synthase from *Acetobacter xylinum*. *Science(Washington)* **230**, 822-825.

Lin,F.C., Brown Jr,R.M., Drake Jr,R. and Haley,B.E. (1990) Identification of the uridine 5'-diphosphoglucose (UDP-Glc) binding subunit of cellulose synthase in *Acetobacter xylinum* using the photoaffinity probe 5-azido-UDP-Glc. *Journal of Biological Chemistry* **265**, 4782-4784.

Lin,Y. and Tanaka,S. (2006) Ethanol fermentation from biomass resources: current state and prospects. *Appl Microbiol Biotechnol* **69**, 627-642.

Lisdiyanti,P., Navarro,R.R., Uchimura,T. and Komagata,K. (2006) Reclassification of Gluconacetobacter hansenii strains and proposals of *Gluconacetobacter saccharivorans* sp. nov. and *Gluconacetobacter nataicola* sp. nov. *International journal of systematic and evolutionary microbiology* **56**, 2101-2111.

Lüaskiewicz,B. (1998) Solubility of bacterial cellulose and its structural properties. *Journal of applied polymer science* **67**, 1871-1876.

Malm,C.J., Risberg,B., Bodin,A., Backdahl,H., Johansson,B.R., Gatenholm,P. and Jeppsson,A. (2012) Small calibre biosynthetic bacterial cellulose blood vessels: 13-months patency in a sheep model. *Scandinavian Cardiovascular Journal* **46**, 57-62.

Maneerung,T., Tokura,S. and Rujiravanit,R. (2008) Impregnation of silver nanoparticles into bacterial cellulose for antimicrobial wound dressing. *Carbohydrate Polymers* **72**, 43-51.

Margeot,A., Hahn-Hagerdal,B., Edlund,M., Slade,R. and Monot,F.d.r. (2009) New improvements for lignocellulosic ethanol. *Current Opinion in Biotechnology* **20**, 372-380.

Masaoka,S., Ohe,T. and Sakota,N. (1993) Production of cellulose from glucose by *Acetobacter xylinum*. *Journal of Fermentation and Bioengineering* **75**, 18-22.

Matsumoto,M., Yamamoto,M. and Kondo,K. (2012) Use of Bacterial Cellulose from Nata de Coco as Base Polymer for Liquid Membranes Containing Ionic Liquids. *Australian Journal of Chemistry*.

Maunu,S., Liitia,T., Kauliomaki,S., Hortling,B. and Sundquist,J. (2000) 13C CPMAS NMR investigations of cellulose polymorphs in different pulps. *Cellulose* **7**, 147-159.

Mayer,R., Ross,P., Weinhouse,H., Amikam,D., Volman,G., Ohana,P., Calhoon,R.D., Wong,H.C., Emerick,A.W. and Benziman,M. (1991) Polypeptide composition of bacterial cyclic diguanylic acid-dependent cellulose synthase and the occurrence of immunologically crossreacting proteins in higher plants. *Proceedings of the National Academy of Sciences* **88**, 5472-5476.

McNeil,M., Darvill,A.G., Fry,S.C. and Albersheim,P. (1984) Structure and Function of the Primary Cell Walls of Plants. *Annual Review of Biochemistry* **53**, 625-663.

Mikkelsen,D., Flanagan,B.M., Dykes,G.A. and Gidley,M.J. (2009) Influence of different carbon sources on bacterial cellulose production by *Gluconacetobacter xylinus* strain ATCC 53524. *Journal of Applied Microbiology* **107**, 576-583.

Mills,E., Pultz,I.S., Kulasekara,H.D. and Miller,S.I. (2011) The bacterial second messenger cyclic-di-GMP: mechanisms of signalling. *Cellular microbiology* **13**, 1122-1129.

Mohite,B.V., Kamalja,K.K. and Patil,S.V. (2012) Statistical optimization of culture conditions for enhanced bacterial cellulose production by *Gluconoacetobacter hansenii* NCIM 2529. *Cellulose* 1-12.

Morgan,J.L., Strumillo,J. and Zimmer,J. (2012) Crystallographic snapshot of cellulose synthesis and membrane translocation. *Nature*.

Nakagaito,A.N., Iwamoto,S. and Yano,H. (2005) Bacterial cellulose: the ultimate nano-scalar cellulose morphology for the production of high-strength composites. *Applied Physics A: Materials Science & Processing* **80**, 93-97.

Nakagaito,A.N. and Yano,H. (2008) The effect of fiber content on the mechanical and thermal expansion properties of biocomposites based on microfibrillated cellulose. *Cellulose* **15**, 555-559.

Nakai,T., Moriya,A., Tonouchi,N., Tsuchida,T., Yoshinaga,F., Horinouchi,S., Sone,Y., Mori,H., Sakai,F. and Hayashi,T. (1998) Control of expression by the cellulose synthase bcsA promoter region from *Acetobacter xylinum* BPR 2001. *Gene* **213**, 93-100.

Nakai,T., Tonouchi,N., Konishi,T., Kojima,Y., Tsuchida,T., Yoshinaga,F., Sakai,F. and Hayashi,T. (1999) Enhancement of cellulose production by expression of sucrose synthase in *Acetobacter xylinum*. *Proceedings of the National Academy of Sciences* **96**, 14-18.

Nishi,Y., Uryu,M., Yamanaka,S., Watanabe,K., Kitamura,N., Iguchi,M. and Mitsuhashi,S. (1990) The structure and mechanical properties of sheets prepared from bacterial cellulose. *Journal of Materials Science* **25**, 2997-3001.

Nishiyama,Y., Langan,P. and Chanzy,H. (2002) Crystal structure and hydrogen-bonding system in cellulose Iβ from synchrotron X-ray and neutron fiber diffraction. *Journal of the*

American Chemical Society **124**, 9074-9082.

Nishiyama,Y., Sugiyama,J., Chanzy,H. and Langan,P. (2003) Crystal structure and hydrogen bonding system in cellulose Iα from synchrotron X-ray and neutron fiber diffraction. *J Am Chem Soc* **125**, 14300-14306.

Noro,N., Sugano,Y. and Shoda,M.A.K.O. (2004) Utilization of the buffering capacity of corn steep liquor in bacterial cellulose production by *Acetobacter xylinum*. *Applied Microbiology and Biotechnology* **64**, 199-205.

Norouzian,D., Farhangi,A., Tolooei,S., Saffari,Z., Mehrabi,M.R., Chiani,M., Ghassemi,S., Farahnak,M. and Akbarzadeh,A. (2011) Study of nano-fiber cellulose production by *Glucanacetobacter xylinum* ATCC 10245. *Pakistan Journal of Biological Sciences: PJBS* **14**, 780-784.

Nguyen,V.T., Flanagan,B., Gidley,M.J. and Dykes,G.A. (2008) Characterization of cellulose production by a *Gluconacetobacter xylinus* strain from Kombucha. Current microbiology **57**, 449-453.

O'sullivan,A.C. (1997) Cellulose: the structure slowly unravels. *Cellulose* **4**, 173-207.

Orts,W.J., Shey,J., Imam,S.H., Glenn,G.M., Guttman,M.E. and Revol,J.F. (2005) Application of cellulose microfibrils in polymer nanocomposites. *Journal of Polymers and the Environment* **13**, 301-306.

Park,J., Jung,J. and Park,Y. (2003a) Cellulose production by *Gluconacetobacter hansenii* in a medium containing ethanol. *Biotechnology Letters* **25**, 2055-2059.

Park,J., Park,Y. and Jung,J. (2003b) Production of bacterial cellulose by *Gluconacetobacter hansenii* PJK isolated from rotten apple. Biotechnol Bioproc E **8**, 83-88.

Park,M., Park,S. and Hyun,J. (2012) Use of magnetic nanoparticles to manipulate the metabolic environment of bacteria for controlled biopolymer synthesis. *ACS applied materials & interfaces* **4**, 5114-5117.

Park,S., Baker,J.O., Himmel,M.E., Parilla,P.A. and Johnson,D.K. (2010) Research cellulose crystallinity index: measurement techniques and their impact on interpreting cellulase performance.

Ramana,K.V., Tomar,A. and Singh,L. (2000) Effect of various carbon and nitrogen sources on cellulose synthesis by *Acetobacter xylinum*. *World Journal of Microbiology and Biotechnology* **16**, 245-248.

Ross,P., Weinhouse,H., Aloni,Y., Michaeli,D., Weinberger-Ohana,P., Mayer,R., Braun,S., De Vroom,E., Van der Marel,G.A. and Van Boom,J.H. (1987) Regulation of cellulose synthesis in *Acetobacter xylinum* by cyclic diguanylic acid.

Ross,P., Mayer,R. and Benziman,M. (1991) Cellulose biosynthesis and function in bacteria.

Microbiological Reviews **55**, 35-58.

Sanchez,O.J. and Cardona,C.A. (2008) Trends in biotechnological production of fuel ethanol from different feedstocks. *Bioresource Technology* **99**, 5270-5295.

Sano,M.B., Rojas,A.D., Gatenholm,P. and Davalos,R.V. (2010) Electromagnetically controlled biological assembly of aligned bacterial cellulose nanofibers. *Annals of biomedical engineering* **38**, 2475-2484.

Sarkar,N., Ghosh,S.K., Bannerjee,S. and Aikat,K. (2012) Bioethanol production from agricultural wastes: An overview. *Renewable Energy* **37**, 19-27.

Saxena,I.M. and Brown,R.M. (1995) Identification of a second cellulose synthase gene (acsAII) in *Acetobacter xylinum*. *Journal of Bacteriology* **177**, 5276-5283.

Saxena,I., Kudlicka,K., Okuda,K. and Brown Jr,R.M. (1994) Characterization of genes in the cellulose-synthesizing operon (acs operon) of *Acetobacter xylinum*: implications for cellulose crystallization. *Journal of Bacteriology* **176**, 5735.

Saxena,I.M. and Brown Jr,R.M. (2000) Cellulose synthases and related enzymes. *Current opinion in plant biology* **3**, 523-531.

Saxena,I.M., Brown Jr,R.M., Fevre,M., Geremia,R.A. and Henrissat,B. (1995) Multidomain architecture of beta-glycosyl transferases: implications for mechanism of action. *Journal of Bacteriology* **177**, 1419.

Saxena,M.I. and Brown,R.M. (2005) Cellulose Biosynthesis: Current Views and Evolving Concepts. *Annals of Botany* **96**, 9-21.

Schramm,M., Gromet,Z. and Hestrin,S. (1957) Synthesis of cellulose by *Acetobacter xylinum*. 3. Substrates and inhibitors. *Biochemical Journal* **67**, 669.

Schramm,M. and Hestrin,S. (1954) Factors affecting Production of Cellulose at the Air/ Liquid Interface of a Culture of *Acetobacter xylinum*. *Journal of General Microbiology* **11**, 123-129.

Schrecker,S.T. and Gostomski,P.A. (2005) Determining the water holding capacity of microbial cellulose. *Biotechnology Letters* **27**, 1435-1438.

Seto,A., Saito,Y., Matsushige,M., Kobayashi,H., Sasaki,Y., Tonouchi,N., Tsuchida,T., Yoshinaga,F., Ueda,K. and Beppu,T. (2006) Effective cellulose production by a coculture of *Gluconacetobacter xylinus* and *Lactobacillus mali. Applied Microbiology and Biotechnology* **73**, 915-921.

Sharma,N., Prasad,G.S. and Choudhury,A.R. (2012) Utilization of corn steep liquor for biosynthesis of pullulan, an important exopolysaccharide. *Carbohydrate Polymers*.

Shoda,M. and Sugano,Y. (2005) Recent advances in bacterial cellulose production.

Biotechnol. Bioprocess Eng. **10**, 1-8.

Singh,A., Pant,D., Korres,N.E., Nizami,A.S., Prasad,S. and Murphy,J.D. (2010) Key issues in life cycle assessment of ethanol production from lignocellulosic biomass: Challenges and perspectives. *Bioresource Technology* **101**, 5003-5012.

Siro,I. and Plackett,D. (2010) Microfibrillated cellulose and new nanocomposite materials: a review. *Cellulose* **17**, 459-494.

Son,H.J., Kim,H.G., Kim,K.K., Kim,H.S., Kim,Y.G. and Lee,S.J. (2001) Optimization of fermentation conditions for the production of bacterial cellulose by a newly isolated Acetobacter. *Biotechnology and applied biochemistry* **33**, 1-5.

Son,H.J., Kim,H.G., Kim,K.K., Kim,H.S., Kim,Y.G. and Lee,S.J. (2003) Increased production of bacterial cellulose by *Acetobacter* sp. V6 in synthetic media under shaking culture conditions. *Bioresource Technology* **86**, 215-219.

Sureshkumar,M., Siswanto,D.Y. and Lee,C.K. (2010) Magnetic antimicrobial nanocomposite based on bacterial cellulose and silver nanoparticles. *J. Mater. Chem.* **20**, 6948-6955.

Sutherland,I.W. (1998) Novel and established applications of microbial polysaccharides. *Trends in Biotechnology* **16**, 41-46.

Svensson,A., Nicklasson,E., Harrah,T., Panilaitis,B., Kaplan,D.L., Brittberg,M. and Gatenholm,P. (2005) Bacterial cellulose as a potential scaffold for tissue engineering of cartilage. *Biomaterials* **26**, 419-431.

Swissa,M. and Benziman,M.O.S.H. (1976) Factors affecting the activity of citrate synthase of *Acetobacter xylinum* and its possible regulatory role. *Biochemical Journal* **153**, 173.

Tanskul,S., Amornthatree,K. and Jaturonlak,N. (2013) A new cellulose-producing bacterium, Rhodococcus sp. MI 2: Screening and optimization of culture conditions. *Carbohydrate Polymers* **92**, 421-428.

Tantratian,S., Tammarate,P., Krusong,W., Bhattarakosol,P. and Phunsri,A. (2005) Effect of dissolved oxygen on cellulose production by *Acetobacter* sp. *J. Sci. Res. Chula Univ* **30**, 179-186.

Tengerdy,R.P. and Szakacs,G. (2003) Bioconversion of lignocellulose in solid substrate fermentation. *Biochemical Engineering Journal* **13**, 169-179.

Teramoto,Y., Lee,S.H. and Endo,T. (2008) Pretreatment of woody and herbaceous biomass for enzymatic saccharification using sulfuric acid-free ethanol cooking. *Bioresource Technology* **99**, 8856-8863.

Tokoh,C., Takabe,K. and Fujita,M. (2002) Cellulose synthesized by *Acetobacter xylinum* in the presence of plant cell wall polysaccharides. *Cellulose* **9**, 65-74.

Toyosaki,H., Naritomi,T., Seto,A., Matsuoka,M., Da,T. and Yoshinaga,F. (1995) Screening of Bacterial Cellulose-producing *Acetobacter* Strains Suitable for Agitated. Biosci. *Biotech. Biochem* **59**, l498-l502.

Trovatti,E., Freire,C.S., Pinto,P.C., Almeida,I.F., Costa,P., Silvestre,A.J., Neto,C.P. and Rosado,C. (2012) Bacterial cellulose membranes applied in topical and transdermal delivery of lidocaine hydrochloride and ibuprofen: In vitro diffusion studies. *International Journal of Pharmaceutics*.

Tuckerman,J.R., Gonzalez,G., Sousa,E.H.S., Wan,X., Saito,J.A., Alam,M. and Gilles-Gonzalez,M.A. (2009) An Oxygen-Sensing Diguanylate Cyclase and Phosphodiesterase Couple for c-di-GMP Control. *Biochemistry* **48**, 9764-9774.

Ul-Islam,M., Ha,J.H., Khan,T. and Park,J.K. (2013) Effects of glucuronic acid oligomers on the production, structure and properties of bacterial cellulose. *Carbohydrate Polymers* **92**, 360-366.

Ummartyotin,S., Juntaro,J., Sain,M. and Manuspiya,H. (2012) Development of transparent bacterial cellulose nanocomposite film as substrate for flexible organic light emitting diode (OLED) display. *Industrial Crops and Products* **35**, 92-97.

Valla,S. and Kjosbakken,J. (1981) Isolation and characterization of a new extracellular polysaccharide from a cellulose-negative strain of *Acetobacter xylinum*. *Canadian Journal of Microbiology* **27**, 599-603.

Valla,S. and Kjosbakken,J. (1982) Cellulose-negative mutants of *Acetobacter xylinum*. *Journal of General Microbiology* **128**, 1401-1408.

Vandamme,E.J., De Baets,S., Vanbaelen,A., Joris,K. and De Wulf,P. (1998) Improved production of bacterial cellulose and its application potential. *Polymer Degradation and Stability* **59**, 93-99.

Vanderhart,D.L. and Atalla,R.H. (1984) Studies of microstructure in native celluloses using solid-state carbon-13 NMR. *Macromolecules* **17**, 1465-1472.

Watanabe,K., Tabuchi,M., Morinaga,Y. and Yoshinaga,F. (1998) Structural Features and Properties of Bacterial Cellulose Produced in Agitated Culture. *Cellulose* **5**, 187-200.

Weinhouse,H.A.I.M. and Benziman,M.O.S.H. (1976) Phosphorylation of glycerol and dihydroxyacetone in *Acetobacter xylinum* and its possible regulatory role. *Journal of Bacteriology* **127**, 747-754.

Weinhouse,H. and Benziman,M. (1972) Regulation of gluconeogenesis in *Acetobacter xylinum*. *European Journal of Biochemistry* **28**, 83-88.

Weinhouse,H. and Benziman,M. (1974) Regulation of hexose phosphate metabolism in *Acetobacter xylinum*. *Biochemical Journal* **138**, 537.

White,A.R. and Brown,M.R. (1981) Enzymatic hydrolysis of cellulose: visual characterization of the process. *Proceedings of the National Academy of Sciences* **78**, 1047-1051.

Yamamoto,H., Horii,F. and Hirai,A. (1996) In situ crystallization of bacterial cellulose II. Influences of different polymeric additives on the formation of celluloses Iα and Iβ at the early stage of incubation. *Cellulose* **3**, 229-242.

Yamamoto,H., Horii,F. and Odani,H. (1989) Structural changes of native cellulose crystals induced by annealing in aqueous alkaline and acidic solutions at high temperatures. *Macromolecules* **22**, 4130-4132.

Yang,G., Xie,J., Hong,F., Cao,Z. and Yang,X. (2012) Antimicrobial activity of silver nanoparticle impregnated bacterial cellulose membrane: Effect of fermentation carbon sources of bacterial cellulose. *Carbohydrate Polymers* **87**, 839-845.

Yang,Y.K., Park,S.H., Hwang,J.W., Pyun,Y.R. and Kim,Y.S. (1998) Cellulose production by *Acetobacter xylinum* BRC5 under agitated condition. *Journal of Fermentation and Bioengineering* **85**, 312-317.

Zaar,K. (1979) Visualization of pores (export sites) correlated with cellulose production in the envelope of the gram-negative bacterium *Acetobacter xylinum*. *The Journal of cell biology* **80**, 773-777.

Zhou,L.L., Sun,D.P., Hu,L.Y., Li,Y.W. and Yang,J.Z. (2007) Effect of addition of sodium alginate on bacterial cellulose production by *Acetobacter xylinum*. *Journal of industrial microbiology & biotechnology* **34**, 483-489.

CHAPTER 2

Selecting high cellulose producing *Gluconacetobacter hansenii* strain ATCC 23769 phenotypes using antibiotic screening

William D. Graham,[1,2] Stephanie L. Mathews,[1,2] Christina Stolarchuk,[1]

Joel Pawlak,[2] and Amy M. Grunden[1,*], *Manuscript in preparation*

[1]Department of Microbiology, North Carolina State University, Raleigh NC 27695

[2]Department of Forest Biomaterials, North Carolina State University Raleigh NC 27695

Abstract

Aims: To demonstrate that the addition of antibiotics to wild type cultures of *Gluconacetobacter hansenii* strain ATCC 23769 is an effective method of selecting high cellulose producing phenotypes.

Methods and Results: A sample of *G. hansenii* strain 23769 was plated onto Schramm Hestrin media and examined by light microscopy for heterogeneity in colony morphology. Three colony sets displaying differences in size and texture were observed. To obtain homogeneity in colony morphology and in theory eliminate lower cellulose producing phenotypes, the aminoglycoside antibiotic kanamycin was added to the media. The addition of the kanamycin at a concentration of 50 μg ml^{-1} resulted in elimination of all colony morphotypes with the exception of high cellulose-producing morphotype 1 (CM1). To investigate the level of protection bacterial cellulose provides *G. hansenii* against antibiotics, CM1 cells were cultured in SH media containing 5% (v/v) cellulase and titrated with increasing concentrations of kanamycin. In cultures containing cellulase, a complete loss in kanamycin resistance was observed.

Conclusions: The treatment of wild type *G. hansenii* 23769 cultures with the aminoglycoside, kanamycin, is an effective method for selecting higher cellulose yield phenotypes.

Significance and Impact of Study: The results from our study suggest the existence of an uncharacterized mechanism for the regulation of cellulose synthesis by *G. hansenii* in response to antimicrobial stimuli.

2.1 Introduction

The current fragile state of global economics as a consequence of diminishing natural resources has led to renewed interest in cellulose related research. The development of an efficient process for converting cellulose into fermentable sugars is a vital component for the advancement of a global economy that is not dependent on fossil fuels. This international initiative has led to innovative developments such as carbon recycling and biofuel production (Kumar *et al*. 2009; Sims *et al*. 2010). Although promising, the effort to make cellulosic biomass commercially viable on a global scale is hindered by the inefficiencies associated with cellulose liberation and saccharification (Chandel *et al*. 2011; McKendry 2002a; McKendry 2002b). A novel path for enhancing the economic viability of cellulose processing is the exploitation of bacteria that can produce cellulose from five carbon sugars, like xylose, which are low value by-products of lignocellulosic conversion (Ishihara *et al*. 2002). Although chemically identical to plant based cellulose, the properties of bacterial cellulose (BC) are unique, exhibiting greater mechanical strength, higher water holding ability and increased crystallinity (Yamanaka *et al*. 1989). Synthesized independent of hemicellulose and lignin, the ultra-pure network of BC make it ideal for biomedical, biosensor, industrial and food applications (Czaja *et al*. 2006; Ignatov *et al*. 2001; Klemm *et al*. 2005). Extensive research has been performed on a number of cellulose producing bacteria investigating the up-regulation of cellulose production as a result of genetic modification and metabolic manipulation (Desvaux *et al*. 2001; Li *et al*. 2012). Strains of *Gluconacetobacter hansenii* (*G. hansenii*) are the most widely used as a consequence of their ability to synthesize cellulose from a variety of carbon substrates (Mikkelsen *et al*. 2009; Ramana *et al*. 2000). At present, these studies have been moderately successful,

producing genetic variants of *G. hansenii* capable of more efficient cellulose production (Chien *et al*. 2006; Li *et al*. 2012; Nakai *et al*. 1999). Despite these advancements, the biochemical solution for reducing the ratio of sugar consumed to cellulose produced has remained elusive, making the process extremely inefficient and economically unviable (Ashjaran *et al*. 2012; Ishihara *et al*. 2002). The cultivation of *G. hansenii* for optimal cellulose synthesis presents an additional challenge due to the spontaneous generation of cellulose negative phenotypes (Cel^-) which under agitated conditions can dominate a culture (Schramm and Hestrin 1954). In a study performed by Valla and Kjosbakken 1982 and later by Williams and Cannon *et al*. 1989, molecular analysis of *G. hansenii* Cel^- phenotypes revealed that the majority of the mutations observed did not reside in the structural genes of cellulose synthesis, because cellulose synthesis could be reinitiated through exposure to the antibiotic tetracycline (Valla and Kjosbakken 1982; Williams and Cannon 1989). These observations may indicate that cellulose synthesis by *G. hansenii* may be subject to a molecular switch that deserves further investigation (Ross *et al*. 1987). Aminoglycosides are a class of antibiotics that prevent dissociation and recycling of bacterial ribosomes by binding to 23s rRNA *in vivo* (Scheunemann *et al*. 2010). In an effort to identify additional mechanisms for enhanced cellulose production by *Gluconacetobacter hansenii* (*G. hansenii*) we investigated the influence of the aminoglycoside kanamycin on cellulose synthesis.

G. hansenii, formerly *Acetobacter xylinum*, is a well-characterized rod-shaped, gram negative cellulose-excreting bacterium (Lisdiyanti *et al*. 2006). A model organism for investigating bacterial polysaccharide synthesis and secretion, the complete genome sequence of *G. hansenii* strain 23769 was published in 2010, making the organism ideal for biochemical characterization and genetic manipulation (Iyer *et al*. 2010). The potential for *G. hansenii* to serve as a target for bioengineered improvements is promising; however, the

genetic modification of *G. hansenii* through molecular cloning is arduous and has proven to be problematic. Recombinant gene expression in *G. hansenii* is difficult to maintain at high efficiency as a result of the complexity associated with the organism's plasmid-chromosomal DNA interaction *in vivo* (Tonouchi *et al*. 1994; Valla *et al*. 1987). At present, researchers are able to avoid this complication by constructing shuttle vectors from native *G. hansenii* plasmids (Tonouchi *et al*. 1994; Wong *et al*. 1990). Shuttle vectors are expensive to design and are strain restricted (Fujiwara *et al.* 1992). As a consequence of these limiting factors, researchers are using the published genome with greater efficiency to characterize the gene expression patterns of *G. hansenii* during cellulose synthesis (Kongruang 2008; Mohite *et al*. 2012). More specifically, biochemical and physiological assays aimed at finding the optimal conditions for cellulose synthesis, have illuminated the expression pattern of the key metabolic enzyme pyruvate kinase, which helps moderate the flux of glucose into the cellulose synthesis pathway (Li *et al*. 2012). This approach to evaluating cellulose synthesis has led to a better understanding of how factors such as pH, oxygen availability, and carbon source can regulate cellulose synthesis on a metabolic level (Hutchens *et al*. 2007; Hwang *et al*. 1999; Krystynowicz *et al*. 2002). These findings are significant for the continual improvement of BC synthesis by *G. hansenii* with future implications of bioengineering *G. hansenii* to produce cellulose on an industrial scale.

Although *G. hansenii* can synthesize cellulose from a variety of carbon sources (Masaoka *et al*. 1993), the most efficient production of cellulose is achieved when glucose is used as the primary carbon source (Ramana *et al*. 2000). Different from other carbon sources, glucose can be shuttled directly into the cellulose synthesis pathway (Ross *et al*. 1991). The metabolism of glucose, however, results in the accumulation of gluconate and a concurrent decline in culture pH (Keshk and Sameshima 2006). Optimum cellulose

synthesis is achieved at a pH range of 4 – 5. When the culture pH falls below 4 as a consequence of gluconate accumulation, cellulose synthesis declines. Once all of the glucose in the media has been oxidized, the bacteria begin to metabolize the gluconate. A gradual increase in culture pH is observed as the bacteria consume the gluconate. Cellulose synthesis and cell division resume once the pH levels climb above 4 (Hwang *et al*. 1999). This pH trend is more evident under agitated conditions when oxygen levels in the media are high. Studies performed on cultures under agitation, where glucose is in excess, observed a more rapid decline in culture pH in addition to lower pH levels (Masaoka *et al*. 1993; Vandamme *et al*. 1998). In this study, we use culture pH determinations as a means of monitoring cellular metabolism.

The colony morphology of *G. hansenii* can present as small wrinkled colonies or larger smooth colonies (Haigler and Benziman 1982; Rashid *et al*. 2003). The variation in colony morphology is a direct result of extracellular cellulose synthesis (Meissner *et al*. 2007). The smaller colony variants extrude cellulose in a manner that promotes cellular aggregation giving rise to the wrinkled appearance. The larger colonies are phenotypically deficient in cellulose synthesis resulting in a smooth appearance (Cannon and Anderson 1991). Moderate cellulose producing colony phenotypes exhibit a hybrid appearance and are generally smooth but small in size (D'Argenio and Miller 2004). In this study, we refer to cellulose producing colonies that exhibit a wrinkled appearance as colony morphotype 1 (CM1), small smooth colonies that produce a moderate amount of cellulose are referred to as colony morphotype 2 (CM2), and cellulose negative cells that have a large smooth colony appearance are referred to as colony morphotype 3 (CM3) (Fig. 2-1).

Analogous to other biofilm associated bacteria, the synthesis and secretion of cellulose by *G. hansenii*, is tightly regulated by the second messenger molecule cyclic

diguanylate (cyclic di-GMP)(Borlee *et al*. 2010; Jenal and Malone 2006; Tal *et al*. 1998). The lack of cellulose production from smooth colony morphotypes suggests a deficiency in cyclic di-GMP signaling (Saxena *et al*. 1994; Strap *et al*. 2011a). This idea is further supported by the flat nature of cellulose deficient colonies compared to the raised structure

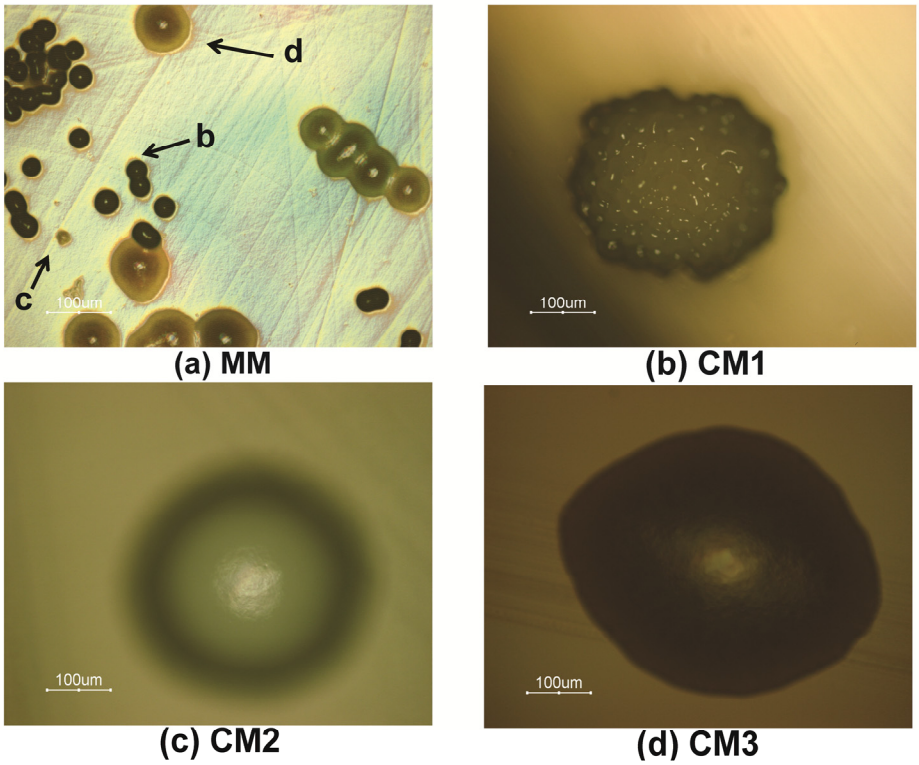

Figure 2-1 *G. hansenii* colony morphologies represented in ATCC 23769. All colonies were grown on SH media for 96 h and examined by light microscopy. (a) Wildtype ATCC 23769 containing a mixture of all three morphotypes (MM), (b) Colony morphotype 1 (CM1), (c) Colony morphotype 2 (CM2), (d) Colony morphotype 3 (CM3).

exhibited by the smaller wrinkled colonies. Early biochemical studies aimed at the characterization of cyclic di-GMP regulating proteins in *G. hansenii,* identified a family of surface bound proteins that contained heme-binding domains that function as oxygen

sensors (Chang *et al.* 2001). In the presence of oxygen, cellulose positive cells are able to aggregate in a manner that promotes maximum aeration (Hwang *et al*. 1999; Jenal and Malone 2006; Starkey *et al*. 2009). Extensive research on a variety of biofilm associated bacteria have identified cyclic di-GMP signaling as an essential component for cellular response to environmental stimuli (D'Argenio and Miller 2004). Furthermore, a review of more recent studies suggest that a correlation exists between the observed increase in *in vivo* cyclic di-GMP levels of isolated pathogenic bacteria and the significant rise in microbial resistance to common antibiotics (Hickman *et al*. 2005; Rogers *et al*. 2012).

Reminiscent of a biofilm, *G. hansenii* is encased in a polysaccharide matrix primarily composed of cellulose (Jung *et al*. 2005). In this study we examine the ability of cellulose to provide antimicrobial resistant properties to *G. hansenii* while highlighting a novel method of enriching *G. hansenii* cultures with cellulose producing phenotypes. We also explore the inefficient production of cellulose when Cel^- phenotypes are present under static conditions using a biological relevant cellulase assay that examines the percentage of cells associated with pellicle formation over a culture period.

2.2 Materials and methods

Bacterial strain and culture conditions

The strain of *Gluconacetobacter hansenii* that was used in this study was ATCC 23769 obtained from the American Type Culture Collection, Manassas, VA (ATCC). The dehydrated sample was aseptically reconstituted initially in 0.4 ml of Schramm and Hestrin media (SH) (Hestrin and Schramm 1954) then diluted into a total volume of 5 ml of SH media containing 20% glycerol (v/v) to establish a stock solution. A working stock was then

established by inoculating 0.5 ml of stock solution into 10 ml of SH media and incubating under static conditions for 96 h at 30°C. For this study the working stock containing the original cell suspension from ATCC 23769 was given the designation mixed morphotype culture (MM). From the MM stock a series of dilution plates were established using SH agar medium. After 96 h of incubation at 30°C, 10-fold serially diluted plates provided the highest resolution for colony morphology analysis by light microscopy. As observed in previous studies, three separate colony morphotypes were seen (Haigler 1982). For this study, these morphotypes were given the designation, colony morphotype 1 (CM1) (cellulose producing), colony morphotype 2 (CM2) (moderate cellulose producer) and colony morphotype 3 (CM3) (cellulose negative mutant). Each colony morphotype was then selected and inoculated into 5 ml of SH media and incubated at 30°C for 96 h under static conditions. These cultures were then used to generate stock plates for each colony morphotype. The stock plates were stored at 4°C to preserve bacteria and lower risk of contamination. The primary media used for this study was Schramm and Hestrin (SH) media. The media components of SH media are 0.12% citric acid, 2% glucose, 0.5% peptone, 0.27% sodium phosphate (dibasic), 0.5% yeast extract and 0.57% magnesium sulfate (Hestrin and Schramm 1954). The comparative analysis of cellulose production by CM1 morphotypes, as a result of media conditions, involved the use of Yamanaka medium (YM). The media components of YM media are 5% sucrose, 0.5% yeast extract, 0.5% ammonium sulfate, 0.3% potassium hydrogen sulfate, and 0.005% magnesium sulfate heptahydrate (Yamanaka *et al*. 1989). A modified version of YM media containing 1% (v/v) ethanol (YME) was also used in this study (Krystynowicz *et al*. 2002).

Initial antibiotic screening

The initial antibiotic screening was performed by plating each colony morphotype onto a plate containing the aminoglycoside kanamycin at a concentration of 50 μg ml^{-1}. The selection plates were incubated at 30°C for 96 h and colony growth assessed by visualization and light microscopy. Additionally, a liquid culture screen was also performed using only the MM stock to show this method is effective at screening cellulose negative phenotypes out of liquid based aliquots. The screen was done by inoculating 150 ml of SH media with 0.5 ml of MM working stock and incubating under static conditions for 96 h. The cells were then plated onto SH media and SH kanamycin media and incubated for 96 h at 30°C. The 10-fold dilution plates were assessed for colony growth and morphotype diversity by unaided visualization and later by light microscopy to confirm initial observations.

Cellulase culture antibiotic titration assay

To perform this assay the cellulase cocktail, CTec2 (Novozyme, Franklinton, NC); was mixed into sterile SH media at a concentration of 5% (v/v) to ensure complete cellulose digestion. The pH of the media was then adjusted to 5 and filter sterilized using a 0.22 micron filter (Corning, Corning, NY). Five ml volumes of filter sterilized 5% (v/v) cellulase media (5% cellulase media) were then aliquoted into 10 ml tubes. Kanamycin was then added to each tube at concentration of 0 μg ml^{-1}, 50 μg ml^{-1}, 100 μg ml^{-1}, 225 μg ml^{-1}, or 500 μg ml^{-1}. CM1 colonies were selected from the primary MM stock plate to ensure the experiment was performed with wild type colonies. The selected colonies were inoculated into the 10 ml tubes containing the 5% cellulase media. The average optical density at λ = 660 nm per ml of culture (OD_{660} ml^{-1}) post inoculation was 0.028 ± 0.017. In parallel, test tubes containing unaltered SH media were supplemented with kanamycin in identical concentrations and inoculated with CM1 cells isolated from MM primary stock plates. The

test tubes were incubated under static conditions for 72 h at 30°C. Bacterial growth was assessed by measuring the OD_{660} ml^{-1}. As controls, test tubes containing SH media and SH 5% cellulase media with no cells were also incubated for 72 h at 30°C and assessed by the OD_{660} ml^{-1} to confirm sterility of growth media and ensure no detectable background from cellulase mixture was observed. As a final control a series of tubes containing *Escherichia coli* strain BL21 were titrated with antibiotic to confirm potency of the antibiotic (data not shown).

Determination of cellulose production

Cellulose production as it relates to pellicle formation was assessed by harvesting the pellicle from the surface of the media and immersing it into a boiling solution of 1 mol l^{-1} NaOH for 30 min. The pellicle was then washed overnight in 255 mmol l^{-1} acetic acid to reduce the pH and remove residual media components. The pellicles were rinsed thoroughly in DiH_2O until the observed pH reached 7. The purified pellicles were then freeze dried and the yield of cellulose quantified by weight (g) (Klemm *et al*. 2001; Maneerung *et al*. 2012).

General growth curves

All growth curves were generated by inoculating 250 ml of media with 1 ml of primary inoculum at an OD_{660} of 0.19. The cultures were incubated at 30°C for a total of 288 h. A volume of 1 ml was removed from the cultures every 24 h to assess pH and bacterial growth by OD_{660}. The pH of the culture was measured using an Acument pH/eV benchtop meter (Fisher Scientific, Springfield, NJ). Static cultures were used in this study to assess the cellulose production of the different morphotypes; additionally relative growth comparisons

were made between the different morphotypes. The OD_{660} ml^{-1} of static cultures was obtained by swirling the flask vigorously to remove cells associated with the surface of the pellicle. Although this method does not account for the cells contained in pellicle biomass it provides a relative comparison between the cultures and has been the general method used in previous studies (Brown Jr and Kanda 2004; Jung *et al*. 2010; Masaoka *et al*. 1993). Cultures were inoculated with 0.5 ml of MM or CM1 stock grown with an OD_{660} ml^{-1} of 19 in 150 ml of SH media and grown under agitated conditions at 135 rpm.

In consideration of the extended growth period and larger volume of cells, the culture concentration of cellulase was adjusted to 1% (v/v) from the 5% (v/v) used previously. This was done to prevent the over accumulation of glucose in the media as a consequence of cellulose saccharification. Excess concentrations of glucose may result in below average pH values as a result of glucose oxidation (Masaoka *et al*. 1993; Nakai *et al*. 1999; Wu and Liu 2013). To develop the cellulase assay two culture methods were evaluated for their influence on the culture environment of CM1 cells. Agitated conditions were used to initially evaluate the two methods because a more accurate OD_{660} ml^{-1} could be obtained as a result of low cellulose production in addition to the enhanced metabolism of *G. hansenii* under aeration. The first method, which we refer to as the 1% cellulase media assay, involved the co-culturing of cellulase with CM1 cells. The filter sterilized 1% cellulase media was inoculated with 1 ml of CM1 cells at an OD_{660} of 0.19 per ml. These cultures were then incubated at 30°C for 288 h under agitated conditions. Bacterial growth and culture pH was assessed every 24 h. As a control, each experimental set included a flask with no inoculum to ensure the cell growth observed was not a result of media contamination and to ensure no detectable background from cellulase mixture was observed. The second method, which we refer to as the 1% cellulase time point assay, was performed by culturing CM1 cells in

SH media and at specific time points administering 1% (v/v) cellulase. A series of cultures containing 250 ml of SH media were inoculated with 1 ml of CM1 inoculum at a concentration of 0.19 OD_{660} ml^{-1}. The cultures were then incubated at 30°C under static or agitated conditions. At time points 96, 168 and 264 h, filter sterilized cellulase was administered to three cultures per time point at a final concentration of 1% (v/v). The cultures were placed back at 30°C overnight for maximum cellulose saccharification. After 24 h cellulase digestion, the OD_{660} ml^{-1} of each culture was determined. As a control, filter sterilized cellulase was also inoculated into 250 ml cultures containing no bacteria and incubated for 24 h to ensure the observed OD_{660} ml^{-1} was not the result of media contamination and to ensure no detectable background from cellulase mixture was observed.

Statistical analysis

A student's *t*-test (2 tailed; unequal variance) was used to evaluate statistical significance of similarity in the BC yield of CM1 cells cultured in SH-kan with respect to SH media with $p>0.05$.

2.3 Results

Initial antibiotic screen

Upon receipt of *G. hansenii* 23769 from American Type Culture Collection (ATCC), the dehydrated samples were reconstituted in SH media (MM Stock) and plated onto SH agar plates. The plates were analyzed by light microscopy for colony diversity (Fig.2-1a). Consistent with previous studies (Haigler and Benziman 1982; Rashid *et al*. 2003), three

different colony morphotypes were observed. Each colony subtype, CM1, CM2 and CM3, was isolated and streaked onto separate plates and the number of colonies for each was comparable. When examined by light microscopy, CM1 cells were small and wrinkled in appearance (Fig. 2-1b). CM2 (Fig. 2-1c) cells were smooth in appearance and small. Both CM1 and CM2 colonies were raised. CM3 (Fig. 2-1d) colonies were smooth and larger than CM1 and CM2 colonies (Fig. 2-1). A liquid culture of MM cells were plated onto SH plates containing kanamycin. After 96 h only CM1 colonies were observed. A colony from each morphotype was streaked onto SH agar plate containing 50 μg ml^{-1} kanamycin and incubated at 30°C. Only CM1 cells were able to grow in the presence of kanamycin after 96 h of incubation. Under these conditions, the number of CM1 colonies were comparable to those without kanamycin. CM2 colonies were present but small. No CM3 colonies were observed. (data not shown).

To characterize the cellulose production of each colony morphotype, pellicle yield was assessed from static cultures inoculated with colonies from each morphotype incubated at 30°C for 96 h. After incubation the cellulose (pellicle) yield of each morphotype was visually assessed. CM1 cells produced the thickest pellicle followed by CM2 cells which produced a very thin almost translucent pellicle. CM3 cells produced no visible pellicle.

Cellulase culture antibiotic titration assay

Bacteria are able to respond swiftly to a variety of environmental cues through key signaling pathways. One notable response to environmental stress is the formation of bacterial biofilms which enhance microbial resistance to antibiotics through a range of mechanisms that generally involve the cooperative secretion of polysaccharides (Meisen et al. 2008). In an effort to investigate the antimicrobial resistant properties of BC, CM1 cells

were cultured in SH media containing increasing concentrations of kanamycin and 5% (v/v) cellulase for cellulose degradation (Fig. 2-2a). Cultures without kanamycin and cellulase suggest that the addition of cellulase did not retard the growth of CM1 cells in SH media. To account for the percentage of cells enmeshed in the cellulose pellicles, a comparison between cultures containing 5% (v/v) cellulase (5% cellulase media) and the cultures without cellulase (SH media) was performed by analyzing the percent change in cell concentrations between each kanamycin concentration point. The first concentration point of 50 μg ml^{-1} kanamycin, resulted in a 95.5% ± 0.5 drop in the observed OD_{660} ml^{-1} reading for 5% cellulase media cultures. In contrast, a much lower decrease of 64.4% ± 1.5 was observed in SH media cultures. Pellicle production of SH media cultures was enhanced in response to the presence of kanamycin at 50 μg ml^{-1} (Fig. 2-2b). A loss of pellicle production was observed when the antibiotic concentration reached 225 μg ml^{-1}. The OD_{660} ml^{-1} reading for SH media cultures, despite the absence of a formed pellicle, continued to decrease with the addition of 500 μg ml^{-1} kanamycin. (*n = 6* where 3 biological and 3 technical replicates were performed).

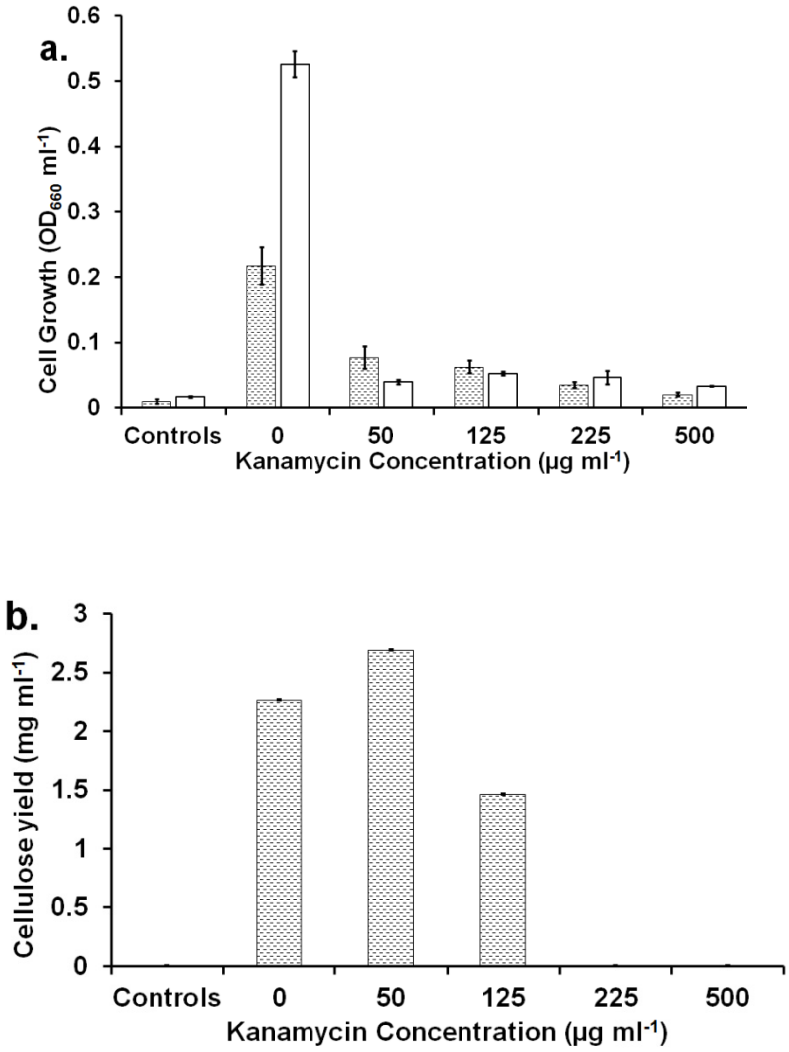

Figure 2-2 The role of bacterial cellulose (BC) in providing antibiotic resistance to *G. hansenii* CM1 cells. (a) The cell growth of *G. hansenii* CM1 was assessed by optical density at 660 nm (OD_{660}) when cultured in the presence of 5% cellulase (v/v) and titrated with antibiotics. All cultures were grown in a media volume of 5 ml and incubated for 72 h under static conditions (*n = 6*). (b) Pellicle yield of cultures containing no cellulase. The controls for this experiment consisted of SH media and SH media with 5% cellulase (v/v) without any cells incubated for the same 72 h period. A BL21 strain of *E. coli* was also used as a control to confirm potency of kanamycin, no growth was observed (data not shown). (▒) Cells cultured in SH media, (□) Cells cultured in 5% cellulase (v/v). (Averaged OD_{660} ml^{-1} of tubes after initial inoculation = 0.028 ± 0.017).

Growth rate of CM1 cells compared to MM cells

CM1 cell growth was compared to MM cell growth to determine the effect of cellulose production on growth rate. Under agitated conditions (Fig. 2-3), the growth rate of CM1 cells and MM cells were similar by OD_{660} ml^{-1}. The pH profile of CM1 cultures was different than MM cultures, CM1 cultures reached a slightly lower pH of 3.34 ± 0.01 after 72 h while MM cultures reached 3.60 ± 0.01 after 144 h *(n = 6*). The cellulose production, as measured by purified pellicle weight, (Table 2-1) from CM1 cultures was 3.48 ± 0.12 times higher compared to MM cultures (*n = 3*). CM1 cells were then evaluated for their ability to produce cellulose under static conditions (Fig. 2-4). The growth profile of CM1 cells and MM cells were similar under static conditions. The culture pH of CM1 cells under static conditions decreased in value at a slower rate compared to MM cultures. MM cultures reached a lower pH of 3.37 ± 0.03 after 288 h compared to CM1 cultures which reached a pH of 3.47 ± 0.03 (*n = 6*). The same trend in cellulose production (Table 2-1) that was observed under agitated conditions continued under static conditions, where the observed cellulose production by CM1 cells was 15 times higher compared to MM cultures (*n = 3* where 3 biological repeats were performed).

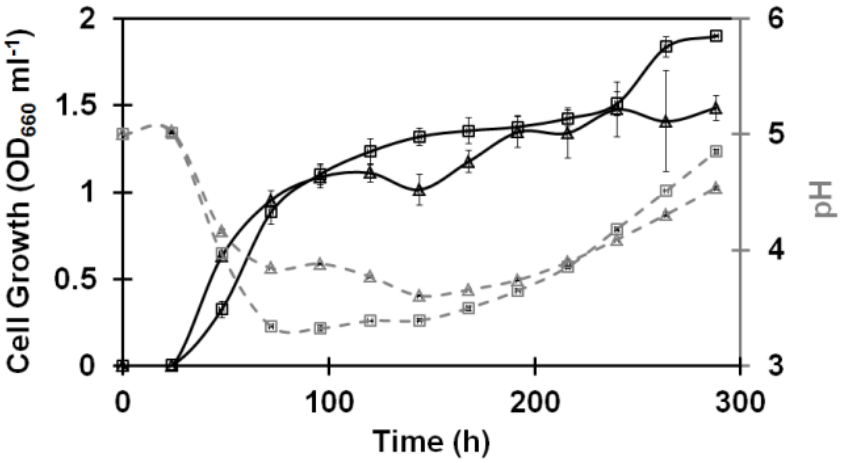

Figure 2-3 Growth rate and metabolism comparison of *G. hansenii* MM cells and CM1 cells at 30°C under agitated conditions. OD_{660} readings were taken every 24 h for 288 h (Y1) and plotted with the change in culture pH (Y2). (◘) CM1 cells, (Δ) MM cells (*n* = *6*).

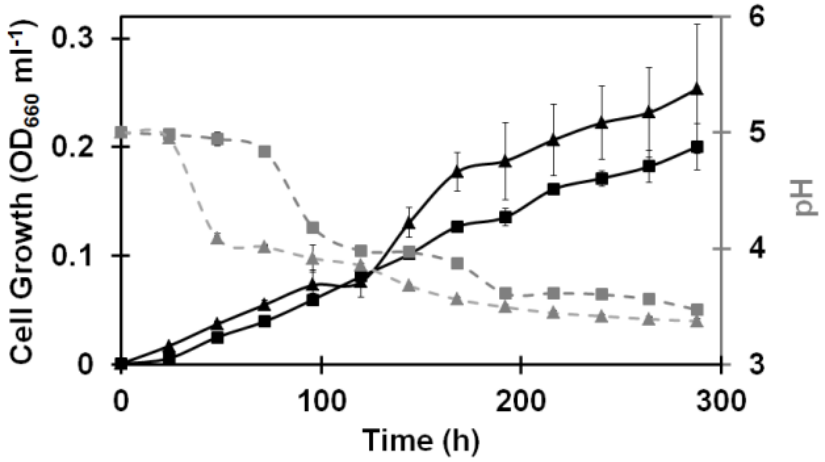

Figure 2-4 Growth rate and metabolism comparison of *G. hansenii* static cultures at 30°C containing MM cells and CM1 cells. OD_{660} readings were taken every 24 h for 288 h (Y1) and plotted with the change in culture pH (Y2). (■) CM1 cells, (▲) MM cells (*n* = *6*).

Table 2-1 Bacterial cellulose productivity based on *G. hansenii* morphotype and media conditions

G. hasenii Morphotype(s)	Media conditions	BC yield g l^{-1}
ATCC 23769 Mixed Morphotypes (MM)		
	HS-agitated	0.163 ± 0.005
	Hestrin Schramm (HS)-Static	0.129 ± 0.030
	Yamanaka media (YM)-Static	1.064 ± 0.085
G. hansenii-Morphotype 1 (CM1)		
	HS-Agitated	0.567 ± 0.018
	HS-Static	1.947 ± 0.099
	HS-50 µg/mL Kanamycin-Static	**2.144 ± 0.025**
	YM-Static	1.128 ± 0.032
	YM + 1% Ethanol-Static	1.252 ± 0.064

(*n=3*)
p = 0.009 where the null hypothesis states that BC yield from HS static cultures = BC yield from HS-Kan cultures with $p > 0.05$

Effect of cellulase on CM1 cell growth

The growth profile for CM1 cells cultured in the presence of cellulase (Fig. 2-5) did not show a significant variation in cell growth compared to CM1 cells grown in SH media under the same conditions. A closer examination, however, of the pH profiles produced from this study suggest a change occurs on perhaps the metabolic level when CM1 cells are cultured over a long period of time with cellulase as a consequence of excess glucose. The culture pH of CM1 cells cultured in 1% cellulase media were more acidic compared to SH media cultures and 1% cellulase time point assay cultures. Based on these results, 1% cellulase time point assays are an effective way of performing in-culture cellulose digestions with no detectable influence on culture conditions based on OD_{660} ml^{-1} and pH (*n = 3* where 3 biological repeats were performed).

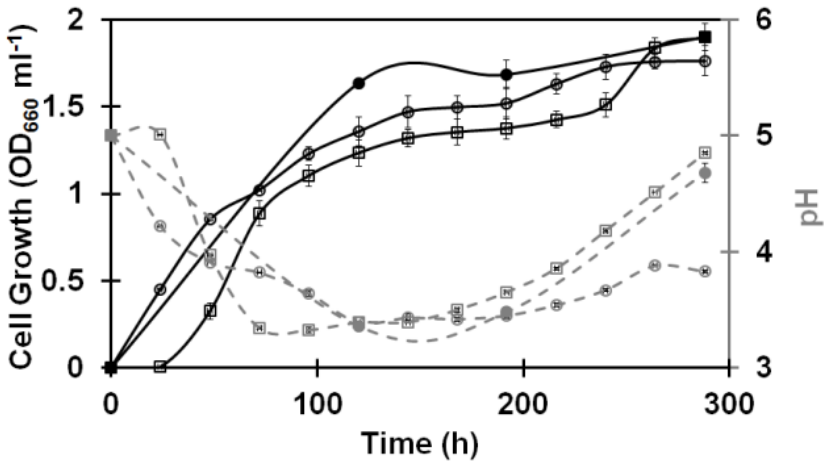

Figure 2-5 The influence of cellulase on *G. hansenii* CM1 cells under agitated conditions**.** Growth rate and metabolism comparison of *G. hansenii* CM1 cells cultured under agitated conditions at 30°C in 1% (v/v) SH cellulase media compared to CM1 cells cultured in SH media and exposed to 1% (v/v) cellulase at time points 120, 192 and 288 h. OD_{660} readings were taken every 24 h for 288 h (Y1) and plotted with the change in culture pH (Y2). (□) SH media (*n = 6*), (○) 1% (v/v) cellulase media (*n = 6*), (●) 1% (v/v) cellulase time point assay (*n = 3*).

The optimization of the in-culture cellulose digestion assay provided a unique opportunity to examine the number of cells that are associated with pellicle formation over a culture period. More specifically, the 1% cellulase time point assay was performed on a series of static cultures for MM and CM1 cells at time points 96, 168 and 264 h (Fig. 2-6). The resulting OD_{660} ml^{-1} were considered to represent 100% cell growth. Based on these values the percentage of cells entangled in pellicle was determined using OD_{660} ml^{-1} of cultures grown in parallel (Table 2-2). The percentage of CM1 cells associated with pellicle biomass at all three time points never falls below 80.76% ± 1.15. A large population of MM cells remain in culture until the 288 h time point demonstrating the inefficiency associated with not removing Cel^- phenotypes from the culture population. (*n = 3* where 3 biological repeats were performed).

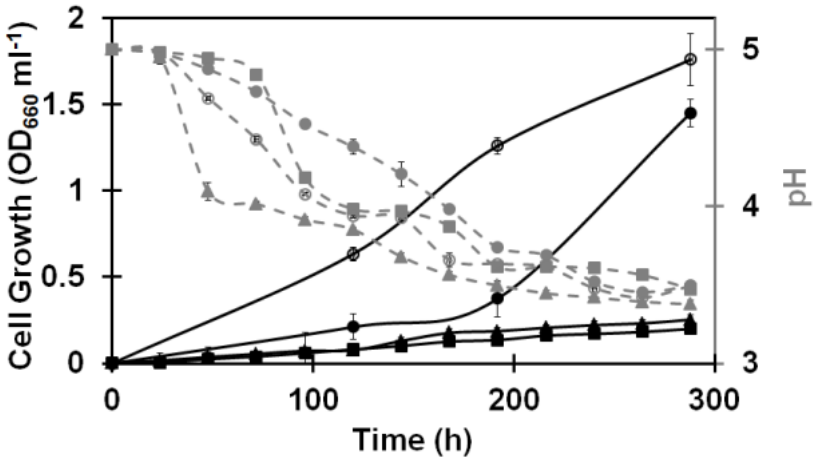

Figure 2-6 The influence of cellulose on the OD_{660} readings of *G. hansenii* MM and CM1 cells under static conditions**.** Growth rate comparison between *G. hansenii* CM1 cells and MM cells cultured under static conditions and exposed to 1% (v/v) cellulase at time points 120, 192 and 288 h. OD_{660} readings were taken every 24 h (Y1) and plotted with the change in pH of the culture (Y2). (▲) MM static culture (*n = 6*), (■) CM1 static culture (*n = 6*), (●) MM 1% (v/v) cellulase time point assay static cultures (*n = 3*), (o) CM1 1% cellulase time point assay (*n = 3*).

Table 2-2. The percentage of cells contained in CM1 and MM pellicles

	% Cells in pellicle		
G. hansenii Morphotype(s)	120 (h)	192 (h)	288 (h)
ATCC 23769 (MM)	61.76% ± 13.40	53.51% ± 13.18	87.1% ± 0.70
Colony Type 1 Morphotype (CM1)	80.76% ± 1.15	87.76% ± 0.46	89.32% ± 0.91

The following equation was used to calculate the above values:
% =[(OD_{660} Cellulase Time Point – OD_{660} Static growth) / (OD_{660} Cellulase Time Point)] x 100%

(*n = 3*)

The influence of kanamycin on CM1 cellulose synthesis

To determine if cellulose synthesis by CM1 cells is enhanced when cultured with a moderate concentration of antibiotic, CM1 cells were cultured statically in SH media with 50 μg ml^{-1} kanamycin (SH-kan). In parallel CM1 cells were inoculated into a series of different media that were previously characterized for their enhancement of cellulose synthesis by *G. hansenii* (Park *et al*. 2003). CM1 inoculated cultures of SH media, SH-kan, YM and YME were grown statically for 288 h with pH and OD_{660} ml^{-1} readings taken every 24 h (Fig. 2-7). At the conclusion of the 288 h growth period, the pellicles from each culture were harvested and purified. The total yield of cellulose produced was determined by the weight of the resulting purified BC relative to the total volume of culture (Table 2-1). CM1 cells cultured in kanamycin media produced the largest amount of cellulose. When the cellulose yield from CM1 cells cultured in the presence of kanamycin was statistically evaluated using students's t-test (two tailed) for similarity to the cellulose yield obtained from cells cultured in SH media only, the probability of similarity was 0.009, suggesting the observed difference in cellulose yield is statistically accurate. YM media was able to promote pellicle formation in MM cultures but was ineffective at supporting pellicle production by CM1 cells. CM1 cells produced the lowest amount of cellulose under static conditions when cultured in YM media. The results presented in figure 2-7, suggest that the low yield was a result of slow cell growth. This observation can also be seen in the pH profile (Fig. 2-7b). The addition of ethanol to the YM media was effective at improving cell growth, but still inefficient in promoting cellulose yield in comparison to CM1 cells cultured in kanamycin media ($n = 3$ where 3 biological repeats were performed).

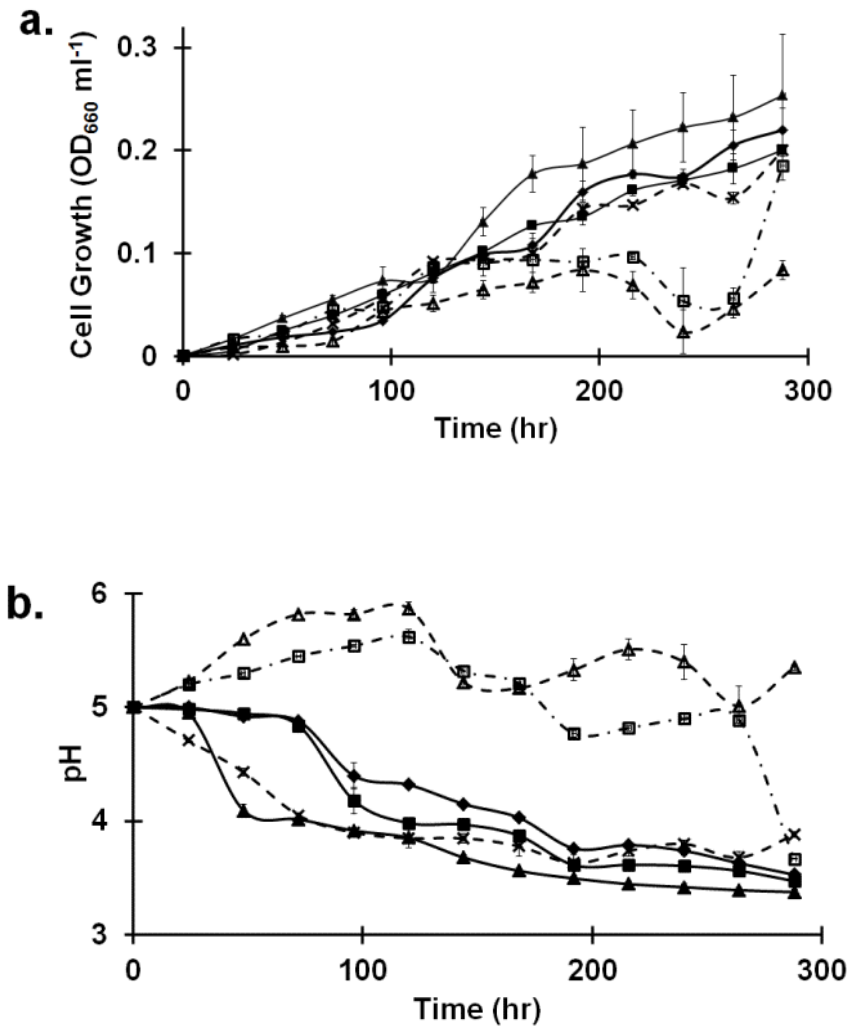

Figure 2-7 The effect of kanamycin on the growth rate and metabolism of *G. hansenii* CM1 cells under static conditions (a) Growth curve comparison of *G. hansenii* MM and CM1 cells in SH media, SH media + kanamycin, YM media and YM media + 1% ethanol after 288 h incubation (*n* = *3*). (b) Change in culture pH over the 288 h growth period (*n* = *3*). (▲) MM cells in SH media, (■) CM1 cells in SH media, (△) MM cells in YM media, (□) CM1 cells in YM media, (χ) CM1 Cells in YM media + 1 % (v/v) ethanol, (♦) CM1 cells in SH media + 50 μg ml^{-1} kanamycin.

2.4 Discussion

Initial antibiotic screen

The commercialization of BC on a global scale is strongly dependent on reducing the cost associated with high yield BC synthesis. The solution to this multi-faceted problem has been investigated from many different angles, including the optimization of culture conditions with respect to carbon and nitrogen sources, pH control and aeration (Hwang *et al*. 1999; Mohite *et al*. 2012; Schramm and Hestrin 1954). Divergent from most microbial production models, BC is most efficiently produced from static cultures. The cultivation of *G. hansenii* under agitated conditions, as shown here, results in a decrease in cellulose synthesis. There are numerous factors that contribute to this phenomenon (Embuscado *et al*. 1994), with the predominant factor involving the generation of cellulose negative phenotypes (Jung *et al*. 2005). Under agitated conditions the cellulose negative cells are more efficient at cellular metabolism and become the dominant phenotype in the population, resulting in a reduction in cellulose synthesis (Jung *et al*. 2005; Park *et al*. 2004). At present, researchers hypothesize that this mutation is a result of a breakdown in cyclic di-GMP associated signaling (Rashid *et al*. 2003). Known for its role in biofilm formation, cyclic di-GMP participates in a second messenger signaling cascade that directs cellular response to environmental cues such as antimicrobials, pH and oxygen availability (Strap *et al*. 2011b). To exploit the full potential of *G. hansenii* as a biocatalyst for cellulose production, the expression of cellulose negative phenotypes must be reduced and the pathways associated with BC synthesis must be explicitly understood. This begins with the isolation of the highest and most efficient cellulose producing phenotypes. In the case of *G. hansenii* 23769, the highest cellulose yields are obtained from small, wrinkled colony morphotypes

(Haigler and Benziman 1982) that are referred to in this study as CM1 (Fig. 2-1). The selection of these colonies was successfully achieved through the inclusion of the aminoglycoside, kanamycin, into the growth media. Functioning in the same manner as a biofilm, we theorize that the cellulose architecture provides protection against the moderate exposure of the bacteria to kanamycin. The cellulose negative phenotypes are unable to synthesize this additional layer of protection (Jung *et al*. 2005), resulting in the mutants' inability to grow in the presence of antibiotic. The incorporation of antibiotics into culture media may help in reducing the number of mutations that arise in the *G. hansenii* cultures and provide an effective method for exerting selective pressure for obtaining cellulose producing *G. hansenii* cells.

Cellulase culture antibiotic titration assay

The results from the initial antibiotic screen highlight the biofilm aspects of BC synthesis and secretion by *G. hansenii*. Generally associated with adherence, biofilms are widely studied for their antimicrobial resistance properties (Broderick et al. 2013). The addition of cellulase to the culture media of CM1 cells with increasing concentrations of kanamycin resulted in a complete loss in kanamycin resistance. This observation illustrates the antimicrobial resistance properties cellulose provides *G.hansenii* (Fig. 2-2). The OD_{660} ml^{-1} of 5% cellulase media cultures dosed with kanamycin never achieved a concentration above basal levels. In comparison, a progressive decrease in the OD_{660} ml^{-1} is witnessed as the concentration of kanamycin is increased in SH media cultures. As a consequence of pellicle formation, the OD_{660} ml^{-1} of SH media cultures are lower than the OD_{660} ml^{-1} readings for 5% cellulase media cultures; however, pellicle formation is still observed (Fig. 2-2). The mechanism associated with the observed increase in cellulose synthesis at the 50 µg ml^{-1}

kanamycin concentration point (Fig. 2-2b) is unclear. The observations of Valla *et al* 1982 suggest the addition of kanamycin stimulated a population of Cel^- phenotypes to reinitiate cellulose synthesis through a not yet characterized mechanism (Valla and Kjosbakken 1982). Despite this mechanistic ambiguity, the conclusions are clear, the introduction of kanamycin into the growth media of *G. hansenii* results in an increase in cellulose production.

Growth rate of CM1 cells compared to MM cells under agitated conditions

The efficiency of cellulose synthesis by *G. hansenii* is highly dependent on carbon and oxygen availability (Hutchens *et al*. 2007; Hwang *et al*. 1999). This statement is exemplified by the results presented in figure 2-3, where the growth rate of MM and CM1 cultures appear to be similar yet the cellulose yield for MM cultures is significantly lower than CM1 cultures (Table 2-1). Although MM cultures contain a percentage of CM1 cells, the presence of cellulose negative phenotypes results in the reduction of nutrient available for cellulose producing cells. These results demonstrate the importance of enriching *G. hansenii* cultures with CM1 cells through selective prescreening to maximize BC production.

Growth rate of CM1 cells compared to MM cells under static conditions

Under static conditions, oxygen diffusion is low resulting in a decrease in cell growth but an increase in cellulose synthesis at the liquid-air interface of the media (Schramm and Hestrin 1954). In contrast, to the growth profiles observed under agitated conditions, the growth rate appears to be higher in MM cultures compared to CM1 cultures under static conditions. Despite this observation the cellulose yield from CM1 cultures is still substantially higher than MM cultures (Table 2-1). Without evaluating the percentage of

cells contained in the pellicles, it is difficult to make a true comparison in cell growth using OD_{660} ml^{-1}. A key point to note, however, is the significant variation in error that is generated when evaluating MM cultures (Fig. 2-4). MM cultures contain both CM1 cells and planktonic cellulose negative cells. The representative ratios between the two phenotypes are inconsistent between cultures resulting in a high variation in pellicle associated cells. In consideration of this fact, a comparison of the culture pH profiles provides a more definitive presentation of the difference in culture types under static conditions. The pH profiles of CM1 and MM cells are slightly different with CM1 cells exhibiting a slower growth profile. In comparison to the pH profiles observed under agitated conditions, both CM1 and MM cultures are able to achieve a lower pH as a consequence of oxygen availability. Although the pH profile of MM culture reaches a lower pH, the profile is the same. A distinctly different profile is observed for CM1 cells when comparing agitated and static conditions. Cellulose synthesis is higher under static conditions resulting in the shuttling of glucose into the cellulose synthesis pathway. CM1 cells accumulate at the liquid-air interface for maximum aeration (Schramm and Hestrin 1954). The limitation in surface area results in a smaller and slower cell growth profile thus lowering the rate of gluconate accumulation (Krystynowicz *et al*. 2002). In comparison, the pH profile of MM cultures remains consistent with the profile observed under agitated conditions. An evaluation of the cellulose yields for agitated and static MM culture supports this observation as the cellulose yields are comparable. As stated previously and observed in CM1 cultures, cellulose is most efficiently produced under static conditions as a result of oxygen tension at the air-liquid interface. Cellulose negative phenotypes are unable to synthesize cellulose and are relegated to the bottom of the culture. Over time oxygen becomes depleted and the cells die (Ross *et al*. 1991).

1% (v/v) Cellulase assay and percentage of pellicle associated bacteria

The addition of cellulase to pellicle producing cultures is a common method used to obtain a more accurate OD_{660} reading (Brown Jr and Kanda 2004); however, the incubation time and concentration of cellulose vary among studies. Here we demonstrate a potential problem with co-culturing cellulose producing bacteria with cellulase over long culture periods. The comparison between the two 1% cellulase culture methods resulted in the 1% cellulase time point assay providing the best results. The 1% cellulase media did not offer a viable assay as a result of cellulase being present in the media at inoculation. Newly synthesized BC was hydrolyzed at a high rate to glucose. The excess glucose was oxidized by CM1 cells (Vandamme *et al*. 1998) resulting in a pH profile vastly different compared to CM1 cells cultured in SH media (Fig. 2-5). To minimize the influence of excess glucose, the 1% cellulase time point assay was used. Exhibiting the same growth and pH profile as CM1 cells under normal conditions, the assay was then used to determine the relative percentage of bacteria associated with pellicle formation from MM and CM1 cultures at specific time points (Fig. 2-6). The percentages presented in table 2-2 provide an interesting insight into pellicle formation over time. The percent of CM1 cells associated with pellicles was as expected, demonstrating the effectiveness of reducing Cel^- phenotypes from the culture population. The trend exhibited by MM cultures, however, interestingly resulted in a large increase in pellicle cell incorporation occurring at the end of the growth curve. This observation is consistent with our earlier statement. Cellulose negative phenotypes are unable to reach the liquid-air interface because they are unable to synthesize cellulose. As time progresses the cellulose negative phenotypes die as a consequence of oxygen depletion (Ross *et al*. 1991). Although the percentage of cells associated with the pellicle is higher, the pellicle yield is still much lower compared to enriched CM1 cultures. It will take

several generations and expensive culture time to enrich a culture through natural oxygen depletion. This demonstrates how inefficient it is not to remove cellulose negative phenotypes from the culture population as well highlight the novelty of our method.

Influence of kanamycin on cellulose synthesis

To fully characterize the influence of kanamycin on cellulose synthesis, CM1 and MM colonies were selected from original MM stock plates and inoculated into a series of cultures previously reported to enhance cellulose production by *G. hansenii* on a metabolic level (Krystynowicz *et al*. 2002). The cultures containing SH media, SH-kan media, YM media and YME media were incubated under static conditions for 288 h and evaluated for cell growth (Fig. 2-7a), metabolism (Fig. 2-7b) and cellulose yield (Table 2-1). A slow growth profile was observed for both CM1 and MM cells cultured in YM media (Fig. 2-7a). However, the cellulose yield of MM cells cultured in YM media significantly increased (Table 2-1). The primary source of carbon in YM media was sucrose, allowing *G. hansenii* to shuttle available hexoses generated from metabolism into the cellulose synthesis pathway (Nakai *et al*. 1999). Different from glucose, the metabolism of sucrose by *G. hansenii* does not result in excess gluconate (Chien et *al.* 2006*)*, thereby raising the pH profile. In MM-YM cultures, the CM1 cell population is able to synthesize cellulose more efficiently as a result of available carbon substrate. As stated previously, sucrose is not directly oxidized into gluconate, resulting in a higher concentration of available substrate for cellulose synthesis (Fig. 2-7a) (Nakai *et al*. 1999). This explains the increase in cellulose production by MM cultures in the presence of YM media. A review of the growth and pH profile of YME cultures containing CM1 cells suggest the ethanol was easily metabolized by *G. hansenii* into acetate. Despite providing an additional source for ATP generation (Li et al. 2012), the

cellulose yield from YME cultures was the lowest. Previous studies investigating the influence of ethanol on *G. hansenii* growth and cellulose synthesis have found ethanol to be effective at removing cellulose negative phenotypes from the population (Park *et al*. 2003). A more recent study on the influence of ethanol on cellulose synthesis implies the metabolism of ethanol, by *G. hansenii*, results in the accumulation of metabolic by-products that negatively impact cellulose synthesis (Li *et al*. 2012). CM1 cells cultured in the presence of 50 μg ml^{-1} kanamycin exhibited the highest yield in cellulose production. An examination of the growth and pH profile suggest the cell growth and rate of metabolism observed is identical to CM1 cells cultured in SH media.

2.5 Conclusion:

Exhibiting high purity, high crystallinity, high water retention and excellent biodegradability, the potential commercial applications for BC are considerable. Restricted only in cost, the enhancement of BC synthesis for industrial gain has been investigated on a metabolic, molecular and engineering level (Chao *et al*. 2000; Mohite *et al*. 2012; Tal *et al*. 1998). Although vastly different in experimental approach, the same conclusion is consistently reached; the efficiency of cellulose production is significantly enhanced when cellulose negative phenotypes are reduced. In this study we illustrate the importance of this conclusion using kanamycin resistance as a selectable marker. As is true for other biofilm associated EPS matrices (Hoffman et al. 2005) cellulose provides high yielding BC producing bacteria with kanamycin resistance. When evaluated for cellulose production, *G . hansenii* cells cultured in 50 μg ml^{-1} kanamycin produced a higher amount of cellulose compared to cells cultured in SH media. This observation suggests the potential of an

additional mechanism not yet explored for the regulation of cellulose synthesis. A model organism for cellulose synthesis, the availability of the complete genome should allow future studies to examine BC synthesis in response to antimicrobial stimuli in greater detail. In conclusion, our results demonstrate a novel method for enriching *G. hansenii* cultures with high yield BC cells and demonstrates the protective capacity of bacterial cellulose that is reminiscent of biofilm associated EPS.

2.6 References

Ashjaran,A., Yazdanshenas,M.E., Rashidi,A., Khajavi,R. and Rezaee,A. (2012) Overview of bio nanofabric from bacterial cellulose. *Journal of The Textile Institute* **104**, 121-131.

Borlee,B.R., Goldman,A.D., Murakami,K., Samudrala,R., Wozniak,D.J. and Parsek,M.R. (2010) Pseudomonas aeruginosa uses a cyclic-di-GMP-regulated adhesin to reinforce the biofilm extracellular matrix. *Molecular Microbiology* **75**, 827-842.

Broderick,A.H., Breitbach,A.S., Frei,R., Blackwell,H.E. and Lynn,D.M. (2013) Surface-Mediated Release of a Small-Molecule Modulator of Bacterial Biofilm Formation: A Non-Bactericidal Approach to Inhibiting Biofilm Formation in Pseudomonas aeruginosa. *Advanced Healthcare Materials* n/a.

Brown Jr,M.R. and Kanda,T. (2004) The relationship between cellulase activity and oligosaccharides and cellulose productions by Acetobacter xylinum ATCC23769.

Cannon,R.E. and Anderson,S.M. (1991) Biogenesis of Bacterial Cellulose. *Critical Reviews in Microbiology* **17**, 435-447.

Chandel,A.K., Chandrasekhar,G. and Silva,M.B. (2011) The realm of cellulases in biorefinery development. *Critical Reviews in Biotechnology* **32**, 187-202.

Chang,A.L., Tuckerman,J.R., Gonzalez,G., Mayer,R., Weinhouse,H., Volman,G., Amikam,D., Benziman,M. and Gilles-Gonzalez,M.A. (2001) Phosphodiesterase A1, a Regulator of Cellulose Synthesis in Acetobacter xylinum, Is a Heme Based Sensor. *Biochemistry* **40**, 3420-3426.

Chao,Y., Ishida,T., Sugano,Y. and Shoda,M. (2000) Bacterial cellulose production by Acetobacter xylinum in a 50-L internal-loop airlift reactor. *Biotechnology and Bioengineering* **68**, 345-352.

Chien,L.J., Chen,H.T., Yang,P.F. and Lee,C.K. (2006) Enhancement of Cellulose Pellicle Production by Constitutively Expressing Vitreoscilla Hemoglobin in Acetobacter xylinum. *Biotechnology Progress* **22**, 1598-1603.

Czaja,W.K., Young,D.J., Kawecki,M. and Brown,R.M. (2006) The Future Prospects of Microbial Cellulose in Biomedical Applications. *Biomacromolecules* **8**, 1-12.

D'Argenio,D.A. and Miller,S.I. (2004) Cyclic di-GMP as a bacterial second messenger. *Microbiology* **150**, 2497-2502.

Desvaux,M., Guedon,E. and Petitdemange,H. (2001) Carbon Flux Distribution and Kinetics of Cellulose Fermentation in Steady-State Continuous Cultures of Clostridium cellulolyticum on a Chemically Defined Medium. *Journal of Bacteriology* **183**, 119-130.

Embuscado,M.E., Marks,J.S. and BeMiller,J.N. (1994) Bacterial cellulose. I. Factors affecting the production of cellulose by Acetobacter xylinum. *Food Hydrocolloids* **8**, 407-418.

Fujiwara,M., Fukushi,K., Takai,M., Hayashi,J., Fukaya,M., Okumura,H. and Kawamura,Y. (1992) Construction of shuttle vectors derived fromAcetobacter xylinum for cellulose-producing bacterium Acetobacter xylinum. *Biotechnol Lett* **14**, 539-542.

Haigler, C. H. (1982) Alteration of cellulose Assembly in Acetobacter xylinum by fluorescent brightening agents, direct dyes, and cellulose derivatives. University of North Carolina at Chapel Hill.

Haigler, C. H. and Benziman, M. (1982) Biogenesis of cellulose I microfibrils occurs by cell-directed self-assembly in Acetobacter xylinum. pp. 273-297. Plenum Press, London, New York.

Hestrin,S. and Schramm,M. (1954) Synthesis of cellulose by Acetobacter xylinum. II. Preparation of freeze-dried cells capable of polymerizing glucose to cellulose. *The Biochemical journal* **58**, 345-352.

Hickman,J.W., Tifrea,D.F. and Harwood,C.S. (2005) A chemosensory system that regulates biofilm formation through modulation of cyclic diguanylate levels. *Proceedings of the National Academy of Sciences of the United States of America* **102**, 14422-14427.

Hoffman,L.R., D'Argenio,D.A., MacCoss,M.J., Zhang,Z., Jones,R.A. and Miller,S.I. (2005) Aminoglycoside antibiotics induce bacterial biofilm formation. *Nature* **436**, 1171-1175.

Hutchens,S.A., Levin,R.V., O'Neill,H.M. and Evans,B.R. (2007) Statistical analysis of optimal culture conditions for Gluconacetobacter hansenii cellulose production. *Letters in Applied Microbiology* **44**, 175-180.

Hwang,J.W., Yang,Y.K., Hwang,J.K., Pyun,Y.R. and Kim,Y.S. (1999) Effects of pH and dissolved oxygen on cellulose production by Acetobacter xylinum BRC5 in agitated culture. *Journal of Bioscience and Bioengineering* **88**, 183-188.

Ignatov,S.G., Ferguson,J.A. and Walt,D.R. (2001) A fiber-optic lactate sensor based on bacterial cytoplasmic membranes. *Biosensors and Bioelectronics* **16**, 109-113.

Ishihara,M., Matsunaga,M., Hayashi,N. and Tíler,V. (2002) Utilization of d-xylose as carbon source for production of bacterial cellulose. *Enzyme and Microbial Technology* **31**, 986-991.

Iyer,P.R., Geib,S.M., Catchmark,J., Kao,T.h. and Tien,M. (2010) Genome Sequence of a Cellulose-Producing Bacterium, Gluconacetobacter hansenii ATCC 23769. *Journal of Bacteriology* **192**, 4256-4257.

Jenal,U. and Malone,J. (2006) Mechanisms of cyclic-di-GMP signaling in bacteria. *Annual review of genetics* **40**, 385-407.

Jung,H.I., Lee,O.M., Jeong,J.H., Jeon,Y.D., Park,K.H., Kim,H.S., An,W.G. and Son,H.J. (2010) Production and Characterization of Cellulose by Acetobacter sp. V6 Using a Cost-Effective MolassesGÇôCorn Steep Liquor Medium. *Applied biochemistry and biotechnology* **162**, 486-497.

Jung,J.Y., Park,J.K. and Chang,H.N. (2005) Bacterial cellulose production by Gluconacetobacter hansenii in an agitated culture without living non-cellulose producing cells. *Enzyme and Microbial Technology* **37**, 347-354.

Keshk,S. and Sameshima,K. (2006) Influence of lignosulfonate on crystal structure and productivity of bacterial cellulose in a static culture. *Enzyme and Microbial Technology* **40**, 4-8.

Klemm,D., Heublein,B., Fink,H.P. and Bohn,A. (2005) Cellulose: Fascinating Biopolymer and Sustainable Raw Material. *Angewandte Chemie International Edition* **44**, 3358-3393.

Klemm,D., Schumann,D., Udhardt,U. and Marsch,S. (2001) Bacterial synthesized cellulose: artificial blood vessels for microsurgery. *Progress in Polymer Science* **26**, 1561-1603.

Kongruang,S. (2008) Bacterial Cellulose Production by Acetobacter xylinum Strains from Agricultural Waste Products. *Appl Biochem Biotechnol* **148**, 245-256.

Krystynowicz,A., Czaja,W., Wiktorowska-Jezierska,A., Gonalves-Mickiewicz,M., Turkiewicz,M. and Bielecki,S. (2002) Factors affecting the yield and properties of bacterial cellulose. *Journal of industrial microbiology & biotechnology* **29**, 189-195.

Kumar,P., Barrett,D.M., Delwiche,M.J. and Stroeve,P. (2009) Methods for Pretreatment of Lignocellulosic Biomass for Efficient Hydrolysis and Biofuel Production. *Industrial & Engineering Chemistry Research* **48**, 3713-3729.

Li,Y., Tian,C., Tian,H., Zhang,J., He,X., Ping,W. and Lei,H. (2012) Improvement of bacterial cellulose production by manipulating the metabolic pathways in which ethanol and sodium citrate are involved. *Appl Microbiol Biotechnol* **96**, 1479-1487.

Lisdiyanti,P., Navarro,R.R., Uchimura,T. and Komagata,K. (2006) Reclassification of Gluconacetobacter hansenii strains and proposals of Gluconacetobacter saccharivorans sp. nov. and Gluconacetobacter nataicola sp. nov. *International Journal of Systematic and Evolutionary Microbiology* **56**, 2101-2111.

Maneerung,T., Tokura,S. and Rujiravanit,R. (2012) Impregnation of silver sulfadiazine into bacterial cellulose for antimicrobial and biocompatible wound dressing. *Biomedical Materials* **7**, 065006.

Masaoka,S., Ohe,T. and Sakota,N. (1993) Production of cellulose from glucose by Acetobacter xylinum. *Journal of Fermentation and Bioengineering* **75**, 18-22.

McKendry,P. (2002a) Energy production from biomass (part 1): overview of biomass. *Bioresource Technology* **83**, 37-46.

McKendry,P. (2002b) Energy production from biomass (part 2): conversion technologies. *Bioresource Technology* **83**, 47-54.

Meisen,S., Wingender,J. and Telgheder,U. (2008) Analysis of microbial extracellular polysaccharides in biofilms by HPLC. Part I: development of the analytical method using two complementary stationary phases. *Anal Bioanal Chem* **391**, 993-1002.

Meissner,A., Wild,V., Simm,R., Rohde,M., Erck,C., Bredenbruch,F., Morr,M., R+¦mling,U. and H+ñussler,S. (2007) Pseudomonas aeruginosa cupA-encoded fimbriae expression is regulated by a GGDEF and EAL domain-dependent modulation of the intracellular level of cyclic diguanylate. *Environmental Microbiology* **9**, 2475-2485.

Mikkelsen,D., Flanagan,B.M., Dykes,G.A. and Gidley,M.J. (2009) Influence of different carbon sources on bacterial cellulose production by Gluconacetobacter xylinus strain ATCC 53524. *Journal of Applied Microbiology* **107**, 576-583.

Mohite,B., Kamalja,K. and Patil,S. (2012) Statistical optimization of culture conditions for enhanced bacterial cellulose production by Gluconoacetobacter hansenii NCIM 2529. *Cellulose* **19**, 1655-1666.

Nakai,T., Tonouchi,N., Konishi,T., Kojima,Y., Tsuchida,T., Yoshinaga,F., Sakai,F. and Hayashi,T. (1999) Enhancement of cellulose production by expression of sucrose synthase in Acetobacter xylinum. *Proceedings of the National Academy of Sciences* **96**, 14-18.

Park,J., Hyun,S. and Jung,J. (2004) Conversion of G. hansenii PJK into non-cellulose-producing mutants according to the culture condition. *Biotechnol Bioproc E* **9**, 383-388.

Park,J., Jung,J. and Park,Y. (2003) Cellulose production by Gluconacetobacter hansenii in a medium containing ethanol. *Biotechnology Letters* **25**, 2055-2059.

Ramana,K.V., Tomar,A. and Singh,L. (2000) Effect of various carbon and nitrogen sources on cellulose synthesis by Acetobacter xylinum. *World Journal of Microbiology and Biotechnology* **16**, 245-248.

Rashid,M.H., Rajanna,C., Ali,A. and Karaolis,D.K.R. (2003) Identification of genes involved in the switch between the smooth and rugose phenotypes of Vibrio cholerae. *FEMS Microbiology Letters* **227**, 113-119.

Rogers,G.B., Carroll,M.P. and Bruce,K.D. (2012) Enhancing the utility of existing antibiotics by targeting bacterial behaviour? *British Journal of Pharmacology* **165**, 845-857.

Ross,P., Weinhouse,H., Aloni,Y., Michaeli,D., Weinberger-Ohana,P., Mayer,R., Braun,S., De Vroom,E., Van der Marel,G.A. and Van Boom,J.H. (1987) Regulation of cellulose synthesis in Acetobacter xylinum by cyclic diguanylic acid.

Ross,P., Mayer,R. and Benziman,M. (1991) Cellulose biosynthesis and function in bacteria. *Microbiological Reviews* **55**, 35-58.

Saxena,I.M., Kudlicka,K., Okuda,K. and Brown,R.M. (1994) Characterization of genes in the cellulose-synthesizing operon (acs operon) of Acetobacter xylinum: implications for cellulose crystallization. *Journal of Bacteriology* **176**, 5735-5752.

Scheunemann,A.E., Graham,W.D., Vendeix,F.A. and Agris,P.F. (2010) Binding of aminoglycoside antibiotics to helix 69 of 23S rRNA. *Nucleic acids research* **38**, 3094-3105.

Schramm,M. and Hestrin,S. (1954) Factors affecting Production of Cellulose at the Air/ Liquid Interface of a Culture of Acetobacter xylinum. *Journal of General Microbiology* **11**, 123-129.

Sims,R.E.H., Mabee,W., Saddler,J.N. and Taylor,M. (2010) An overview of second generation biofuel technologies. *Bioresource Technology* **101**, 1570-1580.

Starkey,M., Hickman,J.H., Ma,L., Zhang,N., De Long,S., Hinz,A., Palacios,S., Manoil,C., Kirisits,M.J., Starner,T.D., Wozniak,D.J., Harwood,C.S. and Parsek,M.R. (2009) Pseudomonas aeruginosa Rugose Small-Colony Variants Have Adaptations That Likely Promote Persistence in the Cystic Fibrosis Lung. *Journal of Bacteriology* **191**, 3492-3503.

Strap,J.L., Latos,A., Shim,I. and Bonetta,D.T. (2011a) Characterization of Pellicle Inhibition in Gluconacetobacter xylinus 53582 by a Small Molecule, Pellicin, Identified by a Chemical Genetics Screen. *PLoS ONE* **6**, 1-9.

Strap,J.L., Latos,A., Shim,I. and Bonetta,D.T. (2011b) Characterization of Pellicle Inhibition in Gluconacetobacter xylinus 53582 by a Small Molecule, Pellicin, Identified by a Chemical Genetics Screen. *PLoS ONE* **6**, 1-9.

Tal,R., Wong,H.C., Calhoon,R., Gelfand,D., Fear,A.L., Volman,G., Mayer,R., Ross,P., Amikam,D., Weinhouse,H., Cohen,A., Sapir,S., Ohana,P. and Benziman,M. (1998) Three cdg Operons Control Cellular Turnover of Cyclic Di-GMP in Acetobacter xylinum: Genetic Organization and Occurrence of Conserved Domains in Isoenzymes. *Journal of Bacteriology* **180**, 4416-4425.

Tonouchi,N., Tsuchida,T., Yoshinaga,F., Horinouchi,S. and Beppu,T. (1994) A host-vector system for a cellulose-producing Acetobacter strain. *Bioscience, biotechnology, and biochemistry* **58**, 1899-1901.

Valla,S., Coucheron,D. and Kjosbakken,J. (1987) The plasmids of Acetobacter xylinum and their interaction with the host chromosome. *Mole Gen Genet* **208**, 76-83.

Valla,S. and Kjosbakken,J. (1982) Cellulose-negative mutants of Acetobacter xylinum. *Journal of General Microbiology* **128**, 1401-1408.

Vandamme,E.J., De Baets,S., Vanbaelen,A., Joris,K. and De Wulf,P. (1998) Improved production of bacterial cellulose and its application potential. *Polymer Degradation and Stability* **59**, 93-99.

Williams,W.S. and Cannon,R.E. (1989) Alternative environmental roles for cellulose produced by Acetobacter xylinum. *Applied and environmental microbiology* **55**, 2448-2452.

Wong,H.C., Fear,A.L., Calhoon,R.D., Eichinger,G.H., Mayer,R., Amikam,D., Benziman,M., Gelfand,D.H., Meade,J.H. and Emerick,A.W. (1990) Genetic organization of the cellulose synthase operon in Acetobacter xylinum. *Proceedings of the National Academy of Sciences* **87**, 8130-8134.

Wu,J.M. and Liu,R.H. (2013) Cost-effective production of bacterial cellulose in static cultures using distillery wastewater. *Journal of Bioscience and Bioengineering* **115**, 284-290.

Yamanaka,S., Watanabe,K., Kitamura,N., Iguchi,M., Mitsuhashi,S., Nishi,Y. and Uryu,M. (1989) The structure and mechanical properties of sheets prepared from bacterial cellulose. *J Mater Sci* **24**, 3141-3145.

CHAPTER 3

The influence of Mechanical and Chemical based pretreatments on native cellulose structure

William D. Graham[1,2], Andrew Moore[1], Stephanie L. Mathews[1,2], Christina Stolarchuk[2], Sunkyu Park[1] Joel J. Pawlak[1,*], Amy Grunden[2], *Manuscript in preparation*

[1]Department of Forest Biomaterials, North Carolina State University, Raleigh NC 27695

[2]Department of Microbiology, North Carolina State University, Raleigh NC 27695

Abstract

The global initiative for economic reform has catalyzed a new era of cellulosic research. Abundant worldwide, cellulose has become the primary candidate precursor for the development of ethanol based fuels, biocompatible medical implants and energy efficient liquid crystal displays. This diversity in application has led to the establishment of many different levels of cellulose research that range from the macro scale to the nano-scale. In this study, we highlight the nano-scale and discuss the importance of understanding the structural characteristics of cellulose. Composed of amorphous and crystalline regions, the x-ray diffraction (XRD) pattern of cellulose is highly dependent on the polymers inherent crystalline properties. Using bacterial cellulose (BC) as a model, we demonstrate the importance of proper sample preparation and how crystalline index values can be significantly influenced by pressure or through the milling/cryogenic homogenization of BC fibers. The influence of salinity on the crystalline structure of never dried BC was investigated by XRD, and it was demonstrated that the addition of salt at a concentration of 19 mmol l^{-1} restores intensity to peaks 110 (14.6°) and $1\bar{1}0$ (16.4°) of wet cellulose. Additionally, an observed shift of 1° in peak $1\bar{1}0$ as a consequence of aqueous water leaving BC during desiccation is reported. When purified BC samples are dried using a freeze dryer, the native structure of the BC is preserved and the 1º shift from 16.4° to 17.4° in the $1\bar{1}0$ peak is not observed in resulting XRD diffractograms.

3.1 Introduction

The commercial, industrial and academic interest in cellulose has led to the development of unique collaborations that blend biological concepts with engineering based problem solving. This melding of philosophies has resulted in the development of revolutionary technologies that involve medical, industrial and textile applications (Gatenholm and Klemm 2010; Ummartyotin *et al*. 2012). Despite these technological advancements, the liberation and processing of cellulose from plant matter is still extremely inefficient, resulting in the accumulation of low value organic materials such as lignin and hemicellulose (Nigam and Singh 2011). A more efficient process that allows for the preservation of higher value sugars associated with hemicellulose would enhance the economic viability of lignocellulosic commodities. A novel method for achieving this goal is characterizing the structural and biochemical relationship between cellulose, hemicellulose and lignin *in vivo*. By thoroughly understanding cellulose structure, enzymes can be engineered for more efficient cellulose saccharification. In this study, we illustrate the importance of properly preparing cellulose for analytical evaluation by x-ray diffraction (XRD).

The proper analysis and evaluation of cellulose structure is essential for the development of better liberation and saccharification techniques. Cellulose consists of a amorphous region and crystalline region (O'sullivan 1997). The crystalline structure of cellulose can change based on pretreatment. The most native state of cellulose is referred to as cellulose I, which is thought to consist of the two polymorphs Iα and Iβ. Through exposure to heat and strong chemicals, the conformation of cellulose I can be shifted to a cellulose II, cellulose III or cellulose IV conformation (Davis *et al*. 1943; Hess and Kissig 1941). A common cellulose allomorph is cellulose II which arises from the regeneration

(exposure to NaOH) or mercerization of cellulose. Cellulose II is thermodynamically more stable compared to cellulose I, making it the preferred conformation for a number of industrial based applications (Kolpak and Blackwell 1976).

Gluconacetobacter hansenii (*G. hansenii*) is a gram negative aerobic bacterium that synthesizes cellulose from a variety of carbon sources (Brown and Saxena 2000). A model organism for cellulose synthesis, *G. hansenii* produces cellulose free of hemicellulose and lignin, making it ideal for cellulose studies. Chemically identical to plant based cellulose, bacterial cellulose (BC) is easily converted to cellulose II using a standard chemical purification technique (Dinand *et al*. 2002).

The analysis of cellulose crystallinity by x-ray diffraction can be accomplished through a variety of calculations. In this study, we use amorphous region subtraction, which involves the subtraction of an amorphous standard from the area beneath the observed cellulose crystalline peaks (Park *et al* 2010). There are at least four crystalline peaks in most cellulose samples that can be observed by XRD; however, for this study, due to the small nature of the fourth peak, we used the 2θ peaks in the regions of 14.6° (110), 16.4° ($1\bar{1}0$) and 22.6° (200). The crystallinity, also referred to as the crystalline index, is then calculated based on the remaining crystalline area relative to the fitted amorphous region (Park *et al*. 2009). In this study, we used a XRD function to optimize amorphous region line fits (Park *et al*. 2010). The antiparallel chain motif of cellulose II results in the overlap of diffraction intensities, making cellulose II unreliable in some cases for true XRD based studies (O'sullivan 1997). We simulate this observation using cryogenic homogenization and pressure. As a means of quantifying this occurrence, an equation was derived to determine the amount of crystals that become aligned and are no longer visible by XRD.

We refer to this value as the % crystalline region shift. Finally we demonstrate how the addition of counter ions to wet cellulose restores amplitude to 2θ peaks at 14.6 °and 16.4°.

3.2 Materials and methods

Bacterial strain and growth conditions

The strain of *Gluconacetobacter hansenii* that was used in this study was ATCC 23769 obtained from the American Type Culture Collection, Manassas, VA (ATCC). The stain was cultured and plated in accordance with the provided ATCC protocol. For this study a primary 250 ml culture was established using Hestrin and Schramm media (SH) (Hestrin and Schramm 1954) under static conditions and maintained at 30°C. SH media components: 12% citric acid, 2% glucose, 0.5% peptone, 0.27% sodium phosphate (dibasic), 0.5% yeast extract and 0.57% magnesium sulfate. To produce pellicles of equal size and depth, disposable petri dishes containing 30 ml of SH media were inoculated with 1 ml of primary culture. The plates were incubated at 30°C for 14 days.

BC purification

Pellicles were purified using a 1% base solution: DiH_2O rinsed pellicles were immersed in a boiling solution of NaOH for two 2 h followed by an acid bath in 255 mM acetic acid overnight (Maneerung *et al*. 2008). Thoroughly rinsed pellicles were placed in 50 ml tubes or cryogenically homogenized, frozen by liquid nitrogen immersion and subsequently freeze dried. Freeze dried samples were placed in a desiccator and held under vacuum. A set of purified BC pellicles were oven dried at 90ºC or allowed to air dry then placed under desiccation.

Ground cellulose preparation

After initial processing, a set of BC samples was cryogenically homogenized using a sterilized, pre-frozen mortar and pestle. Pellicles were placed in the center of the pestle and immersed in liquid nitrogen. Homogenized BC was placed back in a sterile pre-frozen tube, cryogenically stored in liquid nitrogen and freeze dried. Whatman paper No. 1 (FP) was ball milled and passed through a 40 mesh screen.

Chemical analyses

Full (not homogenized) and cryogenically homogenized 3 mg freeze dried samples were analyzed by FT-IR, using a Nexus FT-IR 670 in the range of 4000 to 500 cm^{-1} with a resolution of 4 cm^{-1} and after the accumulation 64 scans. Cryogenically homogenized or milled samples for FT-IR were pressed at 168 MPa, 335 MPa, 600 MPa or 670 Mpa for 10 min using a Perkin Elmer pellet press (Perkin Elmer, Waltham, MA) into 1.5 mm thick disk with a diameter of 13 mm.

Structural analysis

The number-average degree of polymerization (DP_n) for freeze dried BC samples was calculated based on glucose monomers using a BCA reducing end assay. X-ray diffraction (XRD) was performed with a Rigaku Smartlab XRD (Rigaku, The woodlands, TX) using Cu radiation generated at 40 kv and 44 mA. The Bragg angle of 2θ was scanned from 9° to 41° with a step distance and exposure time of 5 s. Freeze dried 20 mg samples were used for analysis. Crystalline index values of treated BC were calculated from XRD spectra using amorphous region subtraction. The resulting spectra were analyzed and normalized

and averaged for comparison. The % crystalline region shift was determined using the following equation where 2θ Peaks = (14.6°, 16.4°, 22.6°):

$$\%\,\text{Crystalline Region Shift} = 100 - \left[\frac{\text{Sum of 2}\theta\text{ Peak amplitudes at Pressure X}}{\text{Sum of 2}\theta\text{ Peak amplitudes at Pressure 0}} \times 100\right]$$

Cellulose water association XRD experiments were performed on never dried cellulose by cutting 4 equal weight squares from DiH_2O saturated cellulose pellicle. Two of the resulting squares were incubated in a solution of DiH_2O or 19 mM saline solution. The remaining two were freeze dried or oven dried. The DiH_2O cellulose square was analyzed at 99.5% DiH_2O saturation and then allowed to air dry for 45 min, weighed and reanalyzed by XRD at 84.2% DiH_2O. The DiH_2O cellulose was air dried overnight and reanalyzed by XRD the following day. The results from the DiH_2O spectra were then compared to the diffractograms of freeze dried, oven dried and saline saturated samples.

Cellulase assays

The purified BC were evaluated for their susceptibility to enzymatic saccharification by 2,4-dinitrosalicyclic acid (DNS) cellulase activity assay (Wood and Bhat 1988). Whatman filter paper grades 1 and 42 served as references (data not shown). The assay was adapted from Balsan *et al.* (2012) (Balsan *et al*. 2012). A total of 0.322 mg of cellulase from *Trichoderma reesei* ATCC 2691 (Sigma, St. Louis MO) was added to 20 mg of cellulose substrate (filter paper or bacterial cellulose) and 2 ml, 0.2 M sodium acetate ($C_2H_3NaO_2$)

buffer, pH 5.5. The mixture was incubated at 50°C for one hour. Enzymatic activity was measured by monitoring the release of reducing sugars. Briefly, 1.5 ml of cellulose-enzyme solution was added to 3 ml of DNS reagent, boiled for 5 minutes, cooled to room temperature under running water, and the absorbance read at 540 nm (Wood and Bhat 1988). Susceptibility of the BC to enzymatic saccharification was determined by the amount of sugar released after a 20 min digestion period.

SEM

Field emission scanning electron microscopy (FE-SEM) was performed on purified BC using a JEOL 6400 cold field emission microscope (JEOL, Peabody, MA, USA).

3.3 Results

FT-IR Transmission

The purified BC samples were analyzed for purity using FT-IR transmission. Both full (BC Sheet) and cryogenically homogenized BC were analyzed to evaluate which sample provided the highest resolution spectra by IR (Fig. 3-1). The cryogenically ground BC (Fig. 3-1b) provided the highest resolution spectrum, closely matching the profile of bleached wood fibers (Fig. 3-1c).

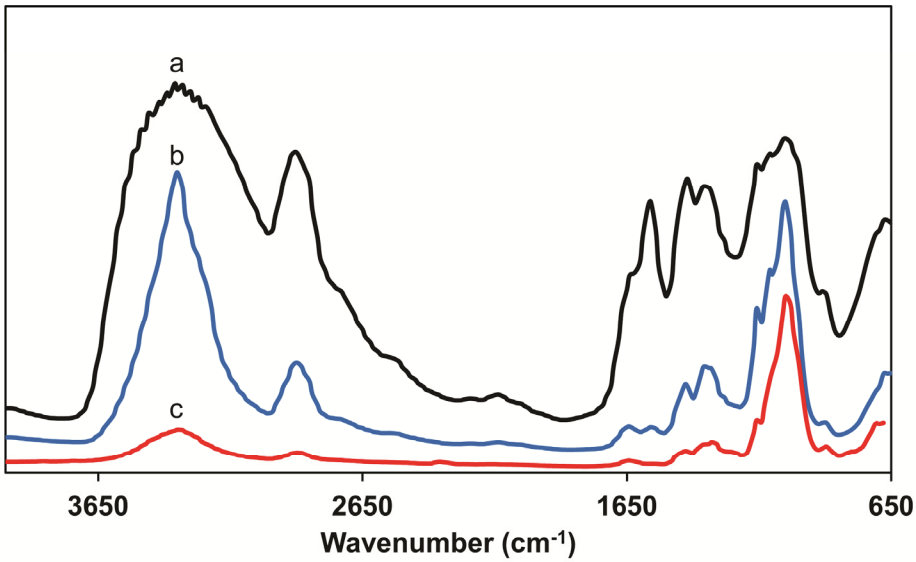

Figure 3-1. FT-IR transmission Spectra of (a) 1% base purified bacterial cellulose (b) 1% base purified bacterial cellulose Cryo-homogenized and pressed (c) wood pulp

XRD Pressing

To characterize the influence of pressure on cellulose fibers when evaluated by XRD, a series of FP and BC samples (full and homogenized) were placed under increasing amounts of pressure. A review of figure 3-2 illustrates the significant change in peak amplitude(s) is observed at varying degrees of pressure in BC samples. The amplitude of peak 16.4° 2θ appears to be the most affected by pressure resulting in an 80% reduction in height with the addition of 670 MPa of pressure. A comparison of the resulting crystalline intensity (C.I.) found in table 3-1 suggest the addition of pressure significantly influences the observed C.I. value as determined by amorphous region subtraction. The C.I. values appear to inversely correlate with the level of pressure applied to the BC sample until a

pressure of 670 MPa is reached, where a slight increase in C.I. value is observed. The addition of 670 MPa also results in the highest %

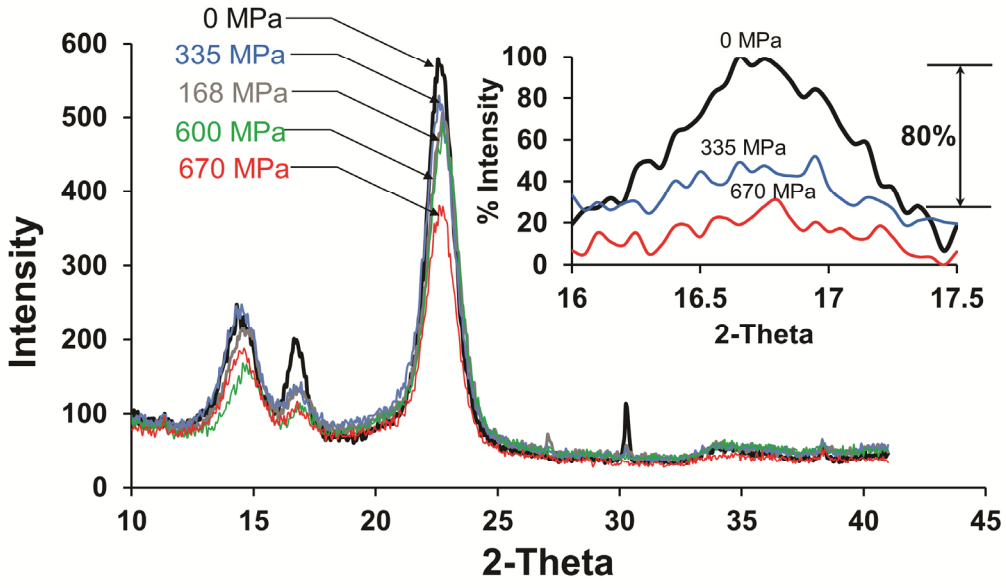

Figure 3-2. XRD of bacterial Cellulose (BC) under varying degrees of pressure: (−) 0 MPa , (−) 168 MPa , (−) 335 MPa, (−) 600 MPa, (−) 670 MPa

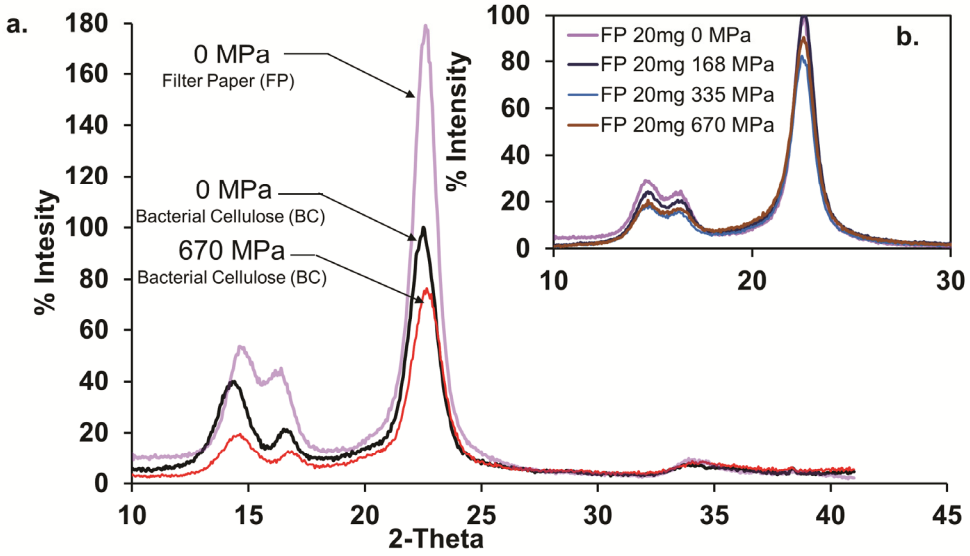

Figure 3-3 Normalized XRD spectra of (a.) 20mg of BC fibers under (–) 0 MPa and (–) 670 MPa compared to 20mg of FP under (–) 0 MPa of pressure. (b.) Normalized XRD spectra of 20mg of FP fibers under varying pressure conditions: (–) 0 MPa , (–) 168 MPa , (–) 335 MPa, (–) 670 MPa.

Table 3-1. Bacterial cellulose peak amplitude and crystallinity at varying degrees of pressure.

Pressure (MPa)	**Peak 1** (14.6°)	**Peak 2** (16.4°)	**Peak 3** (22.6°)	**% Crystalline Region Shift**	**C.I. Vlaue** (amorphous region subtraction)
0	24.80	13.26	61.94	0.00	81.8 ± 0.24
168	17.24	10.19	51.63	20.94	76.6 ± 0.22
335	18.11	11.03	38.05	32.82	74.9 ± 0.25
670	11.61	7.53	47.43	33.44	75.3 ± 3.75

Table 3-2. Filter paper peak amplitude and crystallinity at varying degrees of pressure.

Pressure (Mpa)	**Peak 1** (14.6°)	**Peak 2** (16.4°)	**Peak 3** (22.6°)	**% Crystalline Region Shift**	**C.I. Value** (amorphous region Subtratction
0	18.98	15.89	65.12	0.00	77.4 ± 0.32
168	14.42	12.89	65.12	7.56	76.9 ± 0.28
335	11.26	9.82	51.80	27.12	75.5 ± 0.33
670	11.83	11.05	59.07	18.05	69.1 ± 2.98
1005+	12.49	12.34	57.21	17.93	72.10

crystalline region shift, however, a more uniform depression pattern in peak amplitude is observed. Although the same trend is observed in a FP paper model (Fig. 3-3), a more proportional decrease in magnitude was observed in the 2θ peaks 14.6° and 16.4°. The highest percent crystalline region shift of FP is 27.12, which is observed at 335 MPa (Table 3-2). In an attempt to obtain an increase in FP C.I. as a result of high pressure, FP was pressed under 1,005+ MPa and evaluated by XRD. Although, an increase in C.I. was observed, statistical analysis suggests the change in CI to be negligible. To evaluate the influence of sample quantity on the intensity of the resulting XRD diffractorgrams, the 20 mg spectra of BC was compared to the 20 mg spectra of FP (Fig. 3-3a), resulting in the normalized intensity of FP being 80% higher than BC. The influence of homogenization on sample intensity was also investigated using both BC and FP samples. The cryogenic homogenization and exposure of BC to 670 MPa of pressure resulted in a further reduction in x-ray intensity (Fig. 3-4a), where an 88% drop in

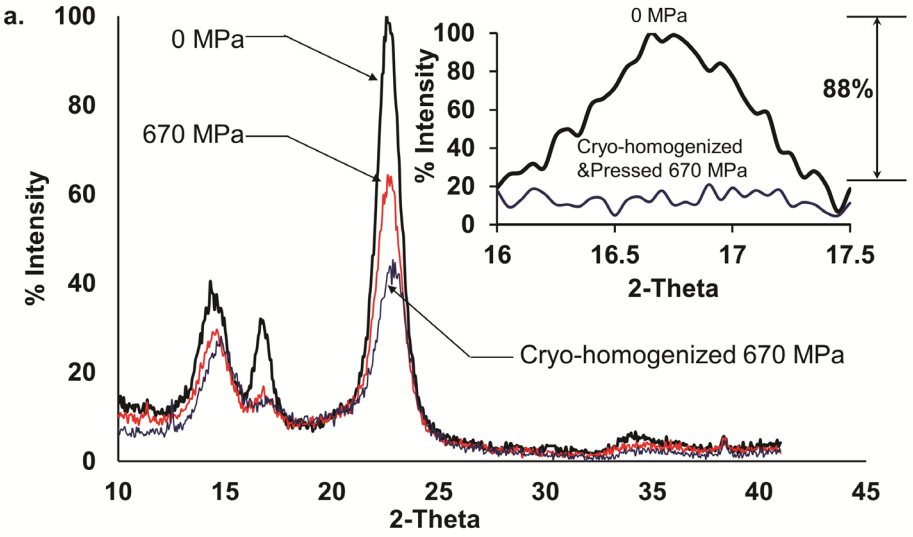

Figure 3-4. Normalized XRD spectra of (a.) 20 mg of BC fibers under (–) 0 MPa, (–) 670 MPa and (–) 670 Mpa post cryo-homogenization. (b.) 20 mg fibers of FP under (–) 0 MPa, (–) 670 MPa and (–) 670 MPa post homogenization.

amplitude is observed in the peak at 16.4°. The same result was observed in milled FP samples where a 57% drop in amplitude was observed in peaks at both 14.6° and 16.4° (Fig. 3-4b). The calculated C.I. values for both BC and FP (Table 3-3 and Table 3-4) were the lowest after homogenization. The % crystalline shift for both samples was also greater than 50% suggesting the pre-homogenization of samples before pressing, results in a significant drop in x-ray intensity.

Table 3-3. Cryo-homogenized bacterial cellulose peak amplitude and crystallinity at varying degrees of pressure

Pressure (MPa)	**Peak 1** (14.6°)	**Peak 2** (16.4°)	**Peak 3** (22.6°)	**% Crystalline Region Shift**	**C.I. Value** (amorphous region subtraction)
0*	24.80	13.26	61.94	0.00	81.8 ± 0.24
670	13.42	7.34	23.48	55.76	65.3 ± 0.45
670*	11.61	7.53	47.43	33.44	75.3 ± 3.75

* Not homogenized

Table 3-4. Homogenized filter paper peak amplitude and crystallinity at varying degrees of pressure**.**

Pressure (MPa)	**Peak 1** (14.6°)	**Peak 2** (16.4°)	**Peak 3** (22.6°)	**% Crystalline Region Shift**	**C.I. Value** (amorphous region subtraction)
0*	18.98	15.89	65.12	0.00	77.4 ± 0.32
670	9.85	8.47	29.65	52.03	59.1 ± 3.98
670*	11.83	11.05	59.07	18.05	69.1 ± 2.98

* Not homogenized

XRD on never dried cellulose

The influence of water on cellulose structure evaluated by XRD was performed using five BC samples of equivalent weight. In figure 3-5a, a similar trend to what was observed in the pressing experiments is observed here, with the 14.6° and the 16.4° peaks experiencing the greatest amount of influence from the addition of DiH_2O. The 22.6° peak is still visible at 99.5% DiH_2O saturation. The addition of salt to the media, however, resulted in the reappearance of peaks at 14.6° and 16.4° (Fig 3-5b). The method used for drying also influences the profile of XRD spectra. The removal of water in the liquid phase results in the shifting of the 2θ peak at 16.4° over to the 17.5° region. Freeze dried samples appear to give a true representation of cellulose crystalline structure as determined by XRD.

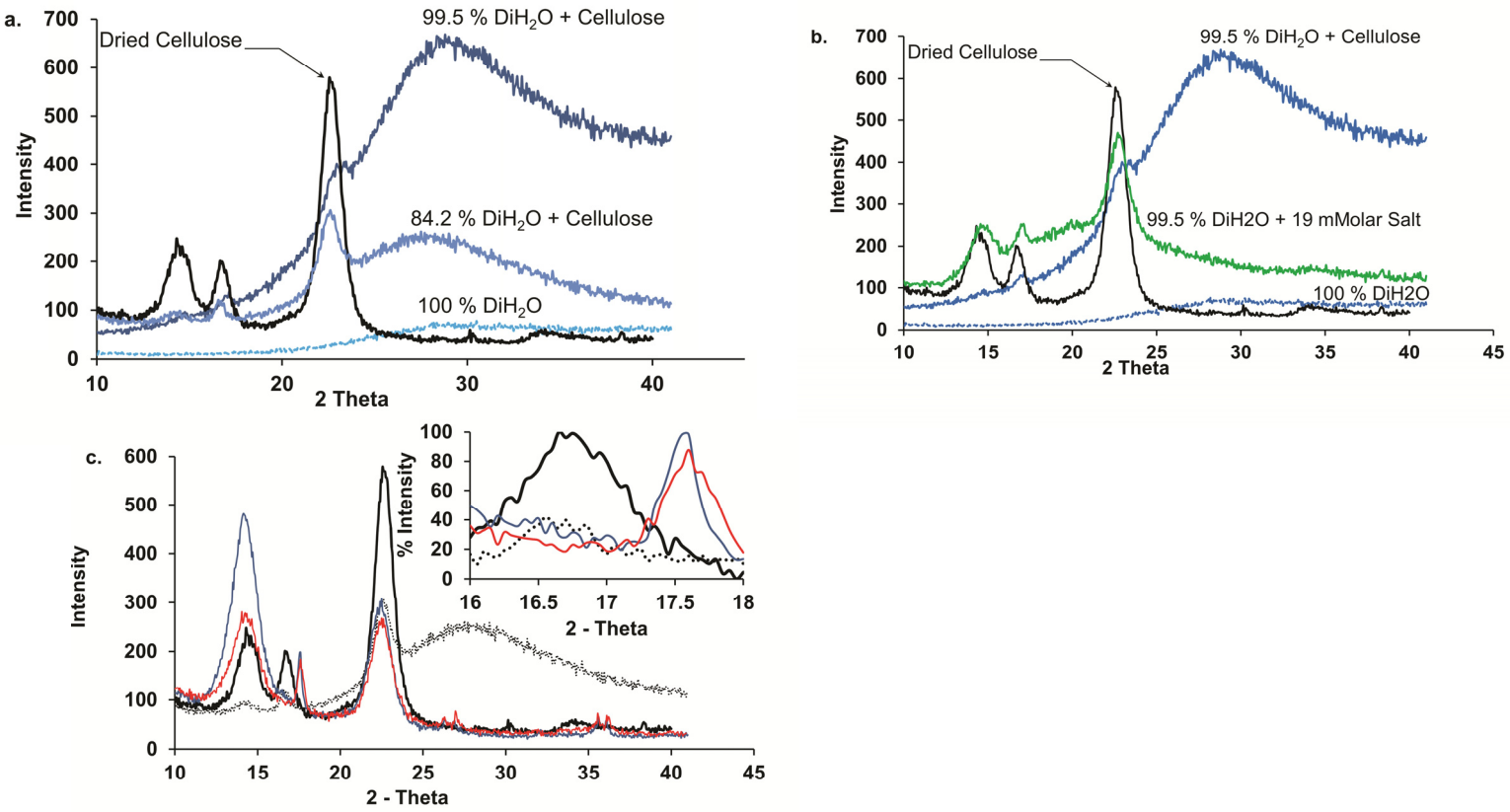

Figure 3-5. XRD spectra of (a.) BC under varying DiH_2O saturation levels. (b.) BC 99.5% staturated with DiH_2O with and without the addition of 19 mM NaCl. (c.) BC dried using (−) freeze drying, (−) air drying, (−) oven drying and (−) BC 85% saturated with DiH_2O.

Influence of homogenization and pressing on DP_n and enzymatic saccharification cryogenically homogenized BC and milled filter paper exhibited reduced DP_n values compared to non-ground (Table 3-5). The best rate of saccharification was observed in ground samples, while a significant decline in enzyme efficiency was observed in pressed samples (Table 3-6).

Table 3-5. Number-average degree of polymerization (DP_n) by the BCA method

Samples	DP_n Value
Bacterial Cellulose (BC)	606 ± 41
homogenized BC	541 ± 42
Filter Paper (FP)	3865 ± 89
Homognized FP	2553 ± 93

Table 3-6. The relationship between bacterial cellulose preparation and cellulase activty evaluated using the DNS D - glucose detection method.

Sample (cryo-ground)	Concentration of D-Glucose mg ml^{-1}		
Cryo-Ground Pellicle	2.33	±	2.28E-01
Non-Ground Pellicle	1.1633	±	7.09E-02
168 MPa	0.135	±	5.02E-03
335 MPa	0.106	±	3.12E-03
670 MPa	0.0915	±	2.20E-03

SEM

The electron micrographs in figure 3-6 illustrate the difference in diameter of BC based fibers compared to plant based fibers.

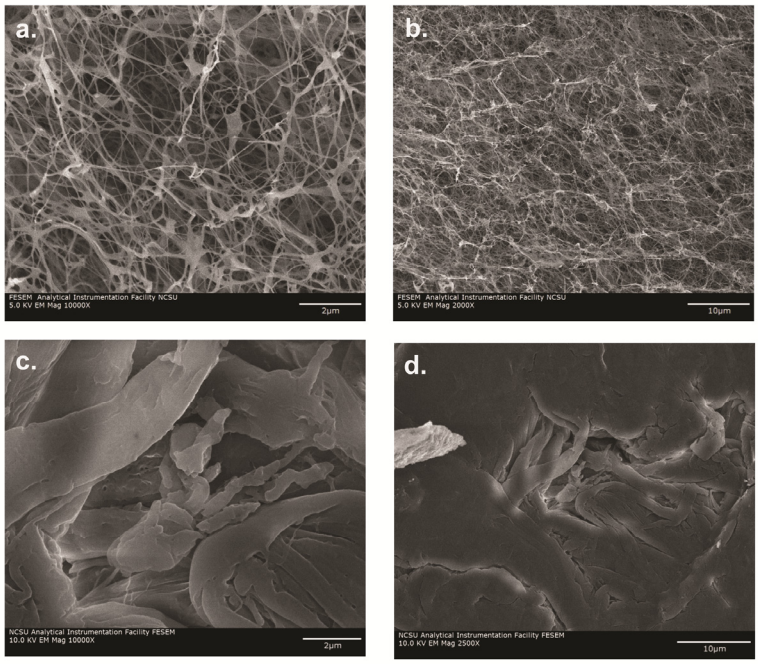

Figure 3-6. Scanning electron microscope images of (a.) Cryogenically homogenized 1% base treated BC at a magnification of 1000X (b.) Cryogenically homogenized 1% base treated BC at a magnification of 2000X (c.) homogenized sample of FP at a magnification of 1000X (d.) homogenized sample of FB at a magnification of 2000X

3.4 Discussion

When performed properly, FT-IR can be a powerful and efficient tool for determining sample purity. The cryogenic homogenization of BC fibers results in better film formation without the addition of hydroscopic thickeners, such as KBr. The spectrum produced from

the homogenized BC was nearly identical to the wood based control fiber suggesting all impurities were successfully removed from the BC pellicle.

As theorized, the addition of pressure resulted in the reorientation of the antiparallel glucan chains into overlapping diffraction patterns (O'sullivan 1997). The 2θ peak at 16.4° appears to be the most influenced by this phenomenon, experiencing an 80% drop in intensity with the addition of 670 MPa of pressure. The calculated C.I. values were significantly affected as a consequence of the variation in peak amplitudes. With the addition of enough pressure, the glucan chains can be oriented back into phase allowing for the relative area beneath the peak(s) to be restored. Since the amorphous region subtraction method is based on ratios (Park *et al*. 2009; Park *et al*. 2010), the calculated C.I. can be observed as increasing, despite a large number of glucan chains falling under the % crystalline region shift category. This trend is observed in BC at a pressure of 670 MPa, where an increase is observed in the C.I. value (Table 3-1.). However an analysis of the XRD spectra in figure 3-2, shows the greatest loss in intensity for all three peaks at 670 MPa. The results from the FP experiments were very similar to BC. The 2θ peaks at 14.6° and 16.4° co-migrated with the addition of pressure whereas the 2θ peak at 16.4° in the BC model significantly decreased in amplitude with the addition of varying degrees of pressure. This observation is likely the result of fiber diameter. BC is 1000 time smaller compared to plant based fibers (Ross *et al*. 1991). The homogenization of both FP and BC resulted in the lowest CI values suggesting that homogenization is not the best way to prepare samples for x-ray diffraction.

The characterization of the interaction of cellulose in water has been difficult at best as a result of not having a clear understanding of native cellulose structure (Chanzy 2011). The characteristic loss in the resolution of 2θ peaks at 14.6° and 16.4° is observed when the

water concentration is the highest. As the sample begins to dry the peaks return, however a shift of almost 1° is observed. Molecular dynamics modeling of cellulose II and its interaction with water suggest that cellulose II crystals do not maintain well under aqueous conditions, resulting in the observed shift in cellulose structure as a result of water leaving (Miyamoto *et al*. 2009). The addition of 19 mM NaCl resulted in the reappearance of 2θ peaks 14.6° and 16.4°, suggesting the salt functioned as a counter ion in solution allowing for more native packing of the cellulose structure under aqueous conditions (Draper *et al*. 2005; Miyamoto *et al*. 2009).

Homogenization of both BC and FP resulted in a slight decrease in DP_n of the cellulose. This may correlate with the enhanced rate of saccharification of the cryogenically homogenized BC. The efficiency of the cellulase is dependent on the accessibility of the substrate (Kuo and Lee 2009). The difference in BC and FP fiber diameter is apparent in the SEM data presented in figure 3-6.

3.5 Conclusion

In conclusion, the results presented in the study demonstrate the high susceptibility of cellulose native structure to mechanical and chemical influence. The addition of pressure results in marked variations in the crystalline profile of BC when evaluated by XRD, which adds an additional layer of complexity when trying to characterize the true native structure of cellulose. More importantly the addition of pressure results in a decline in saccharification efficiency. This a vital point when considering cellulose as a viable candidate for the generation of biofuels and how cellulose is current commercially processed. Using cellulase assays, we also demonstrate how the saccharification efficiency of processed and pressed

wood fibers can be enhanced through milling and other forms of fiber pulverization. In addition to illuminating the mechanical influences on cellulose structure we also shed light on how the glucan chains of cellulose may interact with water. The addition of NaCl to never dried cellulose resulted in a return of crystalline peaks when evaluated by XRD. This suggests that cellulose may interact with water in a very similar manner as nucleic acid. Reminiscent to nucleic acids, the secondary and tertiary structure of cellulose may be highly dependent on steric interactions that strongly influence hydrogen bonding. The addition of salt stabilizes the negative charges running along the backbone (crystalline region) of the glucan chain providing a more structured conformation to the cellulose. Although more research on this observation is required, we demonstrate a novel method for the further characterization of cellulose under aqueous conditions.

3.6 References

Balsan,G., Astolfi,V., Benazzi,T., Meireles,M.A., Maugeri,F., Di Luccio,M., Dal Prí,V., Mossi,A.J., Treichel,H. and Mazutti,M.A. (2012) Characterization of a commercial cellulase for hydrolysis of agroindustrial substrates. *Bioprocess and biosystems engineering* 1-9.

Brown,M.R. and Saxena,I.M. (2000) Cellulose biosynthesis: A model for understanding the assembly of biopolymers. *Plant Physiology and Biochemistry* **38**, 57-67.

Chanzy,H. (2011) The continuing debate over the structure of cellulose: historical perspective and outlook. *Cellulose* **18**, 853-856.

Davis,W.E., Barry,A.J., Peterson,F.C. and King,A.J. (1943) X-Ray Studies of Reactions of Cellulose in Non-Aqueous Systems. II. Interaction of Cellulose and Primary Amines1. *Journal of the American Chemical Society* **65**, 1294-1299.

Dinand,E., Vignon,M., Chanzy,H. and Heux,L. (2002) Mercerization of primary wall cellulose and its implication for the conversion of cellulose IGåÆ cellulose II. *Cellulose* **9**, 7-18.

Draper,D.E., Grilley,D. and Soto,A.M. (2005) Ions and RNA folding. *Annu. Rev. Biophys. Biomol. Struct.* **34**, 221-243.

Gatenholm,P. and Klemm,D. (2010) Bacterial nanocellulose as a renewable material for biomedical applications. *MRS bulletin* **35**, 208-213.

Hess,K. and Kissig,H. (1941) Zur Kenntnis der Hochtemperatur-Modifikation der Cellulose (Cellulose IV). *Zietschrift Physikalische Chemie B* **49**, 235-239.

Hestrin,S. and Schramm,M. (1954) Synthesis of cellulose by Acetobacter xylinum. 2. Preparation of freeze-dried cells capable of polymerizing glucose to cellulose. *Biochemical Journal* **58**, 345.

Kolpak,F.J. and Blackwell,J. (1976) Determination of the structure of cellulose II. *Macromolecules* **9**, 273-278.

Kuo,C.H. and Lee,C.K. (2009) Enhancement of enzymatic saccharification of cellulose by cellulose dissolution pretreatments. *Carbohydrate Polymers* **77**, 41-46.

Maneerung,T., Tokura,S. and Rujiravanit,R. (2008) Impregnation of silver nanoparticles into bacterial cellulose for antimicrobial wound dressing. *Carbohydrate Polymers* **72**, 43-51.

Miyamoto,H., Umemura,M., Aoyagi,T., Yamane,C., Ueda,K. and Takahashi,K. (2009) Structural reorganization of molecular sheets derived from cellulose II by molecular dynamics simulations. *Carbohydrate research* **344**, 1085-1094.

Nigam,P.S. and Singh,A. (2011) Production of liquid biofuels from renewable resources. *Progress in Energy and Combustion Science* **37**, 52-68.

O'sullivan,A.C. (1997) Cellulose: the structure slowly unravels. *Cellulose* **4**, 173-207.

Park,S., Baker,J.O., Himmel,M.E., Parilla,P.A. and Johnson,D.K. (2010) Research Cellulose crystallinity index: measurement techniques and their impact on interpreting cellulase performance.

Park,S., Johnson,D.K., Ishizawa,C.I., Parilla,P.A. and Davis,M.F. (2009) Measuring the crystallinity index of cellulose by solid state 13 C nuclear magnetic resonance. *Cellulose* **16**, 641-647.

Ross,P., Mayer,R. and Benziman,M. (1991) Cellulose biosynthesis and function in bacteria. *Microbiological Reviews* **55**, 35-58.

Ummartyotin,S., Juntaro,J., Sain,M. and Manuspiya,H. (2012) Development of transparent bacterial cellulose nanocomposite film as substrate for flexible organic light emitting diode (OLED) display. *Industrial Crops and Products* **35**, 92-97.

Wood,T.M. and Bhat,K.M. (1988) Methods for measuring cellulase activities. *Methods in enzymology* **160**, 87-112.

CHAPTER 4

Investigation of the structural and thermal behavior of native bacterial cellulose fibers isolated using a protease treatment method

William D. Graham[1,2], Stephanie L. Mathews[1,2], Christina Stolarchuk[2], Andrew Moore[1], Sunkyu Park[1] Joel J. Pawlak[1,*], Amy Grunden[2], *Manuscript in preparation*

[1]Department of Forest Biomaterials, North Carolina State University, Raleigh NC 27695

[2]Department of Microbiology, North Carolina State University, Raleigh NC 27695

Abstract

Cellulose is the most abundant biopolymer on earth. Historically rooted in the paper industry, advancements in colloidal chemistry and the development of novel saccharification techniques have expanded the commercial applications of cellulose to include the production of liquid crystal displays and biofuels. Despite this rejuvenation in cellulosic economics, the establishment of cellulose as a global commodity is significantly hindered by the inefficiencies in cellulose liberation and processing. The current model associated with cellulose liberation from lignin and hemicellulose relies on the use of highly acidic and highly basic reagents resulting in significant alterations to cellulose native structure. In this work we demonstrate how commercially standard liberation techniques significantly influence cellulose structure and function using bacterial cellulose as a model.

Keywords: *Acetobacter xylinum*, *Gluconacetobacter hansenii* 23769, bacterial cellulose, crystallinity and alkalization, cellulose I, cellulose II, purification

4.1 Introduction

Cellulose is the most abundant polymer on earth, making it the most logical candidate precursor for the replacement of fossil fuels (Ayoub *et al*. 2013). The current model for the development of cellulose as a biofuel precursor requires the use of expensive chemical pretreatments that are designed to liberate cellulose from hemicellulose and lignin. The process is extremely inefficient and results in a physical alteration to the native cellulose structure (Kuo and Lee 2009). *Gluconacetobacter hansenii* ATCC 23769 (*G. hansenii*) is a gram negative bacterium that has been well characterized and is considered an archetype for cellulose biosynthesis (Chawla *et al*. 2009). Different from plant associated cellulose, bacterial cellulose (BC) is synthesized in the absence of hemicellulose and lignin. This unique characteristic suggests BC may serve as a model polymer for analyzing cellulose in its most native state. The isolation and characterization of native cellulose is the first step in analyzing the complex biochemical interactions that occur between hemicellulose, lignin and cellulose *in vivo*. A better understanding of *in vivo* lignocellulosic chemistry would aid in the development of more efficient liberation techniques. This study aims to establish a novel BC purification scheme that preserves native cellulose structure with the intent of developing a model for designing more efficient cellulose liberation techniques.

G. hansenii synthesizes highly crystalline cellulose that chemically, is identical to plant derived cellulose. Under static conditions, *G. hansenii* produces the highest yields of cellulose in the form of a cellulose pad referred to as a pellicle (Schramm and Hestrin 1954). The cultivation of *G. hansenii* under agitated condition results in the formation of cellulose spheres (Bielecki *et al*. 2005). Previous studies characterizing BC produced under various culture conditions suggests BC produced under agitation is structurally different from BC produced under static conditions (Czaja *et al*. 2004). More specifically, cellulose produced

under agitated conditions contains a lower Iα mass fraction compared to cellulose produced under static conditions (Czaja *et al*. 2004). Here we investigate if the structural difference observed in the cellulose is a result of culture conditions or a result of the exposure of the cellulose to purification reagents such as 1% (v/w) NaOH.

Similar to plant based models, BC pellicles must undergo purification to remove secondary organic material such as bacterial cells, proteins, media components and other soluble polysaccharides (Nishi *et al*. 1990). The most common method of purification is the exposure of the pellicle to NaOH (alkali) solutions that range in concentration from 2% to 8% (v/w). The immersion of the pellicle in NaOH effectively dissolves the secondary organics associated with impure pellicles (Lüaskiewicz 1998); however, the crystalline structure of native cellulose is significantly altered. The conformation of the cellulose is irreversibly changed from cellulose I polymorph to cellulose II polymorph (O'sullivan 1997). For some industrial applications, the transformation of cellulose I to the more thermal stable cellulose II is desired; however, for the isolation of native cellulose for biochemical and structural analysis, a more biologically relevant purification scheme is required.

Proteinase K (PK), named for its ability to digest keratin, is a highly active protein digesting enzyme (protease) that was first isolated in 1974 from fermenting bovine horn chips in the presence of manure. The isolation of the protease from the fungus *Tritirachium album* Limber was achieved by submerging the fungus in rich media under fermentative conditions and collecting secreted proteins. PK was isolated for its high proteolytic activity against keratin and its ability to digest native proteins indiscriminately by the hydrolysis of peptide bonds under physiologically relevant conditions. The complete biochemical characterization of proteinase K led to the development of a commercially available protease that revolutionized biochemical assays aimed at the preservation of cellular

components (Ebeling *et al*. 2005). More specifically, when mixed with cellular extract, PK works to digest protein discriminately without disturbing cellular components associated with a high degree of hydrogen bonds (Nucleic Acids) (Crowe *et al*. 1991). The utilization of PK for the purification of bacterial cellulose provides a new technique for the isolation of cellulose in its most native state. As detailed in the literature, the structural characterization of cellulose requires the processing of the raw cellulose in a biologically relevant manner that does not disrupt native hydrogen bonding. PK exhibits a high degree of proteolytic activity against native proteins without the addition of chemicals or heat treatment (Ebeling *et al*. 2005). Because of the mild conditions under which it is active, its use in the purification of BC should minimize modification to the structure of cellulose resulting from the purification process.

In this work, we present a novel technique for removing organic impurities from BC using the protein degrading enzyme PK. This method works to preserve cellulose in its most native conformation with future aspirations of modeling the unique biochemical characteristics of the *in vivo* associated cellulose I polymorph. We also demonstrate the inefficiencies associated with the current methods for cellulose liberation. Structural comparisons performed on PK treated BC and alkali treated BC using thermal gravimetic analysis (TGA), differential scanning calorimetry (DSC) and X-ray diffraction (XRD) illustrate how the current process of cellulose liberation results in the enhanced resistance of the cellulose to enzyme mediated saccharification.

4.2 Materials and methods

Bacterial strain and growth conditions

The strain of *Gluconacetobacter hansenii* that was used in this study was ATCC 23769 obtained from the American Type Culture Collection, Manassas, VA (ATCC). The strain was cultured and plated in accordance with the provided ATCC protocol. For this study a primary 250 ml culture was established using Hestrin and Schramm media (SH) (Hestrin and Schramm 1954) under static conditions and maintained at 30°C. SH media components: 12% citric acid, 2% glucose, 0.5% peptone, 0.27% sodium phosphate (dibasic), 0.5% yeast extract and 0.57% magnesium sulfate. To produce pellicles of equal size and depth, disposable petri dishes containing 30 ml of SH media were inoculated with 1 ml of primary culture. The plates were incubated at 30°C for 14 days

BC purification

Pellicles were removed from petri dishes and purified using 1% base treatment, base only treatment or Proteinase K treatment. The pellicles were rinsed thoroughly in DiH_2O for 24 h to remove loose organic debris at the start of each method. The rinse step was carried out at 4ºC for PK treated BC. 1% based treated Pellicles (BH-BC) were immersed in a boiling 1 M solution of NaOH for 2 h. BH-BC were allowed to cool to room temperature then rinsed in DiH_2O and placed in a 255 mM acetic acid bath overnight. The following day acid washed BH-BC samples were rinsed in DiH_2O until a pH of 7 was reached (Maneerung *et al*. 2008). Pellicles treated using the base only method BO-BC samples, were immersed in a 1 M solution of NaOH and placed at 37°C overnight with gentle stirring. BO-BC were rinsed thoroughly and washed in 255 mM acetic acid for 24 h followed by a final rinse step

to achieve a pH of 7 (Earl and VanderHart 1981). Proteinase K treated pellicles (PK-BC), post 4°C rinse, were placed in petri dishes with 30 ml of 50 mM tris-HCl buffer (pH 8) containing 100 μg μl^{-1} Proteinase K (New England Biolabs, Ipswich, MA). Petri dishes were gently stirred for 24 h at 37°C. PK-BC samples were removed from petri dishes and rinsed thoroughly in sterile DiH_2O at 4°C with gentle stirring. Heat treated proteinase K purified BC (PKB-BC) were boiled post treatment. A 50 mM tris-HCl buffer rinsed pellicle (Tris-BC) and a DiH_2O rinsed pellicle (Utr-BC) were also produced. For comparisons and as a control, an untreated set of BC (NP-BC) was also prepared. All samples for this study were placed in 50 mL tubes or cryogenically homogenized, frozen by liquid nitrogen immersion and freeze dried. Freeze dried samples were placed in a desiccator and held under vacuum.

Cryogenic homogenization

After initial processing, a set of BC samples were cryogenically homogenized using a sterilized, pre-frozen mortar and pestle. Pellicles were placed in the center of the pestle and immersed in liquid nitrogen. Homogenized BC was placed in sterile pre-frozen tubes, cryogenically stored in liquid nitrogen and freeze dried.

Chemical analyses

Full and cryogenically homogenized 3 mg freeze dried samples were analyzed by ATR and FT-IR, respectively, using a Nexus FT-IR 670 in the range of 4000 to 500 cm^{-1} with a resolution of 4 $cm^{-}1$ and after accumulation of 32 and 64 scans, respectively. Cryogenically homogenized samples for FT-IR were pressed at 670 Mpa for 10 min using a Perkin Elmer pellet press (Perkin Elmer, Waltham, MA) into 1.5 mm thick disk with a diameter of 13 mm. Elemental composition (C,N) of freeze dried purified BC was

determined by dry combustion elemental analysis using a Leco True-Specs CHN elemental analyzer.

Thermal analysis

Differential scanning calorimeter (DSC) was performed on 3 mg freeze dried samples using a DSCQ100 (TA Inc., New Castle, DE) with standard sealed aluminum pans (900786.901). The temperature range and heating rate was 25°C - 315ºC or 350°C with a heating rate of 10°C min^{-1} followed by isothermal heating for 5 minutes at 315°C or 350°C. Samples analyzed in the 25°C - 315°C range were subjected to a second temperature ramp using the same thermal protocol. An empty sealed pan was used as reference. Thermal gravimetric analysis (TGA) was performed with a TGA Q500 (TA Inc., New Castle, DE) on 20 mg freeze dried samples under air conditions. The temperature range and heating rate were 30°C - 800°C and 10°C min^{-1} with an isothermal hold at 105°C and 800°C for 10 min.

Structural analysis

X-ray diffraction (XRD) was performed with a Rigaku Smartlab XRD (Rigaku, The woodlands, TX) using Cu radiation generated at 40 kv and 44 mA. The Bragg angle of 2θ was scanned from 9° to 41° with a step and exposure time of 5 s. Freeze dried 20 mg samples were used for analysis. Crystalline index value of treated BC was calculated from XRD spectra using amorphous region subtraction. The resulting spectra were analyzed and normalized and averaged for comparison. Field emission scanning electron microscopy (FE-SEM) was performed on purified BC using a JEOL 6400 cold field emission microscope (JEOL, Peabody, MA, USA). Images were analyzed using imagePro 4.5 software (Mediacybernetics, Rockville, MD). All images were converted to 8 bit grey level images

through an automatic threshold conversion. The image analysis software was then used to count and measure the bright objects (fibrils) using automatic analysis function. The width of the objects was reported and calibration was conducted by using the scale bar integrated with each individual SEM image. Image analysis was conducted on ~45 μm x ~55 μm images resulting in the identification of more than 750 individual fibrils for each image. The results of the automatic processing were confirmed by selecting ten fibril widths in higher resolution images and manually measuring the fibril widths (Pereda *et al*. 2011). The number-average degree of polymerization (DP_n) was calculated based on glucose monomer using BCA reducing end assays on freeze dried BC samples (Kongruang *et al*. 2004; Zhang and Lynd 2005).

Cellulase assays

The purified BC samples were evaluated for their susceptibility to enzymatic saccharification using the 2,4-dinitrosalicyclic acid (DNS) cellulase activity assay (Wood and Bhat 1988). Whatman filter paper grades 1 and 42 served as controls (data not shown). The assay was adapted from Balsan *et al*. (2012) (Balsan *et al*. 2012). A total of 0.322 mg of cellulase from *Trichoderma reesei* ATCC 2691 (Sigma, St. Louis MO) was added to 20 mg of cellulose substrate (filter paper or bacterial cellulose) and 2 ml 0.2 M of sodium acetate ($C_2H_3NaO_2$) buffer, pH 5.5. The mixture was incubated at 50°C for one hour. Enzymatic activity was measured by monitoring the release of reducing sugars. Briefly, 1.5 ml of cellulose-enzyme solution was added to 3 ml of DNS reagent, boiled for 5 minutes, cooled to room temperature under running water, and the absorbance read at 540 nm (Wood and Bhat, 1988). Susceptibility of the BC to enzymatic saccharification was determined by the amount of sugar released after a 20 min digestion period.

4.3 Results

Purity of BC

The effectiveness of the treatments described previously to provide pure native cellulose and remove secondary organic material, such as cell debris and media components, was first evaluated by FT-IR ATR shown in figure 4-1. Raised peaks are observed in 1,637.37 cm^{-1} and 2,350.02 cm^{-1} range of NP-BC (Fig. 4-1a) corresponding to a high nitrogen content and CO_2 trapping. Additionally, a broader hydroxyl peak is observed at the 3,349.60 cm^{-1} peak region suggesting water association. Treatment of the pellicles with DiH_2O (Fig. 4-1b) or 50 mM tris-HCl buffer (Fig. 4-1c) was effective at eliminating the CO_2 peak at 2,350.02 cm^{-1}, most likely due to the removal of cell debris; however, elevated peaks were still observed in the 1637.37 cm^{-1} regions. The profile of PK-BC spectra (Fig. 4-1d) was identical to BH-BC (Fig. 4-1e) and avicel (microcrystalline cellulose) (Fig. 4-1F) spectra, suggesting PK-BC samples are equally pure to the standard base treated pellicles. To confirm these results the PK-BC, BH-BC and avicel were examined by FT-IR transmission (Fig. 4-2). The spectral profile of PK-BC was comparable to BH-BC, further confirming the effectiveness of our treatment scheme. The data presented above are based on standard error where n = 6.

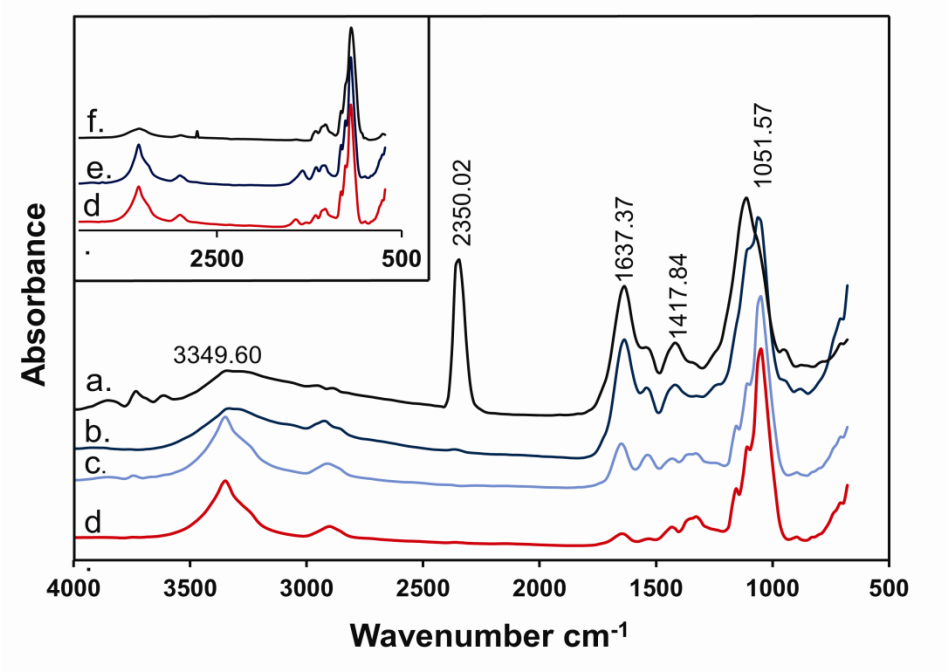

Figure 4-1 Normalized FT-IR ATR spectra of ground (a) Untreated BC (b) DiH_2O rinsed BC (c) 50 mM tris-HCl buffer rinsed BC (d) PK treated BC (e) 1% base treated BC (f) Avicel (n = 6).

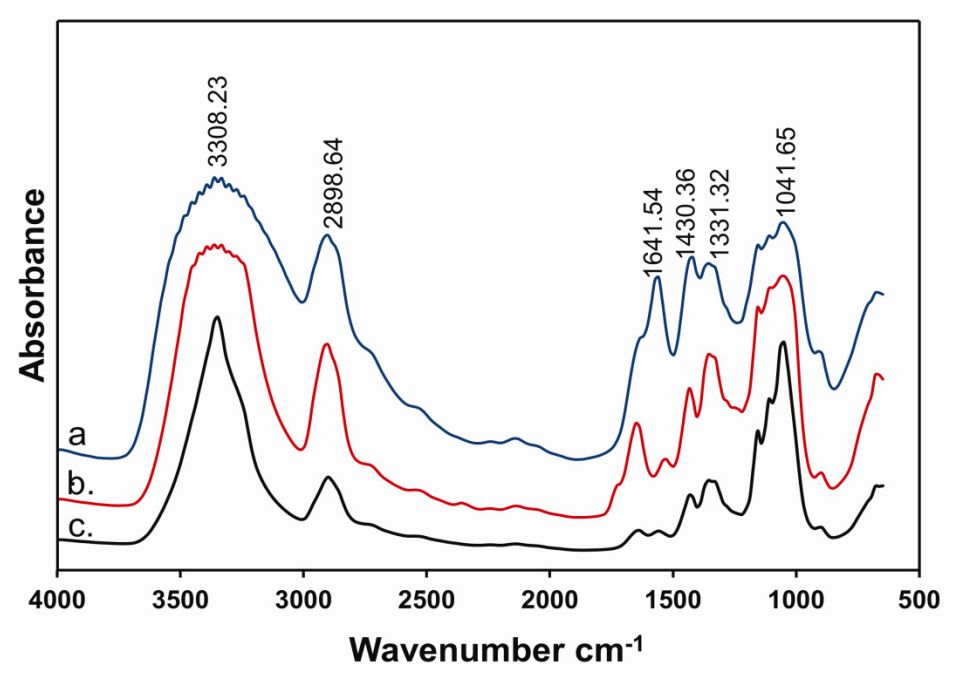

Figure 4-2 Normalized FT-IR transmission spectra of ground (a) 1% base treated BC (b) PK treated BC (c) Avicel (n = 6).

As a final evaluation of BC purity, an elemental analysis (C,N) was performed on all BC pellicles and the results are represented in table 4-1. Although the lowest percentage of nitrogen is observed in the BH-BC, the nitrogen content of PK-BC is close to 10-fold lower than NP-BC and factors no less than five fold below Tris-BC and Utr-BC (n = 3).

Table 4-1. Bacterial cellulose elemental analysis

Sample	% Carbon	% Nitrogen
PK treated BC (PK-BC)	43.16 ± 0.11	0.43 ± 0.02
1% Base treated BC (PK-BH)	43.53 ± 0.04	0.31 ± 0.08
Untreated BC (NP-BC)	44.51 ± 0.13	4.68 ± 1.24
50 mM tris-HCl buffer rinsed BC	45.32 ± 0.24	3.27 ± 0.85
DiH2O rinsed BC (Utr-BC)	31.88 ± 0.07	2.96 ± 0.96

Thermal characterization

To characterize the impact of our treatment on the thermal stability of BC, DSC was performed on all BC pellicles (Fig. 4-3). BH-BC pellicles (Fig. 4-3a) exhibited a normal thermal profile whereas PK-BC undergoes thermal decomposition at a lower temperature, suggesting PK-BC displays a reduced thermal stability relative to BH-BC. An uncharacteristic transition point is also observed in PK-BC at 270°C. Also displaying a reduced thermal structure compared to BH-BC, Utr-BC (Fig. 4-3c), NP-BC (Fig. 4-3d) and Tris-BC (Fig. 4-3e), exhibited additional endothermic peaks in the 50°C to 160°C range, with NP-BC displaying a significantly large endothermic peak at 137°C (n = 3). Based on the purity data, these additional endothermic peaks are likely the result of secondary organics from media components and cell debris. To further characterize the observed transition point in PK-BC at 270°C, a smaller range thermal protocol was used, where the temperature range was condensed to 25°C - 315°C max temperature, to prevent thermal degradation. A second ramp was also used to examine the reversibility of the transition. The DSC thermographic profile of PK-BC (Fig. 4-4a) consistently displayed a slight transition around 270°C; however the transition was irreversible as it was not observed on the second ramp cycle (n = 3). Further thermodynamic studies were performed on PK-BC and BH-BC using TGA where the influence of heat pretreatment was explored using PKB-BC and BO-BC. In figure 4-5a the same results observed in the DSC are observed in the TGA with PK-BC displaying a lower thermal profile in comparison to the 1% base treated BC and the industrially treated avicel. Figure 4-5b is a graphical representation of the temperature PK-BC, BO-BC, PKB-BC and BH-BC undergo the maximum amount of weight loss. The addition of heat to PK-BC and BO-BC results in a thermal stable shift from 314.81 ± 1.45 to

341.14 ± 2.21 and 326.82 ± 2.37 to 347.72 ± 3.75 respectively. These results demonstrate that our treatment is effective at preserving the native state of bacterial cellulose.

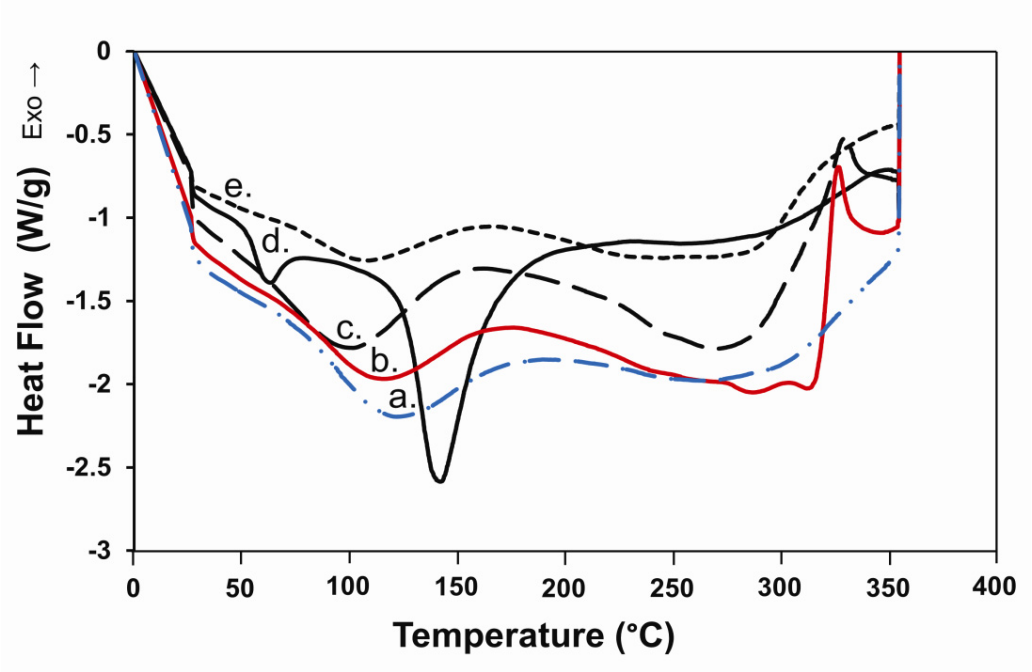

Figure 4-3 DSC Thermograms of ground (a) 1% base treated BC (b) PK treated BC (c) DiH_2O rinsed BC (d) Untreated BC (e) 50mM tris-HCl buffer rinsed BC (n = 3).

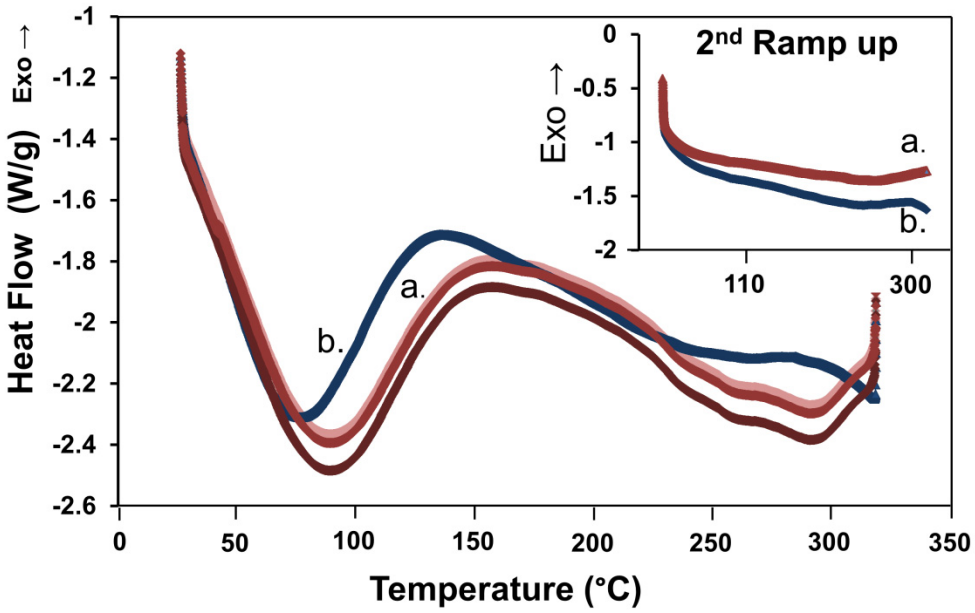

Figure 4-4 DSC Thermograms of ground (a) 1% base treated BC (b) PK treated BC
Insert: Second temperature ramp of treated BC (n = 3)

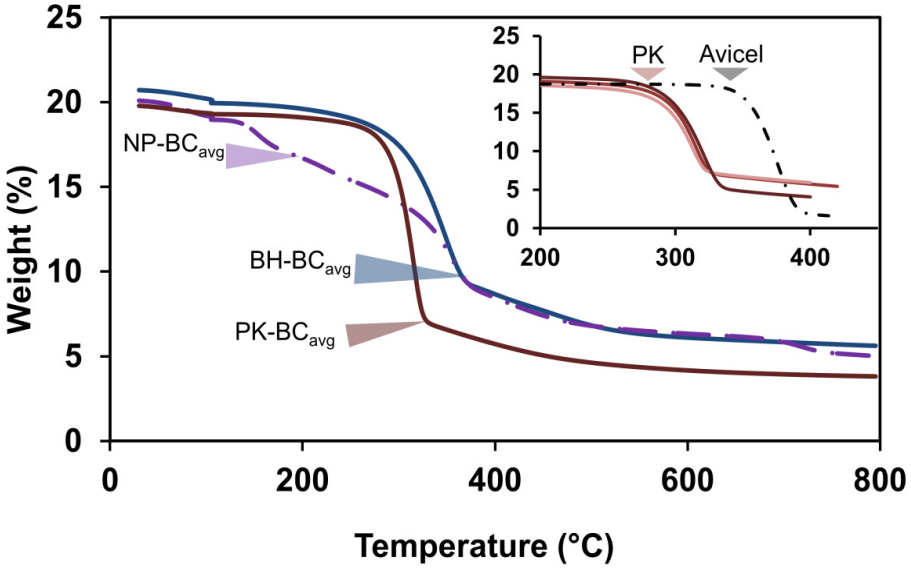

Figure 4-5a TGA Thermograms of Untreated BC (NP-BC), 1% base treated BC (BH-BC) and PK treated BC (PK-BC) and Avicel (n=3).

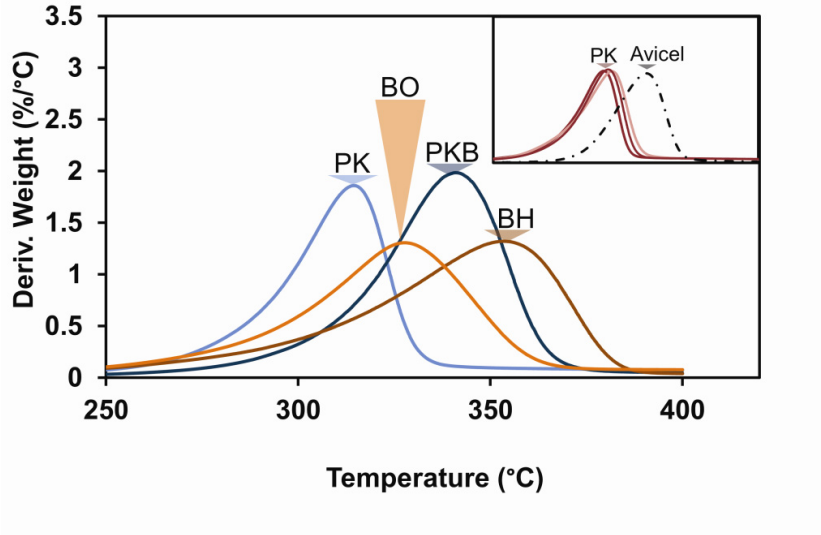

Figure 4-5b TGA thermograms of first derivative weight % of PK-BC, base only treated BC (BO-BC), boiled PK treated BC (PKB) and BH-BC (n = 3).

Structural characterization

The crystalline index (C.I. value) of BH-BC and PK-BC was determined to be XRD and amorphous region subtraction. The XRD spectra of both BH-BC and PK-BC (Fig.4-6) were very similar in profile, explaining the close value in observed C.I. (Table. 4-2). The calculated DP_n value for BH-BC was significantly higher than the DP_n value of PK-BC, further demonstrating the effectiveness of our treatment at preserving glucan chain associated native hydrogen bonding. PK-BC pellicles produced the highest amount of sugar compared to BH-BC pellicles from the cellulase assay, suggesting PK-BC pellicles can undergo enzyme based saccharification at a higher rate compared to BH-BC pellicles.

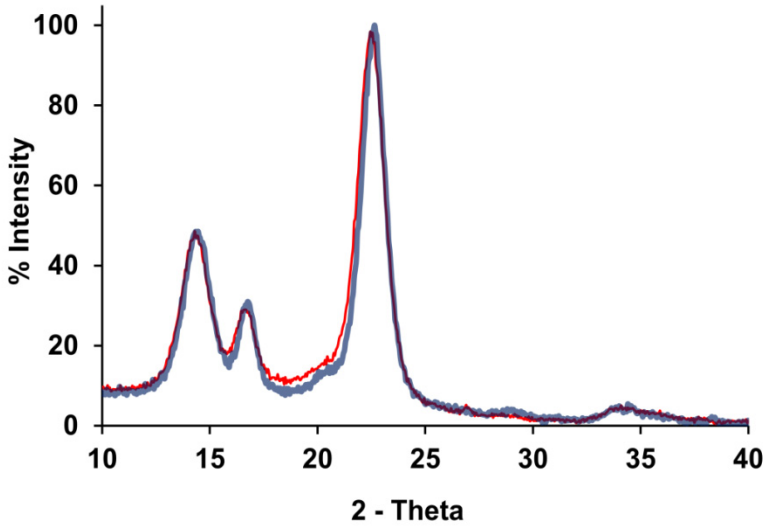

Figure 4-6 XRD spectra overlay comparison of (─) 1% base treated BC and (─) PK treated BC (n = 3).

Table 4-2. Bacterial cellulose fiber physical properties post treatment

Samples	C.I. value	DP_n Value	Cellulase Assay Conc. of D-Glucose mg ml^{-1}
1% Base Treated BC	81.86 ± 0.24	594.45 ± 5.08	2.23 ± 0.23
PK Treated BC	84.21 ± 0.54	225.61 ± 7.69	2.43 ± 0.25

C.I. (n = 3), DP_n (n = 6), Cellulase assay (n = 3)

SEM

SEM images presented in figure 4-7 provide insight into the effects of treatment on the fibrillar structure of the material. Figure 4-7a and 4-7b show the presence of cellular debris found frequently in the rinsed and untreated samples. Figure 4-7c and 4-7d show the differences between the 1% base treated and PK treated samples. Observation of these images indicates that a difference in fibril dimensions exists. A set of lower resolution (larger area) images were used to provide a quantitative measure of the fibril dimension. The image analysis process is described in the experimental methods section. The length of the fibrils was not determined as the dimension often exceeded the area of inspection of the images (i.e. length typically greater than 55 μm). However, the width of the fibrils was determined. Table 4-3 shows a distinct difference in dimension between the two samples with 1 % base samples being 45 % wider than the PK treated samples. This confirms the visual inspection of figure 4-7 where there appears to be a distinct difference in size.

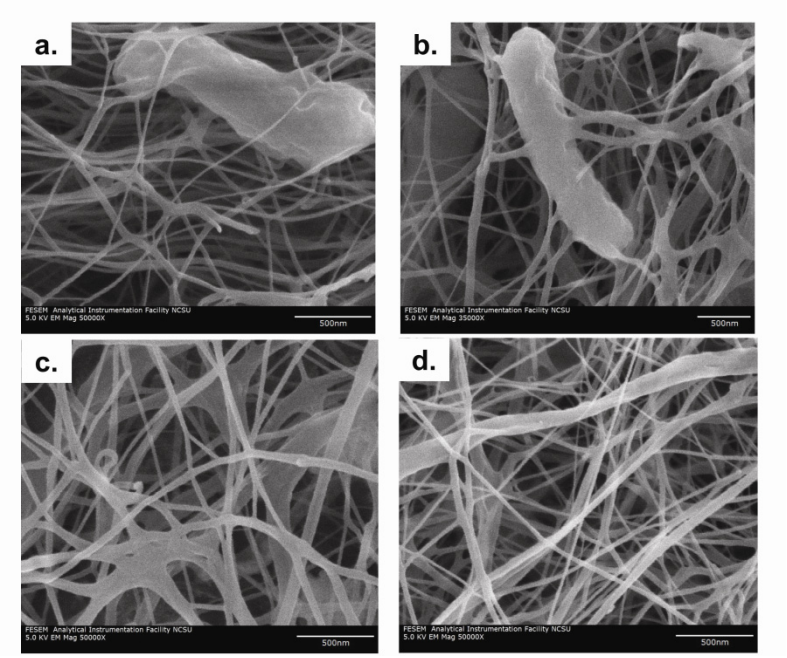

Figure 4-7 SEM images of (a) Untreated BC (b) 50mM tris-HCl treated BC (c) 1% base treated BC (d) PK treated BC

Table 4-3. Average width of bacterial cellulose fibril

Samples	Width Average (nm)	Standard Error (nm)	Sample Size (n)
1% Base Treated BC	177	2	797
PK Treated BC	122	0.4	1003

Bacterial cellulose sphere thermal stability

Cellulose spheres were harvested from agitated cultures to investigate the structural difference between BC produced under static and agitated conditions. The optimized PK treatment method (Fig. 4-8) was used to purify the cellulose spheres. To determine

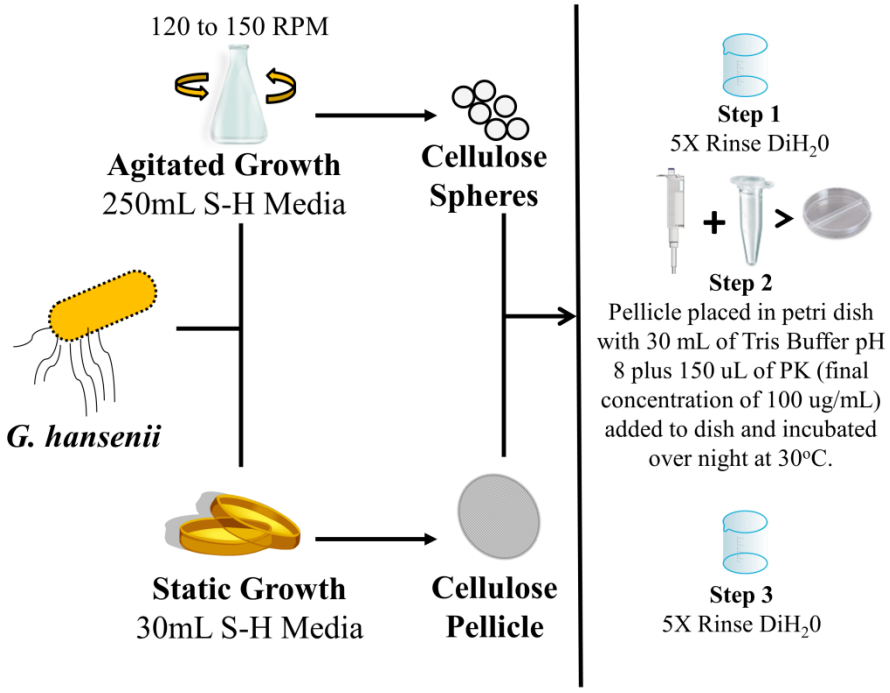

Figure 4-8 Proteinase K (PK) treatment scheme for purifying BC

structural characteristics, the PK purified spheres were analyzed by FT-IR and TGA. The resulting FT-IR spectra mirrored the results from the pellicle purification found in figure 4-2 (data not shown). The analysis by TGA (Fig. 4-9) suggests that, thermodynamically, BC produced under static conditions, is structurally the same as cellulose produced under agitated conditions. Furthermore, BC spheres purified by 1% base treatment exhibited a higher thermal stability compared to BC pellicles (Fig. 4-9b) purified by the same treatment.

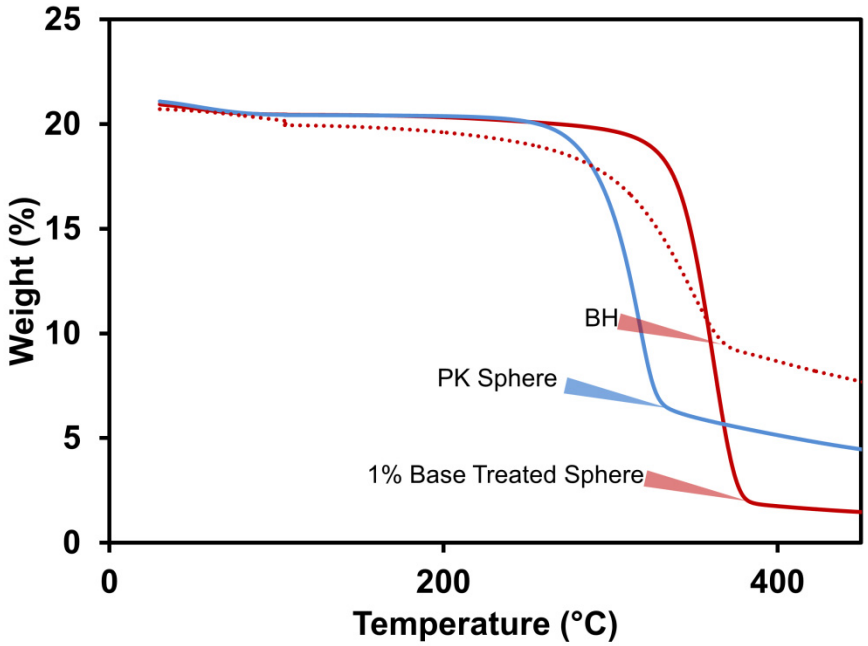

Figure 4-9a TGA thermograms PK treated spheres and 1% base treated BC spheres.

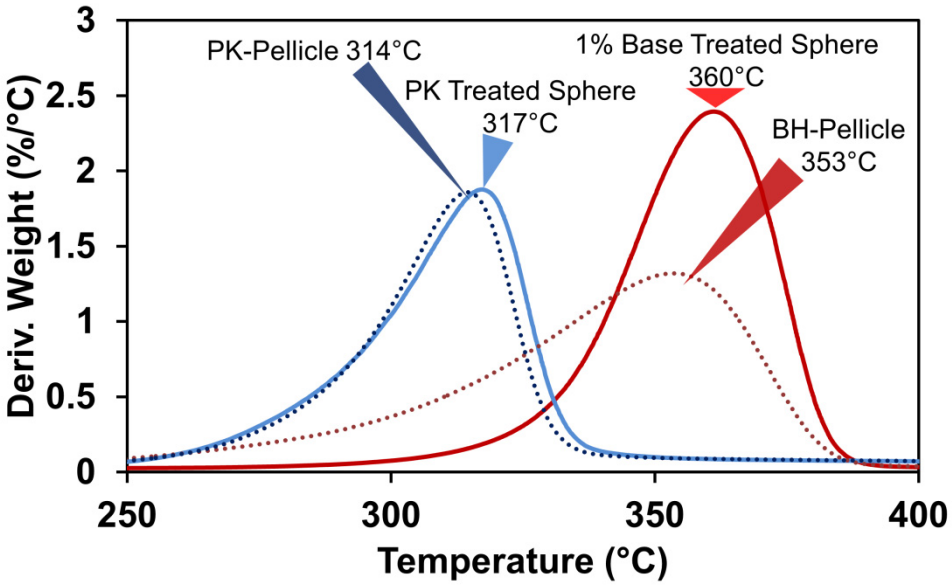

Figure 4-9b TGA thermograms first derivative weight % of (⋯) PK treated spheres,(–) PK treated pellicles (–) 1% base treated BC spheres (⋯) 1% base treated pellicle

4.4 Discussion

Purity of BC

FT-IR ATR was an effective and efficient method of determining the purity of the BC pellicles. Respiration occurring in *G. hansenii* cells results in the release of CO_2, which provides buoyancy to synthesized pellicles (Schramm and Hestrin 1954). The thorough rinsing of the BC pellicles removes loosely associated bacteria and facilitates the release of CO_2 leading to the complete reduction in the CO_2 corresponding peak at 2,350.02 cm^{-1} (Esler *et al*. 2000). The raised peak patterns in the 1,637.37 cm^{-1} region correspond to β-sheet and α-helical structures of proteins (Jackson and Mantsch 1991). The addition of proteinase K results in the reduction of nitrogen content from 2.96% observed in Utr-BC samples to 0.43% ± 0.02 observed in PK-BC samples (Table 4-1). The reduction in nitrogen content can also be observed in the decreased absorbance in the 1.637.37 cm-1 region in the FT-IR transmission spectra. Cryogenically ground BC was used for FT-IR transmission analysis for higher resolution of BC chemical content. The pressed films for BH-BC, PK-BC and avicel gave identical cellulose associated profiles. NP-BC and Utr-BC were also analyzed by FT-IR transmission; however, the amount of impurities contained in these samples resulted in oversaturated spectra. The same trend is observed in the results from elemental analysis (Table 4-1), with NP-BC exhibiting a 10-fold higher concentration of nitrogen. The nitrogen content is reduced with the removal of loosely associated cellular debris, however a five-fold difference is still observed between Utr-BC and PK-BC, as a result of the proteinase K effectively digesting any protein associated with the pellicle.

Thermal characterization

The DSC thermographic profile of PK-BC and BH-BC are nearly identical with the exception of the observed second transition point at 270ºC in PK-BC. It is unclear what this observed transition point is, and as demonstrated in figure 4-4, it appears to be irreversible. The resulting DSC thermographic profiles of NP-BC, Utr-BC and Tris-BC illustrate the impure nature of untreated BC. The lowered thermal stability of PK-BC compared to BH-BC and avicel is the result of the preservation of native cellulose structure (Cellulose I) (O'sullivan 1997). The degradation point of PK-BC is near 324ºC which corresponds to the degradation temperature of the less thermodynamically stable cellulose I polymorph (Nakagaito *et al*. 2005). Thermal stability of BH-BC has been enhanced by the addition of alkali, resulting in the observed increase in degradation temperature to 360ºC, which is characteristic of the cellulose II polymorphs (Nakagaito *et al*. 2005; Yamamoto *et al*. 1989). Although the addition of alkali alone enhanced the thermal stability of BC, as seen in figure 5b, the addition of heat to PK-BC produced a more dramatic change in thermal stability (Nakagaito *et al*. 2005; O'sullivan 1997).

Structural characteristics

The crystalline index of PK-BC is higher compared to BH-BC, which corresponds to the properties of cellulose I and cellulose II polymorphs (Park *et al*. 2010). The XRD spectra of the two samples are nearly identical. The mercerization of cellulose I into cellulose II results in the re-association of glucan chains into a more compacted conformation resulting in enhanced DP (Kuo and Lee 2009). This explains the observed difference in DP_n of PK-BC and BH-BC listed in table 4-2. The compact structure of BH-BC is also evident in the cellulase assay (Table 4-2). The preservation of the native structure allows for better

exposure to saccharification enzymes, leading to more efficient cellulose degradation (Kuo and Lee 2009). The observed enhanced webbing and increased diameter of BH-BC found in figure 7b may also be explained by mercerization of the cellulose (O'sullivan 1997).

Bacterial cellulose sphere thermal stability

The resulting thermograms suggest that BC produced under both agitated and static conditions are thermodynamically the same. Additionally, our results suggest that BC spheres are more susceptible to chemical and thermal influence. This observed difference in thermal stability may be the result of the thin nature of cellulose produced under agitated conditions. In a sphere conformation, a greater surface area of the cellulose is exposed resulting in a high susceptibility to structural shifts as a consequence of heat or chemical influence.

4.5 Conclusion

This work has significant implications in understanding the nature of the cellulose structure as it relates to many fields of application from papermaking to biofuels. This study shows the distinct effect that cellulose purification technique can have on altering the native structure of cellulose. Bacterial cellulose was isolated using a biologically compatible enzyme digestion method. By preventing the exposure to heat, base, or acid, the observed structure and properties of the cellulose are unaltered. The mild enzymatic isolation technique showed that cellulose readily undergoes changes with heat associated pretreatments. This manifests itself in differences in the increased thermal stability of the cellulose and a lower temperature transition as observed in the DSC. XRD did not show

significant differences in the crystalline structure (percent crystallinity or unit cell) suggesting that changes leading to the thermal stability take place outside of the crystalline regions. Furthermore, changes that take place during the heat and base treatment affect the degree of polymerization. Upon heat and base treatment, the DP of the cellulose doubles, which indicates a significant change in the material during treatment. SEM images showed an increase in the fibril width with the addition of base and heat suggesting that the fibrils coalesce during this treatment. A 45 % increase in the fibril width was observed. The changes in the fibrillar and DP of the cellulose lead to slight observed decline in the susceptibility of the fibers to enzymatic hydrolysis (9 %). In conclusion, this work shows that the native cellulose structure is much more susceptible to alteration by what is perceived to be mild chemical and heat treatment than previously understood. Thus, as researchers begin to attempt to identify the controlling factors for cellulose ultrastructure in cellulose biosynthesis, it will be critical to understand the artifacts that may arise due to isolation techniques.

4.6 References

Ayoub,A., Venditti,R.A., Pawlak,J.J., Sadeghifar,H. and Salam,A. (2013) Development of an acetylation reaction of switchgrass hemicellulose in ionic liquid without catalyst. *Industrial Crops and Products* **44**, 306-314.

Balsan,G., Astolfi,V., Benazzi,T., Meireles,M.A., Maugeri,F., Di Luccio,M., Dal Prí,V., Mossi,A.J., Treichel,H. and Mazutti,M.A. (2012) Characterization of a commercial cellulase for hydrolysis of agroindustrial substrates. *Bioprocess and biosystems engineering* 1-9.

Bielecki,S., Krystynowicz,A., Turkiewicz,M. and Kalinowska,H. (2005) Bacterial cellulose. *Biopolymers Online*.

Chawla,P.R., Bajaj,I.B., Survase,S.A. and Singhal,R.S. (2009) Microbial cellulose: fermentative production and applications. *Food Technology and Biotechnology* **47**, 107-124.

Crowe,J.S., Cooper,H.J., Smith,M.A., Sims,M.J., Parker,D. and Gewert,D. (1991) Improved cloning efficiency of polymerase chain reaction (PCR) products after proteinase K digestion. *Nucleic acids research* **19**, 184.

Czaja,W., Romanovicz,D. and Malcolm Brown,R. (2004) Structural investigations of microbial cellulose produced in stationary and agitated culture. *Cellulose* **11**, 403-411.

Earl,W.L. and VanderHart,D.L. (1981) Observations by high-resolution carbon-13 nuclear magnetic resonance of cellulose I related to morphology and crystal structure. *Macromolecules* **14**, 570-574.

Ebeling,W., Hennrich,N., Klockow,M., Metz,H., Orth,H.D. and Lang,H. (2005) Proteinase K from Tritirachium album limber. *European Journal of Biochemistry* **47**, 91-97.

Esler,M.B., Griffith,D.W.T., Wilson,S.R. and Steele,L.P. (2000) Precision trace gas analysis by FT-IR spectroscopy. 2. The 13C/12C isotope ratio of CO2. *Analytical chemistry* **72**, 216-221.

Hestrin,S. and Schramm,M. (1954) Synthesis of cellulose by Acetobacter xylinum. II. Preparation of freeze-dried cells capable of polymerizing glucose to cellulose. *The Biochemical journal* **58**, 345-352.

Jackson,M. and Mantsch,H.H. (1991) Protein secondary structure from FT-IR spectroscopy: correlation with dihedral angles from three-dimensional Ramachandran plots. *Canadian Journal of Chemistry* **69**, 1639-1642.

Kongruang,S., Han,M.J., Breton,C.I.G. and Penner,M.H. (2004) Quantitative analysis of cellulose-reducing ends. *Applied biochemistry and biotechnology* **113**, 213-231.

Kuo,C.H. and Lee,C.K. (2009) Enhancement of enzymatic saccharification of cellulose by cellulose dissolution pretreatments. *Carbohydrate Polymers* **77**, 41-46.

Lüaskiewicz,B. (1998) Solubility of bacterial cellulose and its structural properties. *Journal of applied polymer science* **67**, 1871-1876.

Maneerung,T., Tokura,S. and Rujiravanit,R. (2008) Impregnation of silver nanoparticles into bacterial cellulose for antimicrobial wound dressing. *Carbohydrate Polymers* **72**, 43-51.

Nakagaito,A.N., Iwamoto,S. and Yano,H. (2005) Bacterial cellulose: the ultimate nano-scalar cellulose morphology for the production of high-strength composites. *Applied Physics A: Materials Science & Processing* **80**, 93-97.

Nishi,Y., Uryu,M., Yamanaka,S., Watanabe,K., Kitamura,N., Iguchi,M. and Mitsuhashi,S. (1990) The structure and mechanical properties of sheets prepared from bacterial cellulose. *Journal of Materials Science* **25**, 2997-3001.

O'sullivan,A.C. (1997) Cellulose: the structure slowly unravels. *Cellulose* **4**, 173-207.

Park,S., Baker,J.O., Himmel,M.E., Parilla,P.A. and Johnson,D.K. (2010) Research Cellulose crystallinity index: measurement techniques and their impact on interpreting cellulase performance.

Pereda,M., Amica,G., Racz,I. and Marcovich,N.E. (2011) Structure and properties of nanocomposite films based on sodium caseinate and nanocellulose fibers. *Journal of Food Engineering* **103**, 76-83.

Schramm,M. and Hestrin,S. (1954) Factors affecting Production of Cellulose at the Air/ Liquid Interface of a Culture of Acetobacter xylinum. *Journal of General Microbiology* **11**, 123-129.

Wood,T.M. and Bhat,K.M. (1988) Methods for measuring cellulase activities. *Methods in enzymology* **160**, 87-112.

Yamamoto,H., Horii,F. and Odani,H. (1989) Structural changes of native cellulose crystals induced by annealing in aqueous alkaline and acidic solutions at high temperatures. *Macromolecules* **22**, 4130-4132.

Zhang,Y.-H.P. and Lynd,L.R. (2005) Determination of the number-average degree of polymerization of cellodextrins and cellulose with application to enzymatic hydrolysis. *Biomacromolecules* **6**, 1510-1515.

CHAPTER 5

Summary of work and future prospects

William D. Graham[1,2],

[1]Department of Forest Biomaterials, North Carolina State University, Raleigh NC 27695

[2]Department of Microbiology, North Carolina State University, Raleigh NC 27695

5.1 Review

Bacterial cellulose (BC) is a highly crystalline nano-fiber that is extruded from the cell surface of cellulose synthesizing bacteria in the form of micro-fibrils (Brown *et al*. 1976). These micro-fibrils associate into tightly woven helical structures called ribbons. Depending on the culturing conditions, when grown statically, the micro-fibrils aggregate at the air-liquid interface to form a cellulose pad referred to as pellicles. When cultivated under agitated conditions, cellulose spheres are formed. The nano-fiber morphology of the densely packed BC pellicle results in enhanced absorbent capacity and tensile strength compared to plant derived cellulose (Borzani and Souza 1995). These mechanical and physical characteristics make BC an ideal polymer for a variety of technological advancements that range from biofuel engineering to self-assembling nano-scaffolding for medical applications (David 2009; Fontana *et al*. 1990; Helenius *et al*. 2006; Petersen and Gatenholm 2011). The chemical purity of BC is also of great significance, requiring minimal processing compared to plant cellulose which is generally associated with hemicellulose and lignin. The liberation of plant cellulose results in the isolation of different cellulose polymorphs. Chemical processing causes secondary reactions which perturb the structure of the plant cellulose causing it to change conformations. Different from plant cellulose, BC is synthesized in the absence of hemicellulose and lignin. The current model for BC purification requires the emersion of BC into thermal acid and base solutions to remove cellular debris and extra cellular protein (Maneerung *et al*. 2008). Extensive investigations have been done to determine the structure of cellulose in its most native state (Chanzy 2011). The data generated from these studies however, are based on thermally and chemically treated cellulose. In this study we examine the inherent properties of unprocessed cellulose using unaltered BC synthesized by *Gluconacetobacter hansenii* (*G. hansenii*) as a model.

5.2 Summary of work and future prospects

The solution for the commercial production of BC from *G. hansenii* has proven elusive (Ishihara *et al*. 2002). The enhancement of BC synthesis for industrial purposes has been investigated on a metabolic, molecular and engineering level (Chao *et al*. 2000; Mohite *et al*. 2012; Tal *et al*. 1998). In each of these studies the same conclusion is consistently reached. The enhancement of BC synthesis by *G. hansenii* begins with the removal of cellulose negative phenotypes from culture conditions. In this study we illustrate the importance of this conclusion using kanamycin resistance as a selectable marker. As is true for other biofilm associated EPS matrices (Hoffman *et al*. 2005) cellulose provides high yielding BC producing bacteria with protection from the aminoglycoside kanamycin. When evaluated for cellulose production, *G .hansenii* cells cultured in 50 μg ml^{-1} kanamycin produced a higher amount of cellulose compared to cells cultured in SH media alone. This observation suggests the potential of an additional mechanism not yet explored for the regulation of cellulose synthesis. Furthermore, it is demonstrated that when cultured in the presence of 5% (v/v) cellulase, a complete loss in kanamycin resistance is observed in wild type cultures of *G. hansenii*. A model organism for cellulose synthesis, the availability of the complete genome should allow future studies to examine BC synthesis in response to antimicrobial stimuli in greater detail. More specifically, the link between cellulose synthesis and *in vivo* cyclic di-GMP levels, in response to *G. hansenii* exposure to aminoglycoside antibiotic, should be investigated using the technique(s) outlined in Hoffman *et al* 2005. The results from such a study would not only provide researchers with a powerful tool for understanding biofilm mediated antibiotic resistance, it would also potentially identify an alternative method for the up-regulation of cellulose synthesis by *G. hansenii*.

The ambiguity surrounding the native structure of cellulose is compounded by the absence of an established protocol for the structural analysis of cellulose by x-Ray diffraction (XRD). Using BC as a model, we demonstrate how calculated crystalline index (C.I.) values can be significantly influenced by pressure or through the milling/cryogenic homogenization of BC fibers. The influence of salinity on the crystalline structure of never dried BC was also investigated by XRD, and it was demonstrated that the addition of salt at a concentration of 19 mmol l^{-1} restores intensity to peaks 110 (14.6°) and $1\bar{1}0$ (16.4°) of wet cellulose. This suggests that cellulose may interact with water in a very similar manner as nucleic acid. Reminiscent to nucleic acids, the secondary and tertiary structure of cellulose may be highly dependent on steric interactions that strongly influence hydrogen bonding. The addition of salt stabilizes the negative charges running along the backbone (crystalline region) of the glucan chain providing a more structured conformation to the cellulose. Preliminary in nature, these results help to establish a new model for investigating the structural characteristics of *in vivo* cellulose. Additionally, an observed shift of 1° in peak $1\bar{1}$ 0 as a consequence of aqueous water leaving BC during desiccation is reported. When purified BC samples are dried using a freeze dryer, the native structure of the BC is preserved and the 1º shift from 16.4° to 17.4° in the $1\bar{1}0$ peak is not observed in the resulting XRD diffractograms. The characterization and optimization of BC sample preparation for analysis by XRD resulted in the derivation of protocols designed to provide high resolution spectra for C.I. value determination by amorphous region subtraction. These optimized protocols were used to screen a series of purification techniques that did not require the use of chemicals or heat. The treatment of BC with the protease, proteinase K (PK), resulted in small quantifiable changes in XRD diffractograms, with PK samples

exhibiting increased C.I. values (data not shown). Analysis by FT-IR transmission using ground and pressed BC samples and elemental composition determination confirmed the purity of PK treated BC to be comparable to 1% base treated BC. The structural stability of PK treated BC was analyzed by TGA and DSC, resulting in thermograms that illustrated a reduction of 39° in the thermal stability of PK treated BC compared to 1% base treated BC. This observation suggests a change in the physical chemistry of the cellulose occurs as a result of heat and chemical exposure. Although chemically identical, the properties of the PK treated BC varied in thermal stability and fiber morphology. Displaying a degree of polymerization value (DP_n) nearly one half of the DP_n observed from 1% base treated BC, PK treated BC exhibited enhanced saccharification efficiency and increased water retention (data not shown). These results and the results observed previously under saline conditions, suggests that the native conformation of cellulose is highly dependent on hydrogen bonding which can be influenced by steric interactions *in vivo*.

5.3 Concluding remarks

The novelty of this system is that future research targeted at understanding the complex biochemical interactions between cellulose, hemicellulose and lignin *in vivo*, can use this technique to model the influence of pH and counter ion concentrations on cellulose structure. Furthermore, the results from this study also suggest the possibility of structural proteins that mediate the formation of cellulose secondary and tertiary structures *in vivo*. Future studies aimed at characterizing the biochemical interactions between proteins and cellulose can use this treatment method to model the influence proteins may have on the ultra-structure of cellulose *in vivo,* with future aspirations of identifying novel binding targets for enhanced enzymatic saccharification.

5.4 References

Borzani,W. and Souza,S.J. (1995) Mechanism of the film thickness increasing during the bacterial production of cellulose on non-agitaded liquid media. *Biotechnology Letters* **17**, 1271-1272.

Brown,R.M., Willison,J.H. and Richardson,C.L. (1976) Cellulose biosynthesis in Acetobacter xylinum: visualization of the site of synthesis and direct measurement of the in vivo process. *Proceedings of the National Academy of Sciences* **73**, 4565-4569.

Chanzy,H. (2011) The continuing debate over the structure of cellulose: historical perspective and outlook. *Cellulose* **18**, 853-856.

Chao,Y., Ishida,T., Sugano,Y. and Shoda,M. (2000) Bacterial cellulose production by Acetobacter xylinum in a 50-L internal-loop airlift reactor. *Biotechnology and Bioengineering* **68**, 345-352.

David,B. (2009) Cellulases and biofuels. *Current Opinion in Biotechnology* **20**, 295-299.

Fontana,J., De Souza,A., Fontana,C., Torriani,I., Moreschi,J., Gallotti,B., De Souza,S., Narcisco,G., Bichara,J. and Farah,L. (1990) Acetobacter xylinum; cellulose pellicle as a temporary skin substitute. *Applied Biochemistry and Biotechnology* **24-25**, 253-264.

Helenius,G., Biñckdahl,H., Bodin,A., Nannmark,U., Gatenholm,P. and Risberg,B. (2006) In vivo biocompatibility of bacterial cellulose. *J. Biomed. Mater. Res.* **76A**, 431-438.

Hoffman,L.R., D'Argenio,D.A., MacCoss,M.J., Zhang,Z., Jones,R.A. and Miller,S.I. (2005) Aminoglycoside antibiotics induce bacterial biofilm formation. *Nature* **436**, 1171-1175.

Ishihara,M., Matsunaga,M., Hayashi,N. and Tiler,V. (2002) Utilization of d-xylose as carbon source for production of bacterial cellulose. *Enzyme and Microbial Technology* **31**, 986-991.

Maneerung,T., Tokura,S. and Rujiravanit,R. (2008) Impregnation of silver nanoparticles into bacterial cellulose for antimicrobial wound dressing. *Carbohydrate Polymers* **72**, 43-51.

Mohite,B., Kamalja,K. and Patil,S. (2012) Statistical optimization of culture conditions for enhanced bacterial cellulose production by Gluconoacetobacter hansenii NCIM 2529. *Cellulose* **19**, 1655-1666.

Petersen,N. and Gatenholm,P. (2011) Bacterial cellulose-based materials and medical devices: current state and perspectives. *Applied Microbiology and Biotechnology* **91**, 1277-1286.

Tal,R., Wong,H.C., Calhoon,R., Gelfand,D., Fear,A.L., Volman,G., Mayer,R., Ross,P., Amikam,D., Weinhouse,H., Cohen,A., Sapir,S., Ohana,P. and Benziman,M. (1998) Three cdg Operons Control Cellular Turnover of Cyclic Di-GMP in Acetobacter xylinum: Genetic Organization and Occurrence of Conserved Domains in Isoenzymes. *Journal of Bacteriology* **180**, 4416-4425.

APPENDICES

Appendix A. Bacterial cellulose 1% base treatment protocol

Items you will need

1 L 1 M NaOH	1 L 255 mM Acetic Acid	5 L Sterile DiH_2O
Sleeve of Petri dishes	2 sterile beakers with Sterile stir bars	3 sterile spatulas
1 non sterile beaker	1 non sterile spatula	Timer

If applicable: Mortar and pestle, 50 mL falcon tubes, liquid nitrogen & liquid nitrogen sufficient cooler.

Before beginning this procedure your pellicles should have reached your desired thickness and diameter. The below protocol is designed for processing 4 to 6 pellicles of petri dish thickness and diameter at one time. Upon harvesting the pellicles, obtain a 1 L beaker and a thin long spatula capable of stretching across the mouth of the beaker. When executing this protocol it is strongly advised to wear gloves at all times.

Day 1:

1. Wearing gloves, place a non-sterile spatula over a non-sterile beaker. Now remove pellicle from media and place over spatula. Allow the pellicle to drip for 1 minute. During the dripping process, place the base of disposable petri dish onto the scale and tare the scale. Now obtain a media associated wet weight. To differentiate between the different pellicles use a pair of scissors to make small incisions around the rim of the pellicle to denote the pellicles designation number. Record the unpure wet weight into your notebook or spread sheet.
2. Place pellicle into bottom of the beaker and perform step 1 on remaining pellicles you wish to process.

3. Once you have obtained all unpure wet weights, fill the beaker with DiH_2O and allow the pellicles to rinse. Insert a stir bar and allow the pellicles to rinse on stir plate for 30 min. Repeat this process 3 times, replenishing the DiH_2O each time with fresh DiH_2O. For best results and if time allows rinse pellicles overnight at 4°C.
4. After rinsing, poor off DiH_2O and fill beaker with 800 mL of 1 M NaoH. Place mixture onto hot plate (in a fume hood) and bring to a boil with moderate stirring. Allow pellicles to boil in NaOH for 2 h(George *et al*. 2005). During boiling process autoclave 4L of DiH_2O.
5. After boiling, allow pellicles to cool in NaOH mixture for 30mins. After mixture has cooled to the touch, poor off the NaOH. Immediately add 1 L of sterile DiH_2O and rinse the pellicles for 30 min. During the rinsing process obtain enough petri dishes to match the number of pellicles you are processing. Label the petri dishes accordingly (Pellicle Chem 1, 2….).
6. After rinsing, remove pellicles individually and place them into their designated petri dish. Once all the pellicles have been placed in the petri dishes you labeled in step 5, add 30 mL of 255 mM acetic acid to each petri dish(George *et al*. 2005). Carefully parafilm the closed petri dishes and place them on a rocker over night at room temperature. Before ending the day autoclave 1 1 L beaker covered with foil with a stir bar placed inside. In addition to the beaker(s) autoclave 2 L of DiH_2O to match the remaining 3 L you should still have from step 5.

Day 2

1. Remove pellicles from rocker and poor off 255 mM acetic acid. Rinse each petri dish individually with sterile DiH_2O keeping the pellicle in the petri dish. After plate

rinsing, remove the pellicles from their individual petri dish and place into sterile beaker with sterile stir bar (Prepared in Day 1 step 6). Poor in 1 L of sterile water (again prepared in Day 1 step 6) and place beaker and contents onto a stir plate allowing the pellicles to rinse for 1h.

2. After 1 h rinse, continue to rinse the pellicles with sterile DiH_2O a minimum of 2 more times, changing the DiH_2O out every 30 min. On last wash allow the pellicles to rinse overnight to ensure that the pH of the pellicle equilibrates to a neutral level. Before ending the day autoclave 1 1 L beaker and a long flat spatula that can lay across the mouth of the beaker.

❖ Cryo-grinding: If you intend to cryo-grind the sample you will need to autoclave a mortar and pestle along with an additional spatula. You will also need to use 50 mL tubes for Day 3 step 1.

Day 3

1. Obtain a petri dish for each individual pellicle that you are processing. Label each petri dish with the date and the name of each respective pellicle (Chem… 1, 2, 3). Now take the weights of each petri dish (including lid) and write the weight onto the plate (label the weight as total plate weight). Note: The same process detailed above can be done with 50 mL falcon tubes. If you are going to freeze dry using community freeze dryer or cyro-grind the samples you should use falcon tubes in place of petri dishes unless you are using an open type freeze dryer.
2. Stop the pellicles from spinning and obtain the newly autoclave beaker and spatula that you prepared in Day 2 step 2. Obtain the petri dishes labeled in Day 3 step 1. Remove a pellicle from the DiH_2O and allow it to drip for 1 min. During the dripping

process obtain the respective petri dish that matches the pellicle currently dripping. Using the base of the petri dish only, tare the scale. After 1 min drip, place the pellicle onto the base and obtain a DiH_2O wet weight. Place the DiH_2O wet weight of the pellicle onto the bottom of the petri dish. Label this weight as DiH_2O wet weight. Repeat this process for the remaining set of pellicles.

3. After obtaining the DiH_2O wet weight, the remaining steps will vary depending on mode of experimentation. Pick which option best suites your experimental goal.

❖ 3a. Sample manipulation: At this stage of the processing you can now incubate the pellicle(s) under varying conditions (pH, Salinity, color contrast ect. Note: Enzymatic digestion at this stage will not work as a result of the high water content. To perform enzymatic studies such as cellulase assays, you should dry the pellicle first. After sample manipulation move on to step 3b.

❖ 3b. Freeze Drying

3b.1.a <u>Freeze drying full plates</u>: If you have access to an open top freeze dryer you can freeze the plates using liquid nitrogen directly onto the pellicle or freezing the pellicle in the - 80°C. If using the -80°C freezer, you will need to freeze the pellicles overnight. Note: Freezing the pellicle with liquid nitrogen directly contacting the cellulose pellicle will result in high nitrogen content in the pellicle as well as a decrease in fiber associated pore size.

3b.1.b <u>Freeze drying in 50 mL flacon tubes using liquid nitrogen</u>: If you do not have access to an open top freeze dryer as noted in Day 3 step 1 and you are using a

community freeze dryer, you should have prepared your DiH_2O saturated pellicles in pre-weighted falcon tubes. Obtain a dewer full of liquid nitrogen and a styrofoam or plastic lined cooler. Fill the cooler with liquid nitrogen. Place samples in cooler (cap sealed). While the samples are freezing in the liquid nitrogen, Using a 12 to 18 gauge needle poke holes in the top of a set of fresh 50 mL tubes of equal size and thread as the tubes containing your sample. Place a 2 micron filter into the bottom of the aerated cap. After preparing the tubes turn on freeze dryer allowing ample time for the unit to reach optimum temperature. Once the freeze dryer is ready and the samples are frozen, using a tong remove the samples one by one from the liquid nitrogen and replace caps with aerated caps. Make sure you mark the empty tubes appropriately so that after the drying process the appropriate cap can be placed back onto its corresponding tube to preserve the noted weights of each tube.

3b.1.c Cryo-Grinding: If you are cryo-grinding the samples you will need obtain a dewer full of liquid nitrogen. Also locate a styrofoam or plastic lined cooler. Fill the cooler 2/3 of the way full with liquid nitrogen. Once you have the liquid nitrogen obtain your sterile mortar and pestle. Use the underside of the autoclaved foil (covered the mortar and pestle during autoclaving) as a sterile surface. Place your unwarped pestle and spatula on the sterile foil. Place a paper towel underneath the mortar to prevent sticking. Poor liquid nitrogen into the uncovered mortar and allow the nitrogen to boil completely off freezing the mortar. Poor a second cup of nitrogen into the mortar this time placing the pestle in the middle of the mortar. Allow the nitrogen to boil half way down mortar. Remove the pestle and place the first cellulose sample into the middle of the

mortar. Refill the mortar with liquid nitrogen, submerging the pellicle completely in liquid nitrogen. During the freezing process, place cap back on empty 50 mL tube and place tube into liquid nitrogen bath (styrofoam/plastic cooler). Once the nitrogen has boiled half way down the mortar, refill the mortar with liquid nitrogen. Using the still frozen pestle, gently tap the top of the cellulose pellicle to break the pellicle up into smaller pieces. Once only 1/3 nitrogen is left in the mortar begin grinding the sample. Refill the mortar with liquid nitrogen accordingly based on the remaining sample that needs to be ground.

-Once the sample has been ground to a fine powder, place the tip of the spatula into the liquid nitrogen cooler. Remove the now frozen empty sample tube from the cooler and remove the cap. Place frozen tube into a holder. Using the now frozen spatula carefully direct the ground sample into the frozen sample tube (For larger samples-thicker pellicles, you may need to label and freeze additional tubes).

-Once you have removed all of the powder from the mortar place cap back on tube and place tube back into liquid nitrogen cooler bath. Perform the same procedure on remaining pellicles.

-Once you have finished grinding all of the pellicles, while the samples are still in nitrogen bath, obtain an equal number of 50 mL falcon tubes. Using a 12 to 18 gauge needle poke holes in the top of the new empty 50 mL tubes. Place a 2 micron filter into the bottom of the aerated cap. After preparing the tubes turn on freeze dryer allowing ample time for the unit to reach optimum temperature. Once the freeze dryer is ready and the samples are frozen, using a tong remove the samples one by one from the liquid nitrogen and replace caps with aerated

caps. Make sure you mark the empty tubes appropriately so that after the drying process the appropriate cap can be placed back onto its corresponding tube to preserve the noted weights of each tube.

3b.2. Place the pellicles on the freeze dryer and allow the samples to dry for 2 – 3 days

- 3c. Oven Drying: If you are going to oven dry, you will need to obtain a set on non-stick steel plates or a set of paper clips. Locate a drying oven capable of reaching a minimum 90°C. If you are using paper clips weigh and number each paper clip. Suspend the pellicles from a raised rack position within the drying oven. Make sure you use two paper clips per sample to prevent folding. If available, use an additional two paper clips at the bottom corners of pellicle to weigh down the sample and prevent folding as a result of dehydration. If you have non-stick plates, simply place the pellicles in the plates (sandwiched to prevent folding) and allow pellicles to dry overnight.

Day 6: Dried Sample

1. Obtain dried weight: Remove dried sample from freeze dryer or oven. You will now need to obtain a dried weight by weighing the plate, tube or dried pellicle with paper clips. Using the petri dish weight, tube weight or paper clip weight recorded previously during the processing of the pellicle(s), obtain the dried sample weight simply by subtracting the container/paper clip weight from the total weight. Record the dried weight of the sample onto the final tube or plate the sample will be stored in. Label the dry weight as sample final dry weight.

2. Store samples in a vacuumed desiccator until you are ready to analyze or proceed with the next step in sample preparation.

References

George,J., Ramana,K.V., Sabapathy,S.N., Jagannath,J.H. and Bawa,A.S. (2005) Characterization of chemically treated bacterial (Acetobacter xylinum) biopolymer: Some thermo-mechanical properties. *International Journal of Biological Macromolecules* **37**, 189-194.

Appendix B. Bacterial cellulose proteinase K treatment protocol

Items you will need

Proteinase K	50 mM Tris-HCl Buffer (pH 8)	5 L Sterile DiH_2O
Sleeve of Petri dishes	2 sterile beakers with Sterile stir bars	3 sterile spatulas
1 non sterile beaker	1 non sterile spatula	Timer

If applicable: Mortar and pestle, 50 mL falcon tubes, liquid nitrogen & liquid nitrogen sufficient cooler.

Before beginning this procedure your pellicles should have reached your desired thickness and diameter. The below protocol is designed for processing 4 to 6 pellicles of petri dish thickness and diameter at one time. Upon harvesting the pellicles, obtain a 1 L sterile beaker, 2 L Sterile DiH_2O, a separate 1 L beaker and a thin long spatula capable of stretching across the mouth of the beaker. When executing this protocol it is strongly advised that you wear gloves at all times.

Day 1:

1. Wearing gloves, place a non-sterile spatula over the non-sterile beaker. Now remove pellicle from media and place over spatula. Allow the pellicle to drip for 1 minute. During the dripping process, place the base of disposable petri dish onto the scale and tare the scale. Now obtain a media associated wet weight. To differentiate between the different pellicles use a pair of scissors to make small incisions around the rim of the pellicle to denote the pellicles designation number. Record the unpure wet weight into your notebook or spread sheet.

2. Place pellicle into bottom of sterile beaker and perform step 1 on remaining pellicles you wish to process.
3. Once you have obtained all wet weights, fill the beaker with sterile DiH_2O with a sterile stir bar. Allow the pellicles to rinse overnight at 4^oC.

Day 2

1. After overnight rinsing poor off DiH_2O and refill the beaker containing pellicles with fresh sterile DiH_2O and allow pellicles to rinse at 4^oC for 1hr. Repeat this rinsing process 3 more times to remove as much cellularly debris as possible. After final rinse, poor off DiH_2O and proceed to day 2 step 2.
2. Now obtain enough petri dishes to match the number of pellicles you are processing. Label the petri dishes accordingly (pellicle-PK 1, 2….).
3. Remove pellicles individually and place them into their designated petri dish. Once all the pellicles have been placed in the petri dishes you labeled in Day 2 step 2, add 30 mL of 50 mM Tris-HCl buffer (pH 8) to each petri dish.
4. Remove Proteinase K from the -20°C freezer. Add enough proteinase k solution to each petri dish containing pellicle to obtain a final PK concentration of 100 ug/mL(GUNKEL and GASSEN 1989). If the stock is at a concentration is 20 mg/mL you will need to add 150 uL of enzyme mixture to petri dishes.
5. Carefully parafilm the closed petri dishes and place them on a mixing plate in the 37°C incubator for overnight digestion (GUNKEL and GASSEN 1989). Before concluding for the evening autoclave 2 1 L beakers containing stir bars and 5 L of DiH_2O.

Day 3

1. Remove pellicles from 30°C incubator and poor off enzyme mixture. Rinse each petri dish individually with room temperature sterile DiH_2O keeping the pellicle in the petri dish. After plate rinsing, remove the pellicles from their individual petri dish and place into sterile beaker with sterile stir bar (Prepared in Day 2 step 5). Poor in 1 L of sterile water (again prepared in Day 2 step 5) and place beaker and contents onto a stir plate allowing the pellicles to rinse for 1 h at 4°C.
2. After 1 h rinse, continue to rinse the pellicles with sterile DiH_2O a minimum of 3 more times, changing the DiH_2O out every 30 min. On last wash allow the pellicles to rinse overnight at 4ºC to ensure complete removal of Tris-HCl associated salts. Before ending the day autoclave 1 1 L beaker and a long flat spatula that can lay across the mouth of the beaker.

❖ Cryo-grinding: If you intend to cryo-grind the sample you will need to autoclave a mortar and pestle along with an additional spatula. You will also need to use 50 mL tubes for Day 4 step 1.

Day 4

1. Obtain a petri dish for each individual pellicle that you are processing. Label each petri dish with the date and the name of each respective pellicle (PK… 1, 2, 3). Now take the weights of each petri dish (including lid) and write the weight onto the plate (label the weight as total plate weight). Note: The same process detailed above can be done with 50 mL falcon tubes. If you are going to freeze dry using community freeze dryer or cyro-grind the samples you should use falcon tubes in place of petri dishes unless you are using an open type freeze dryer.

2. Stop the pellicles from spinning and obtain the newly autoclave beaker and spatula that you prepared in Day 3 step 2. Obtain the petri dishes labeled in Day 4 step 1. Remove a pellicle from the DiH_2O and allow it to drip for 1 min. During the dripping process obtain the respective petri dish that matches the pellicle currently dripping. Using the base of the petri dish only, tare the scale. After 1 min drip, place the pellicle onto the base and obtain a DiH_2O wet weight. Place the DiH_2O wet weight of the pellicle onto the bottom of the petri dish. Repeat this process for the remaining set of pellicles.
3. After obtaining the DiH_2O wet weight, the remaining steps will vary depending on mode of experimentation. Pick which option best suites your experimental goal.

❖ 3a. Sample manipulation: At this stage of the processing you can now incubate the pellicle(s) under varying conditions (pH, Salinity, color contrast ect.).

Note: Enzymatic digestion at this stage will not work as a result of the high water content. To perform enzymatic studies such as cellulase assays, you should dry the pellicle first.

After sample manipulation move on to step 3b.

❖ 3b. Freeze Drying

3b.1.a Freeze drying full plates: If you have access to an open top freeze dryer you can freeze the plates using liquid nitrogen directly onto the pellicle or freezing the pellicle in the - 80°C freezer. If using the -80°C freezer, you will need to freeze the pellicles overnight. Note: Freezing the pellicle with liquid nitrogen directly contacting the cellulose pellicle will result in high nitrogen content in the pellicle as well as a decrease in fiber associated pore size.

3b.1.b Freeze drying in 50 mL flacon tubes using liquid nitrogen: If you do not have access to an open top freeze dryer as indicated in Day 4 step 1 and you are using a community freeze dryer, you should have prepared your DiH_2O saturated pellicles in pre-weighted falcon tubes. Obtain a dewer full of liquid nitrogen and a styrofoam or plastic lined cooler. Fill the cooler with liquid nitrogen. Place samples in cooler (cap sealed). While the samples are freezing in the liquid nitrogen, Using a 12 to 18 gauge needle poke holes in the top of a set of fresh 50mL tubes of equal size and thread as the tubes containing your sample. Place a 2 micron filter into the bottom of the aerated cap. After preparing the tubes turn on freeze dryer allowing ample time for the unit to reach optimum temperature. Once the freeze dryer is ready and the samples are frozen, using a tong remove the samples one by one from the liquid nitrogen and replace caps with aerated caps. Make sure you mark the empty tubes appropriately so that after the drying process the appropriate cap can be placed back onto its corresponding tube to preserve the noted weights of each tube.

3b.1.c Cryo-Grinding: If you are cryo-grinding the samples you will need to obtain a dewer full of liquid nitrogen. Also locate a styrofoam or plastic lined cooler. Fill the cooler 2/3 of the way full with liquid nitrogen. Now obtain your sterile mortar and pestle. Use the underside of the autoclaved foil (covered the mortar and pestle during autoclaving) as a sterile surface. Place you unwarped pestle and spatula on the sterile foil. Place a paper towel underneath your mortar to prevent sticking. Now poor liquid nitrogen into the uncovered mortar and allow the nitrogen to boil completely off, freezing the mortar. Refill the mortar with nitrogen this time placing the pestle in the middle of the mortar. Allow the nitrogen to boil

half way down mortar. Remove the pestle and place the first cellulose sample into the middle of the mortar. Fill the mortar with nitrogen complete submersing the pellicle. During the freezing process, place cap back on 50 mL tube and place tube into liquid nitrogen cooler. Once the nitrogen has evaporated half way down the mortar, refill the mortar with nitrogen. Gently tap the top of the frozen pellicle to break up the cellulose as the nitrogen boils down. Once only 1/3 nitrogen is left in the mortar begin grinding the sample. Refill the mortar with liquid nitrogen accordingly based on the remaining amount of unground sample.

Once the sample has been ground to a fine powder, place the tip of the spatula into the liquid nitrogen cooler. Remove the sample tube from the cooler and remove the cap. Place frozen tube into a holder. Using the now frozen spatula carefully direct the ground sample into the frozen sample tube (For larger samples-Thicker pellicles, you may need to label and freeze additional tubes.)

Once you have removed all of the powder from the mortar place cap back on tube and place tube back into liquid nitrogen cooler bath. Perform the same procedure on remaining pellicles.

Once you have finished grinding all of the pellicles, while the samples are still in nitrogen bath, obtain an equal number of 50 mL falcon tubes. Using a 12 to 18 gauge needle poke holes in the top of the new empty 50 mL tubes. Place a 2 micron filter into the bottom of the aerated cap. After preparing the tubes turn on freeze dryer allowing ample time for the unit to reach optimum temperature. Once the freeze dryer is ready and the samples are frozen, using a tong remove the samples one by one from the liquid nitrogen and replace caps with aerated caps. Make sure you mark the empty tubes appropriately so that after the drying

process the appropriate cap can be placed back onto its corresponding tube to preserve the noted weights of each tube.

3b.2. Place the pellicles on the freeze dryer and allow the samples to dry for 2 – 3 days

- 3c. Oven Drying: If you are going to oven dry, you will need to obtain a set on non-stick steel plates or a set of paper clips. Locate a drying oven capable of reaching a minimum 90°C. If you are using paper clips weigh and number each paper clip. Suspend the pellicles from an elevated rack in the drying oven. Make sure you use two paper clips per sample to prevent folding. If available use an additional two paper clips at the bottom corners of pellicle to weigh down the sample and prevent folding as a result of dehydration. If you have non-stick plates, simply place the pellicles in the plates (sandwiched to prevent folding) an allow pellicles to dry overnight.

Dried Sample

1. Obtain dried weight: Remove dried sample from freeze dryer or oven. You will now need to obtain a dried weight by weighing the plate, tube or dried pellicle with paper clips. Using the petri dish weight, tube weight or paper clip recorded previously during the processing of the pellicle, obtain the exact dried weight of each sample using subtraction from total weight. Record the dried weight of the sample onto the final tube or plate the sample will be stored in. Label the dry weight as sample final dry weight.

2. Store samples in a vacuumed desiccator until you are ready to analyze or proceed with the next step in sample preparation.

References

GUNKEL,F.A. and GASSEN,H.G. (1989) Proteinase K from Tritirachium album Limber. *European Journal of Biochemistry* **179**, 185-194.

Appendix C. Bacterial cellulose sphere 1% base treatment protocol

Items you will need

1 M NaOH	255 mM Acetic Acid	5 L Sterile DiH_2O
Sleeve of Petri dishes	2 sterile beakers with Sterile stir bars	3 sterile spatulas
1 1 L Non-sterile beaker	1 non sterile spatula	Liquid nitrogen
50 mL Falcon Tubes	Swinging bucket rotor	Styrofoam cooler

Before beginning this procedure your agitated cultures should be mature in growth and have produced a sufficient amount of cellulose spheres (1 week growth after a 0.130 A_{660}/mL inoculation (Hwang *et al*. 1999; Masaoka *et al*. 1993). The below protocol is designed for processing 1 250 mL agitated culture of *G. Hansenii*. Before harvesting the cellulose spheres, obtain 2 50 mL sterile falcon tubes, 1 sterile beaker and a thin long spatula. When executing this protocol it is strongly advised to wear gloves at all times.

Day 1:

1. Wearing gloves, remove agitated culture from 30°C shaker. Place two 50 mL falcon tubes into a holder and remove the caps.
2. Carefully poor 50mL of culture into each tube.
3. Balance the tubes using a weight balance.
4. Spin down the two tubes at 1 ,500 to 3,500 RPM for 10 min using swinging bucket rotor(Chirgwin *et al*. 1979).
5. After centrifugation, gently poor off supernatant into sterile beaker. It may be more efficient to use a pipetor to remove the supernatant to prevent the loss of spheres.

Keep beaker covered with sterile foil at all time to minimize chances of contamination.

6. Repeat steps 2 through 5 until you have centrifuged the entire 250 mL culture.
7. After the entire culture has been centrifuged, rinse the cellulose spheres using non-sterile DiH_2O by filling the 50 mL tubes with DiH_2O and vortex 20 seconds.
8. Balance and centrifuge the 50mL tubes for 10 min at 1,500 RPM to 3,500 RPM using a swinging bucket rotor.
9. Discard supernatant down drain. Be careful not to poor out spheres as the cellulose is not tightly packet. It may be helpful to use a pipetor to remove supernatant.
10. Repeat steps 7 through 9, 5 more times for a total of 6 rinse cycles. (It would be helpful to rebalance the tubes before vortexing the spheres to prevent pipette tip blockage during the weight balancing process).
11. After last rinse (6^{th} rinse cycle) centrifuge the two 50 mL tubes again and discard the supernatant.
12. Obtain 1 1 L non-sterile beaker and a 1L solution of 1 M NaOH (George *et al*. 2005). Fill the two 50 mL tubes containing cellulose sphere with 50 mL of 1 M NaOH solution. Briefly vortex the tubes.
13. Poor the contents of each tube into the 1 Lnon-sterile beaker. Bring the volume of the NaOH in the beaker to 800 mL.
14. Place the beaker containing the cellulose spheres and stir bar onto a hot plate. Boil the cellulose spheres in 1 M NaOH for 2 h on a moderate stir(George *et al*. 2005). During the boiling process allow NaOH to boil down to 500 mL before refilling to the 800 mL starting point.

15. After 2 h boiling period allow the NaOH solution to cool to the touch. During the cooling process obtain 2 sterile 50 mL falcon tubes. Using an analytical scale, weigh both tubes and place the weight of each tube in the lower corner of test tube label.
16. Place the 50 mL tubes into a rack and remove the caps. Obtain cooled beaker containing cellulose spheres and poor of excess NaOH until there is 400 mL of sample and NaOH left in the beaker.
17. Gently fill both 50 mL tubes with cellulose-NaOH mixture. Balance and centrifuge both tubes for 10 min using a swinging bucket rotor at 1,500 RPM to 3,500 RPM for 10 min.
18. After centrifugation, poor off supernatant and repeat step 17 until the entire contents of NaOH beaker is empty.
19. After final centrifugation, add 15 mL of 255 mM acetic acid to both tubes and vortex vigorously.
20. After vortexing, obtain 1 sterile petri dish. Label the petri dish as Agi-chem1, 2, and date. Poor contents of tubes 1 and 2 into petri dish.
21. Gently parafilm petri dish and place on rocker overnight.

Day 2

Before beginning day 2 autoclave 1 1 L beaker with stir bar, 5 L of DiH_2O, and 1 spatula.

1. Remove petri dishes from rocker. Poor the contents of each plate into the autoclaved sterile beaker.
2. Poor in 1 L of room temperature sterile DiH_2O into the beaker and place beaker on stir plate. Allow cellulose to rinse for 1 h.

3. After 1 h rinse, gently poor off 500 mL of DiH_2O and replace with fresh sterile room temperature DiH_20. Be careful to not loose and spheres when changing DiH_2O.
4. Repeat step 3 4 more time (3 L of DiH_20 for total rinse).
5. After 4^{th} rinse cylce, add a final 500 mL of room temperature sterile DiH_2O to the beaker for a total of 1 L of DiH_2O in the beaker and allow the cellulose to rinse overnight.

Day 3

Before beginning day 3 obtain 2 50 mL sterile falcon tubes and label them cellulose spheres-Agitated conditions and the date 1 & 2, Styrofoam cooler & liquid nitrogen. Obtain the weight of each 50 mL tube and place the tube weight on the bottom corner of the tube label.

6. Obtain beaker with rinsing cellulose spheres and gently poor off 600 mL of DiH_2O. Be careful not to lose cellulose spheres.
7. Place two labeled 50 mL falcon tubes into a holder. Remove the caps and gently poor 50 mL of rinsed cellulose into each tube.
8. Balance the tubes using a weight balance and centrifuge the cellulose for 10 min at 1,500 RPM to 3,500 RPM in a swinging bucket rotor.
9. Poor off supernatant into sink. The cellulose spheres are not tightly packed. It may be more efficient to use a pipetor to remove the supernatant.
10. Repeat step 8 through 9 until the entire contents of the beaker are empty.
11. Using the remaining amount of sterile DiH_2O from Day 2, rinse the cellulose by filling each tube with room temperature DiH_2O and vortexing.

12. Balance the tubes and centrifuge for 10 min at 1,500 RPM to 3,500 RPM using a swinging bucket rotor.
13. Repeat steps 11 through 12 3 more times. On final rinse, centrifuge for 20 min.
14. Remove supernatant from the tubes using a pipetor.
15. The remaining steps will vary depending on mode of experimentation. Pick which option best suites your experimental goal.

❖ 15a. Sample manipulation: At this stage of the processing you can now incubate the spheres under varying conditions (pH, Salinity, color contrast ect.).

Note: Enzymatic digestion at this stage will not work as a result of the high water content. To perform enzymatic studies such as cellulase assays, you should dry the pellicle first.

After sample manipulation move on to step 15b.

❖ 15b. Freeze Drying

Freeze drying in 50 mL flacon tubes using liquid nitrogen: After rinse and centrifugation, place samples in cooler (cap sealed). While the samples are freezing in the liquid nitrogen, Using a 12 to 18 gauge needle poke holes in the top of a set of fresh 50 mL tubes of equal size and thread as the tubes containing your sample. Place a 2 micron filter into the bottom of the aerated cap. After preparing the tubes turn on freeze dryer allowing ample time for the unit to reach optimum temperature. Once the freeze dryer is ready and the samples are frozen, using a tong remove the samples one by one from the liquid nitrogen and replace caps with aerated caps. Make sure you mark the empty tubes appropriately so that after the drying process

the appropriate cap can be placed back onto its corresponding tube to preserve the noted weights of each tube.

Place tubes in freeze dryer and allow sample to dry for 2 to 3 days.

- 15c. Oven Drying:

If you are going to oven dry, you will need to obtain a set on non-stick steel plates. Locate a drying oven capable of reaching a minimum 90°C. Using a sterile spatula, gently scrape the cellulose spheres onto the face of one of the non-stick plates. Making a sandwich, press the cellulose between a sister non-stick plate and allow cellulose to dry overnight.

Day 5/6 Dried Sample

1. Remove samples from the freeze dryer or oven and replace aerated caps with original caps. Weigh the tube(s) on the same balance you weighed the tubes on originally. Subtract the empty tube weight found in the lower corner of the tube label from the full tube weight to determine the actual weight of the spheres. Record the sample weight on the side of the tube and or notebook.
2. After obtain the sample weight, store samples in a vacuumed desiccator until you are ready to analyze or proceed with the next step in sample preparation.

References

Chirgwin,J.M., Przybyla,A.E., MacDonald,R.J. and Rutter,W.J. (1979) Isolation of biologically active ribonucleic acid from sources enriched in ribonuclease. *Biochemistry* **18**, 5294-5299.

George,J., Ramana,K.V., Sabapathy,S.N., Jagannath,J.H. and Bawa,A.S. (2005) Characterization of chemically treated bacterial (Acetobacter xylinum) biopolymer: Some thermo-mechanical properties. *International Journal of Biological Macromolecules* **37**, 189-194.

Hwang,J.W., Yang,Y.K., Hwang,J.K., Pyun,Y.R. and Kim,Y.S. (1999) Effects of pH and dissolved oxygen on cellulose production by Acetobacter xylinum BRC5 in agitated culture. *Journal of Bioscience and Bioengineering* **88**, 183-188.

Masaoka,S., Ohe,T. and Sakota,N. (1993) Production of cellulose from glucose by Acetobacter xylinum. *Journal of Fermentation and Bioengineering* **75**, 18-22.

Appendix D. Bacterial cellulose sphere proteinase K treatment protocol

Items you will need

Proteinase K	50 mM Tris-HCl Buffer (pH 8)	5 L Sterile DiH_2O
Sleeve of Petri dishes	2 sterile beakers with Sterile stir bars	3 sterile spatulas
DiH_2O	1 non sterile spatula	Liquid nitrogen
50 mL Falcon Tubes	Swinging bucket rotor	Styrofoam cooler

Before beginning this procedure your agitated cultures should be mature in growth and have produced a sufficient amount of cellulose spheres (1 week growth after a 0.130 A_{660}/mL inoculation (Hwang *et al*. 1999; Masaoka *et al*. 1993)). The below protocol is designed for processing 1 250 mL agitated culture of *G. Hansenii*. Before harvesting the cellulose spheres, obtain 2 50 mL sterile falcon tubes, 1 sterile beaker and a thin long spatula. When executing this protocol it is strongly advised to wear gloves at all times.

Day 1:

1. Wearing gloves, remove agitated culture from 30°C shaker. Place two 50 mL falcon tubes into a holder and remove the caps.
2. Carefully poor 50 mL of culture into each tube.
3. Balance the tubes using a weight balance.
4. Spin down the two tubes at 1,500 RPM to 3,500 RPM for 10 min using swinging bucket rotor(Chirgwin *et al*. 1979).

5. After centrifugation, gently poor off supernatant into sterile beaker. It may be more efficient to use a pipetor to remove the supernatant to prevent the loss of spheres. Keep beaker covered with sterile foil at all time to minimize chances of contamination. (It would be helpful to rebalance the tubes before vortexing the spheres to prevent pipette tip blockage during the weight balancing process)

6. Repeat steps 2 through 5 until you have centrifuged the entire 250 mL culture.

7. After the entire culture has been centrifuged, rinse the cellulose spheres using non-sterile DiH_2O by filling the 50 mL tubes with DiH_2O and vortex 20 sec. For best results used pre-chilled (4°C) sterile DiH_2O when rinsing the cellulose spheres. If possible rinse overnight at 4°C using rocking plate in 4°C refrigerator or cold room.

8. Balance and centrifuge the 50 mL tubes for 10 min at 1,500 RPM to3,500 RPM using a swinging bucket rotor.

9. Discard supernatant down drain. Be careful not to poor out spheres as the cellulose is not tightly packet. It may be helpful to use a pipetor to remove supernatant.

10. Repeat steps 7 through 9, 5 more times for a total of 6 rinse cycles.

11. After last rinse (6^{th} rinse cycle) centrifuge the two 50 mL tubes again and discard the supernatant.

12. Obtain two petri dishes and label them PK-spheres 1 & 2. Fill the two 50 mL tubes containing cellulose sphere with 30 mL of Tris-HCl (pH 8) buffer. Briefly vortex the tubes (GUNKEL and GASSEN 1989).

13. Separately poor the contents of each tube into the two labeled petri dishes that you labeled in step 12.

14. Add 150 uL (stock concentration of 20 mg/mL) of proteinase K to each petri dishes.

15. Gently parafim the petri dishes and place them on a rocker for 1 h with moderate rocking.

16. After 1 h remove the petri dishes from the rocker and place them in 30°C for overnight indigestion.

Day 2

Before beginning day 2 autoclave 1 1 L beaker with stir bar, 5 L of DiH_2O, and 1 spatula.

1. Remove petri dishes from the 30°C incubator. Poor the contents of each plate into the autoclaved sterile beaker.

2. Poor in 1 L of room temperature sterile DiH_2O into the beaker and place beaker on stir plate. Allow cellulose to rinse for 1hr.

3. After 1 h rinse, gently poor off 500 mL of DiH_2O and replace with fresh sterile room temperature DiH_2O. Be careful to not loose and spheres when changing DiH_2O.

4. Repeat step 3 4 more time (3 L of DiH_2O for total rinse).

5. After 4^{th} rinse cycle, add a final 500 mL of room temperature sterile DiH_20 to the beaker for a total of 1 L of DiH_2O in the beaker and allow the cellulose to rinse overnight.

Day 3

Before beginning day 3 obtain 2 50 mL sterile falcon tubes and label them cellulose spheres-Agitated conditions and the date 1 & 2, styrofoam cooler & liquid nitrogen. Obtain the weight of each 50 mL tube and place the tube weight on the bottom corner of the tube label.

6. Obtain beaker with rinsing cellulose spheres and gently poor off 600 mL of DiH_2O. Be careful not to lose cellulose spheres.

7. Place two labeled 50 mL falcon tubes into a holder. Remove the caps and gently poor 50 mL of rinsed cellulose into each tube. (make sure you have obtained a weight for both 50 mL tubes and placed the weight of the tube onto the lower corner of tube label)

8. Balance the tubes using a weight balance and centrifuge the cellulose for 10 min at 1,500 RPM to 3,500 RPM in a swinging bucket rotor.

9. Poor off supernatant into sink. The cellulose spheres are not tightly packed. It may be more efficient to use a pipetor to remove the supernatant.

10. Repeat step 8 through 9 until the entire contents of the beaker are empty.

11. Using the remaining amount of sterile DiH_2O from Day 2, rinse the cellulose by filling each tube with room temperature DiH_2O and vortexing.

12. Balance the tubes and centrifuge for 10 min at 1,500 RPM to 3,500 RPM using a swinging bucket rotor.

13. Repeat steps 11 through 12 3 more times. On final rinse, centrifuge for 20 min.

14. Remove supernatant (DiH_2O rinse) from the tubes using a pipetor.

15. The remaining steps will vary depending on mode of experimentation. Pick which option best suites your experimental goal.

❖ 15a. Sample manipulation: At this stage of the processing you can now incubate the spheres under varying conditions (pH, salinity, color contrast ect.).

Note: Enzymatic digestion at this stage will not work as a result of the high water content. To perform enzymatic studies such as cellulase assays, you should dry the pellicle first.

After sample manipulation move on to step 15b.

❖ 15b. Freeze Drying

Freeze drying in 50 mL flacon tubes using liquid nitrogen: After rinse and centrifugation, place samples in nitrogen bath-cooler (cap sealed). While the samples are freezing in the liquid nitrogen, Using a 12 to 18 gauge needle poke holes in the top of a set of fresh 50 mL tubes of equal size and thread as the tubes containing your sample. Place a 2 micron filter into the bottom of the aerated cap. After preparing the tubes turn on freeze dryer allowing ample time for the unit to reach optimum temperature. Once the freeze dryer is ready and the samples are frozen, using a tong remove the samples one by one from the liquid nitrogen and replace caps with aerated caps. This process should be done fast. The sample

should not thaw before they have been placed on the freeze dryer. Make sure you mark the empty tubes appropriately so that after the drying process the appropriate cap can be placed back onto its corresponding tube to preserve the noted weights of each tube.

Place tubes in freeze dryer and allow sample to dry for 2 to 3 days.

- 15c. Oven Drying:

If you are going to oven dry, you will need to obtain a set on non-stick steel plates. Locate a drying oven capable of reaching a minimum 90°C. Using a sterile spatula, gently scrape the cellulose spheres onto the face of one of the non-stick plates. Making a sandwich, press the cellulose between a sister non-stick plate and allow cellulose to dry overnight.

Day 5/6 Dried Sample

1. Remove samples from the freeze dryer or oven and replace aerated caps with original caps. Weigh the tube(s) on the same balance you weighed the tubes on originally. Subtract the empty tube weight found in the lower corner of the tube label from the full tube weight to determine the actual weight of the spheres. Record the sample weight on the side of the tube and or notebook.

2. After obtaining the sample weight, store samples in a vacuumed desiccator until you are ready to analyze or proceed with the next step in sample preparation.

References

Chirgwin,J.M., Przybyla,A.E., MacDonald,R.J. and Rutter,W.J. (1979) Isolation of biologically active ribonucleic acid from sources enriched in ribonuclease. *Biochemistry* **18**, 5294-5299.

GUNKEL,F.A. and GASSEN,H.G. (1989) Proteinase K from Tritirachium album Limber. *European Journal of Biochemistry* **179**, 185-194.

Hwang,J.W., Yang,Y.K., Hwang,J.K., Pyun,Y.R. and Kim,Y.S. (1999) Effects of pH and dissolved oxygen on cellulose production by Acetobacter xylinum BRC5 in agitated culture. *Journal of Bioscience and Bioengineering* **88**, 183-188.

Masaoka,S., Ohe,T. and Sakota,N. (1993) Production of cellulose from glucose by Acetobacter xylinum. *Journal of Fermentation and Bioengineering* **75**, 18-22.

Appendix E. Instrument methods

Chemical analysis of bacterial cellulose as a result of pretreatment using FT-IR
Instrument: Nexus FT-IR 670

FT-IR ATR experimental plan
- Initial analysis was performed using FT-IR attenuated total reflectance (ATR)
- 3mg of treated freeze dried bacterial cellulose
- Measurement from wavenumbers 4000 toAppe 500 cm^{-1}
- 32 Scans per sample read with a resolution of 32

FT-IR Transmission: Higher resolution spectra
- 3mg of ground and treated freeze dried bacterial cellulose
- Measurement from wavenumbers 4000 to 500 cm^{-1}
- 64 Scans per sample read with a resolution of 32

Chemical analysis of bacterial cellulose as a result of pretreatment using Elemental Analsysis
Instrument: CHN CE440
- 500 mg of Sample
- Analyzed by combustion for Carbon, Nitrogen and hydrogen content

Thermodynamic structural analysis of bacterial cellulose using TGA
Instrument: TA Instrument Q500

TGA experimental plan
- 20mg of treated bacterial cellulose
- Open platinum pan
- Temperature range 30°C to 800°C
- 5minute hold at 110°C to remove water & normalize samples
- Ramp rate of 10° per minute

Thermodynamic structural analysis of bacterial cellulose using DSC
Instrument: TA instrument Q100

DSC experimental plan
- 3mg of treated bacterial cellulose
- Sealed Pan
- Temperature range 25°C to 315°C
- Ramp rate of 10° per minute
- Scan profile consisted of two up scans and one down scan

Bacterial Cellulose Crystalline Region Structural Analysis by XRD
Instrument: Rigku SmartLab 5G

Experimental Plan
- 5 mg of freeze dried cellulose
- Dry stage mounting
- 2θ range 9 to 41 in 0.05 step increments
- Exposure time of 5 seconds

Bacterial Cellulose morphology and structural analysis by Field Emission Scanning Electron Microscopy (FE-SEM)
Instrument: JEOL 6400 is a Cold Field Emission Scanning Electron microscope

Bactieral Cellulose structural analysis by ^{13}C CP-MAS NMR (Solid State NMR)
Instrument: Bruker
- 10 mg Freeze dried ground samples

Appendix F. Curriculum Vitae **William D. Graham**

Email: wdgram@gmail.com

Professional Profile

People oriented scientist with a team first, individual second attitude. I have seven years of professional experience in the field of research, where I have learned a variety of techniques in the field of Molecular and Structural Biochemistry. My experience includes working with nucleic acids and proteins where I have characterized their interactions through thermodynamic studies. My accomplishments in this field include managing and advancing graduate level research projects, the development and adaptation of software for data calculations and manipulation, increased laboratory productivity and efficiency by creating networking solutions for data sharing, laboratory accounting and product procurement. I am a self motivated individual who understands the importance of deadlines and accountability.

Education

NORTH CAROLINA STATE UNIVERSITY — Raleigh, NC
Doctorate in Microbiology & Forest Biomaterials — Spring 2013
Dissertation: *Bacterial Cellulose: A Model for Deconstructing Cellulose Native Structure*

NORTH CAROLINA STATE UNIVERSITY — Raleigh, NC
Masters of Science, Molecular and Structural Biochemistry — July 2010
Thesis: *Isolating HIV NCp7 Peptide Mimics that Target the Anticodon Stem Loop Region of Human Transfer RNA Lysine3 in a Modification Dependent Manner*

NORTH CAROLINA STATE UNIVERSITY — Raleigh, NC
Bachelor of Science, Microbiology — December 2001

Awards & Honors

National Needs Foundation Fellowship (USDA) — 2010 – 2013
NIH America Recovery and Reinvestment Act (ARRA) Minority Grant Recipient — 2009 – 2010

Conferences & Presentations

Chancellor's Ph.D review panelist — Fall 2012
Nano-Cellulose Technology Workshop — Summer 2012
College of Agricultural and Life Sciences HBCU Undergraduate Advisor Panelist — Fall 2011
College of Agricultural and Life Sciences Creating Awareness Key Note Speaker — Summer 2011
North Carolina RNA Symposium Poster Presentation — Summer 2009
American Society of Biochemistry and Molecular Biology Conference Poster — Spring 2009

William D. Graham

Email: wdgram@gmail.com

Microbiology/Molecular Biology Consultant
Sirga Advanced Biopharma, Raleigh, NC 2007 – 2010

- Enhanced Antibiotic Screening
- Peptide Screening & Characterization
- Cloning and Maintaining Bacterial Cell Lines

Research Specialist
NCSU Department of Biochemistry, Raleigh, NC 2002 – 2010

- Protein & Nucleic Acid Purification
- Radioactive Labeling of Nucleic Acids
- Phage Display Library Peptide Screening
- Protocol Development and Experimental Design
- Microplate Reader Fluorescent Screening Assays
- Manage and Maintain Complex Scientific Equipment
- Procure, Manage and Maintain Laboratory Supplies
- Manage Laboratory Safety Procedures & Waste Disposal
- Advancement and Supervision of Graduate Student Projects
- Peptide & RNA Isothermal Titration Calorimetry Binding Studies
- Thermodynamic Characterization of Proteins & Nucleic acids
- Monthly Power Point Presentations on Project Accomplishments

Research Technician II
NCSU Department of Microbiology, Raleigh, NC 2001 – 2002

- Performed Yeast-Two- Hybrid Screens on TGMV Viral Movement Proteins with a *Nicotiana benthamiana* cDNA Library

Laboratory Assistant
NCSU Department of Botany, Raleigh, NC 1998 – 2001

- Performed DNA and RNA Extractions and Purifications
- Created Functional Cataloging for Transgenic Cell Lines
- Responsible for Cell Culture Transfers and Tissue Cultures
- Assisted in the Investigation of Calcium Concentrations in Plant Root Tips & How those Concentrations Influence Gravitropism

Evening Manager/Sales Consultant
Golds Gym, Cary NC 2002 – 2007

- Managed Staff Schedules and Timesheets
- Negotiated the Procurement of Gym Supplies

William D. Graham

Email: wdgram@gmail.com

Teaching & Mentoring

North Carolina Project SEED Mentor	Summer 2011
Teaching Assistant: PSE 332 Pulp Bleaching Chemistry (NCSU)	Spring 2011
Undergraduate Research Mentor	2002 – 2010
Teaching Assistant: BCH 453 Biochemistry of Gene Expression (NCSU)	Spring 2009

Laboratory Skills

- Plant Transformations
- Yeast Transformations
- Fluorescence Microscopy
- Peptide-Ligand Screening
- Nucleic Acid-Ligand Screening
- Cellulose Nano-Crystal Isolation
- U.V. Thermal Structural Analysis
- Gram Staining
- Electrophoresis
- Fluorescent Screening
- Bacterial Transformations
- Ribosomal Binding Assay
- Nucleic Acid Purifications
- Radioactive Isotope Labeling
- PCR
- Western Blots
- Southern Blots
- Aseptic Technique
- Molecular cloning
- Restriction Digest
- Molecular cloning

Instrument Experience

- Fluorescence Microplate Reader
- Ultraviolet Visible Spectrometer
- Thermal Gravimetirc Analyzer (TGA)
- High Pressure Liquid Chromatography (HPLC)
- Fourier transformed infrared spectrometer (FT-IR)
- Jasco Circular Dichroism (CD)
- Isothermal Titration Calorimetry (ITC)
- Differential Scanning Calorimetry (DSC)
- Rigaku S.lab X-Ray Diffractometer (XRD)
- Waters Q-Tof Premier Mass Spectrometer

William D. Graham

Email: wdgram@gmail.com

Publications

Graham, William D., *et al* Functional Recognition of the Modified Human tRNALys3UUU Anticodon Domain by HIV's Nucleocapsid Protein and a Peptide Mimic, *Journal of Molecular Biology* 410.4 (2011): 698.

Graham[†] **WD**., Scheunemann[†] A., Agris PF., Binding of Aminoglycosides to Helix 69 of 23s RNA, *Journal of Molecular Biology* (2010): 3094-3105

Vendeix, FA., Dziergowska, A., Gustillo, EM., **Graham WD**., Anticodon Domain Modifications Contribute to Order to tRNA for Ribosome-Mediated Codon Binding, *J. of Biochemistry* 47.23 (2008): 6117-6129..

Agris, PF., Vendeix FA., **Graham WD**. (2007) tRNA's Wobble Decoding of the Genome: 40 years of Modifications, *Journal of Molecular Biology. 366, 1-1.*

Publications Currently Under Review

Graham, William D, *et al.* (2013) Investigation of the structural and thermal behavior of native bacterial cellulose fibers using a protease treatment method, *Journal of Bioresource and Technology* (submitting).

Graham, William D, *et al*. (2013) Selecting high cellulose producing *Gluconacetobacter hansenii* strain ATCC 23769 phenotypes using antibiotic screening, *Journal of Applied Microbiology* (submitting).

Graham, William D, *et al*. (2013) The influence of mechanical and chemical based pretreatments on native cellulose structure' *ChemSusChem* (submitting).